

DISSERTATION

PATHOLOGY OF FELINE CHRONIC KIDNEY DISEASE: HISTOMORPHOLOGIC  
CHARACTERIZATION OF RENAL AND GASTRIC LESIONS; AND AN INVESTIGATION  
INTO THE EXPRESSION OF RENAL  $\alpha$ -ENOLASE

Submitted by

Shannon M. McLeland

Department of Microbiology, Immunology, and Pathology Department

In partial fulfillment of the requirements

For the Degree of Doctor of Philosophy

Colorado State University

Fort Collins, Colorado

Spring 2015

Doctoral Committee:

Advisor: Steve Dow

Co-Advisor: Michael Lappin

Robert Callan

Colleen Duncan

Jessica Quimby

Copyright by Shannon M. McLeland 2015

All Rights Reserved

## ABSTRACT

### PATHOLOGY OF FELINE CHRONIC KIDNEY DISEASE: HISTOMORPHOLOGIC CHARACTERIZATION OF RENAL AND GASTRIC LESIONS; AND AN INVESTIGATION INTO THE EXPRESSION OF RENAL $\alpha$ -ENOLASE

Feline chronic kidney disease (CKD) is a common disease among older cats and is associated with high morbidity and decreased survival. A definitive cause or potential factors that initiate this highly prevalent disease have been elusive. The overall goal of this body of work was twofold; to better characterize, histopathologically, the renal and associated gastric manifestations of CKD, and secondly, explore the potential role of vaccinations and autoantibodies in cats with CKD.

In the first study the presence and severity of both reversible and irreversible histopathologic lesions were evaluated in the kidneys of cats at each stage of CKD. A total of 46 cats with CKD were classified according to the International Renal Interest Society (IRIS) as: Stage I (3 cats), Stage II (16 cats), Stage III (14 cats), and Stage IV (13 cats). Eleven young, non-azotemic and 10 geriatric, non-azotemic cats were included as controls. The severity of tubular degeneration, interstitial inflammation, fibrosis, and glomerulosclerosis was significantly greater in later stages of CKD compared to early stages of disease. Proteinuria was associated with increased severity of tubular degeneration, inflammation, fibrosis, tubular epithelial single cell necrosis and decreased normal parenchyma. Presence of hyperplastic arteriolosclerosis, fibrointimal hyperplasia, or other vascular lesions was not found to be significantly different

between hypertensive and normotensive cats. Irreversible lesions such as interstitial fibrosis were more common and severe in later stages of CKD (Stage III and IV).

Chronic kidney disease in cats is associated with gastrointestinal signs commonly attributed to uremic gastropathy. Symptomatic therapy is based on documented gastric lesions in other species. The objective of this study was to determine the prevalence and characterize gastric lesions in cats with CKD. Samples from a total of 37 CKD cats and 12 non-azotemic control cats were evaluated. Characterized lesions were compared with serum creatinine concentrations, calcium-phosphorus product (CPP) and serum gastrin concentrations. Gastric ulceration, hemorrhage, edema, and vascular injury, were not observed in cats with CKD. The most significant gastric lesions in CKD cats were fibrosis and mineralization. Sixteen CKD cats (43%) had evidence of gastric fibrosis of varying severity and 14 CKD cats (38%) had gastric mineralization. Cats with CKD were more likely to have gastric fibrosis and mineralization than non-azotemic controls ( $p=0.005$  and  $p=0.021$ , respectively). Only cats with moderate and severe azotemia had gastric mineralization. CPP was correlated to disease severity; severely azotemic CKD cats had significantly greater CPP when compared to non-azotemic controls, and to mildly and moderately azotemic cats ( $p<0.05$ ). Gastrin concentrations were significantly greater in CKD cats when compared to non-azotemic controls ( $p=0.003$ ) but elevated concentrations were not associated with gastric ulceration.

Vaccinations against feline viral rhinotracheitis, calicivirus, and panleukopenia (FVRCP) and vaccine cell lysates (CRFK) can induce autoantibodies that target  $\alpha$ -enolase protein. In addition, a subset of these cats with antibodies against CRFK lysates developed interstitial nephritis when hyperinoculated. Alpha-enolase, a ubiquitous, glycolytic enzyme has been implicated as a self-antigen in various autoimmune diseases, some of which are associated with

active nephritis in human patients. Plasma cell membrane expression of  $\alpha$ -enolase has been identified as a target of autoantibodies.

The focus of these dissertation chapters was threefold. First, to determine if cats with CKD have anti- $\alpha$ -enolase antibodies and if levels of antibodies vary with severity of disease (i.e. IRIS stage) or FVRCP vaccine history. Second, to characterize  $\alpha$ -enolase expression in feline tissues and renal subcellular fractions in health and in feline CKD. Third, to determine if antibodies in the sera from CKD cats are capable of targeting feline endogenous renal proteins. Twenty-nine CKD cats and healthy, unvaccinated control cats (n=8) were included. CKD cats consisted of 9 Stage II cats, 8 Stage III cats, and 12 Stage IV cats.

Cat with CKD, regardless of vaccine history, had significantly greater levels of  $\alpha$ -enolase antibodies than controls ( $p < 0.0001$ ). No difference in the levels of antibodies between vaccine groups or IRIS stage was found. Alpha-enolase protein was differentially expressed in the kidneys of cats with CKD by immunohistochemistry. In healthy kidneys,  $\alpha$ -enolase protein immunoreactivity was moderate in tubular epithelium but absent in glomeruli. In contrast,  $\alpha$ -enolase expression was significantly decreased in tubules that were degenerative or atrophic in kidneys of CKD cats with significantly more expression in glomeruli relative to healthy controls. All but one CKD (n=28) cat had cytosolic  $\alpha$ -enolase while membranous protein expression was less frequent (n=16). However, membranous expression was more common in later stages of disease (i.e. Stage III and IV). Immunoglobulin G from the sera of CKD and non-azotemic cats were shown to target recombinant  $\alpha$ -enolase, as well as, cytosolic and membranous protein at approximately 52 kDa by immunoblot. These data indicate that  $\alpha$ -enolase antibodies are commonly found in sera of cats with CKD and are capable of binding endogenous renal proteins. Lastly,  $\alpha$ -enolase protein is overexpressed in glomeruli with decreased expression in injured

renal tubules of cats with CKD. Together this work indicates that anti- $\alpha$ -enolase antibodies are common in cat sera and that renal  $\alpha$ -enolase protein is altered in both the cellular population expression and cellular localization which has potential physiologic and pathologic implications.

## ACKNOWLEDGEMENTS

I would like to take a moment to acknowledge a few individuals to whom this dissertation and the course of my career would not have been possible. I want to say that any successes in this journey are owed entirely to them and any shortcomings are my own. First and foremost thank you to the members of my committee. Dr. Michael Lappin and Dr. Steve Dow my co-advisors, thank you for supporting my graduate efforts from the beginning. The inception and fruition of this work would not have been possible without them. Dr. Colleen Duncan, graduate committee member and amazing pathology residency mentor (I believe I was your first). You have been so positive and encouraging from the beginning of my residency and I am so grateful. I aspire to be more like you as a pathologist. You make pathology fun and pertinent, engaging veterinary student's interest in a field of medicine that is often viewed as perhaps lifeless. Dr. Robert Callan thank you for being committed to this project and offering invaluable advice. Last but certainly not least Dr. Jessica Quimby, the last member to officially join my committee but has served a role of mentor, counsel, and most of all friend for the last five years. Your passion, dedication, and zeal have been the driving force behind this dissertation.

I would like to acknowledge the Morris Animal Foundation and the Center for Companion Animal Studies for financially supporting the  $\alpha$ -enolase portion of my research. Other individuals that have been behind the scenes that I would like to thank. Dr. Rachel Cianciolo, nephropathologist extraordinaire. You have taught me a great deal about the kidney and you are an incredible pathologist and friend. Much gratitude to Dr. Kathy Lunn for her contributions to the uremic gastropathy chapter. Jennifer Hawley, you gave up countless hours of your time to teach me how to be a researcher and you were always available for questions, thank you. Much of the immunohistochemical and histochemical work in this dissertation is

owed to the hard work of Todd Bass and other members of the histopathology lab of the CSU Diagnostic Medical Center. For the encouragement and support by the members of the CSU pathology department, in particular Dr. EJ Ehrhart, Dr. Mason, Dr. Karen Fox, and Dr. Brett Webb—thank you. On a more personal note to my husband Dr. Tim Kuhnmuensch, thank you, thank you, thank you for all that you are. Lastly, to the cats that donated their kidneys and lives to further our understanding of feline chronic kidney disease. Each one has (had) a name, a home and a loving family. For your sacrifice I am grateful and dedicate this to them:

Amaretto	Dakoda	Katie	Peanut	Winston
Anais	Duster	Keiko	Pretty Girl	Padme
Athelia	Emily	Lucky	Robbie	Darcy
Beethoven	Ginger	Mara	Sammy	Yang
Bigara	Gus	Mathilda	Skitch	Sierra
Blackie	Hopey	Mia	Stash	Angela
Buzz	Jean Tom	Mussette	Tanqueray	Bingley



## TABLE OF CONTENTS

ABSTRACT.....	ii
ACKNOWLEDGEMENTS.....	vi
LIST OF TABLES.....	xii
LIST OF FIGURES.....	xiii
LIST OF PERTINENT PUBLICATIONS.....	xv
CHAPTER 1: LITERATURE REVIEW.....	1
1.1 Feline chronic kidney disease.....	1
1.1.1 Prevalence of feline chronic kidney disease.....	1
1.1.2 Pathology of feline chronic kidney disease.....	1
1.1.3 Renal fibrosis.....	2
1.1.4 Staging of feline chronic kidney disease.....	3
1.2 Uremic gastropathy.....	4
1.2.1 The uremic syndrome.....	4
1.2.2 Pathology of uremic gastropathy.....	5
1.2.2 Gastrin and uremic gastropathy.....	5
1.3 Alpha-enolase autoantibodies and kidney disease.....	6
1.3.1 Renal immunity.....	6
1.3.2 Alpha-enolase: a target for autoantibodies.....	8
1.3.3 Alpha-enolase autoantibodies in the cat.....	10
1.4 Alpha-enolase in health and disease.....	13
1.4.1 Alpha-enolase the glycolytic enzyme.....	13
1.4.2 Alpha-enolase protein in disease.....	13
1.5 Membranous cellular localization of alpha-enolase.....	16
1.5.1 Surface expression in autoimmune disease.....	16
1.5.2 Alpha-enolase: plasminogen receptor.....	17
REFERENCES.....	18
CHAPTER 2: RESEARCH OVERVIEW AND SPECIFIC AIMS.....	27
2.1 Research Overview.....	27
2.2 Specific Aim 1 (Chapter 3: Histopathology of CKD IRIS stages).....	27
2.3 Specific Aim 2 (Chapter 4: Uremic gastropathy).....	28
2.4 Specific Aim 3 (Chapter 5: Alpha-enolase antibodies in serum).....	29

2.5 Specific Aim 4 (Chapter 6: Renal $\alpha$ -enolase protein expression) .....	31
2.6 Specific Aim 5 (Chapter 7: Cellular expression and antigenicity of renal proteins) .....	31
REFERENCES .....	33
<b>CHAPTER 3: A COMPARISON OF BIOCHEMICAL AND HISTOPATHOLOGIC STAGING IN CATS WITH CHRONIC KIDNEY DISEASE .....</b>	<b>37</b>
3.1 Chapter Summary .....	37
3.2 Introduction.....	37
3.3 Materials and Methods.....	39
3.3.1 Case Selection .....	39
3.3.2 Clinicopathologic Data.....	39
3.3.3 Histopathology.....	40
3.3.4 Statistical Analysis.....	43
3.4 Results.....	43
3.4.1 Signalment.....	43
3.4.2 Histopathology.....	45
3.4.3 Clinicopathologic Data.....	59
3.5 Discussion.....	61
REFERENCES .....	69
<b>CHAPTER 4: RELATIONSHIP BETWEEN SERUM CREATININE, SERUM GASTRIN, CALCIUM- PHOSPHORUS PRODUCT AND UREMIC GASTROPATHY IN CATS WITH CHRONIC KIDNEY DISEASE .....</b>	<b>72</b>
4.1 Chapter Summary .....	72
4.2 Introduction.....	73
4.3 Material and Methods .....	74
4.3.1 Animals .....	74
4.3.2 Clinicopathologic Data.....	76
4.3.3 Gastrin Assay .....	76
4.3.4 Gross and Histopathologic Evaluation.....	77
4.3.5 Statistical Analysis .....	78
4.4 Results.....	80
4.4.1 Animals .....	80
4.4.2 Clinicopathological Data.....	80
4.4.3 Histopathology.....	84
4.5 Discussion.....	91

REFERENCES .....	95
CHAPTER 5: IDENTIFICATION AND QUANTIFICATION OF ANTI- $\alpha$ -ENOLASE ANTIBODIES IN SERA OF CATS WITH CHRONIC KIDNEY DISEASE AND IMMUNOPRECIPITATION OF ENDOGENOUS RENAL PROTEINS .....	97
5.1 Chapter Summary .....	97
5.2 Introduction.....	98
5.3 Methods and Materials.....	99
5.3.1 <i>Samples</i> .....	99
5.3.2 <i>Clinicopathologic Data</i> .....	99
5.3.3 <i>Western blot Immunoassay</i> .....	100
5.3.4 <i>Enzyme-linked immunosorbent assay (ELISA)</i> .....	101
5.3.5 <i>Immunoprecipitation (IP)</i> .....	101
5.3.6 <i>Mass Spectrometry</i> .....	102
5.3.7 <i>Statistics</i> .....	103
5.4 Results.....	104
5.4.1 <i>Samples</i> .....	104
5.4.2 <i>Western Blot Immunoassay</i> .....	104
5.4.3 <i>ELISA</i> .....	106
5.4.4 <i>Immunoprecipitation (IP) and Mass Spectrometry</i> .....	110
5.5 Discussion.....	111
REFERENCES .....	114
CHAPTER 6: QUANTIFICATION OF RENAL $\alpha$ -ENOLASE IN FELINE CHRONIC KIDNEY DISEASE .....	116
6.1 Chapter Summary .....	116
6.2 Introduction.....	117
6.3 Methods and Materials.....	118
6.3.1 <i>Samples</i> .....	118
6.3.2 <i>Clinicopathologic Data</i> .....	118
6.3.3 <i>Immunohistochemistry</i> .....	119
6.3.4 <i>Statistics</i> .....	120
6.4 Results.....	121
6.4.1 <i>Signalment and Clinicopathologic Data</i> .....	121
6.4.2 <i>Immunohistochemistry</i> .....	121
6.5 Discussion.....	129

REFERENCES .....	131
CHAPTER 7: CELLULAR LOCALIZATION OF RENAL ALPHA-ENOLASE .....	134
7.1 Chapter Summary .....	134
7.2 Introduction.....	134
7.3 Material and Methods .....	136
7.3.1 <i>Samples</i> .....	136
7.3.2 <i>Subcellular fractionation</i> .....	136
7.3.3 <i>Affinity chromatography</i> .....	138
7.4 Results.....	138
7.4.1 <i>Subcellular fractionation</i> .....	138
7.4.2 <i>Affinity chromatography</i> .....	142
7.5 Discussion.....	143
REFERENCES .....	146
CHAPTER 8: CONCLUDING REMARKS.....	148
8.1 Significance of Work .....	148
8.2 Specific Aim 1 (Chapter 3: Histopathology of CKD IRIS stages) .....	148
8.3 Specific Aim 2 (Chapter 4: Uremic gastropathy) .....	149
8.4 Specific Aim 3 (Chapter 5: Alpha-enolase antibodies in serum and endogenous renal targets) ....	150
8.5 Specific Aim 4 (Chapter 6: Renal $\alpha$ -enolase protein expression) .....	151
8.6 Specific Aim 5 (Chapter 7: Cellular localization of $\alpha$ -enolase).....	153
REFERENCES .....	154

## LIST OF TABLES

### Chapter 3

Table 3.1	Scoring schematic for dichotomous and semi-quantitative histologic variables	42
Table 3.2	Clinical data for controls and CKD cats by stage	44
Table 3.3	Results of dichotomous and continuous histologic variables	46
Table 3.4	Results of categorical histologic variables	47

### Chapter 4

Table 4.1	Scoring system for gastric and renal lesions	79
Table 4.2	Summary of clinicopathologic data in control and CKD cats	82
Table 4.3	Summary of gastric lesions in control and CKD cats	86
Table 4.4	Summary of renal lesions in control and CKD cats	90

### Chapter 5

Table 5.1	Mean absorbance and calculated %ELISA results of $\alpha$ -enolase ELISA	106
-----------	--	-----

### Chapter 6

Table 6.1	Summary of immunoreactivity scores in non-azotemic control and CKD cats	122
Table 6.2	Summary of immunoreactivity scores in CKD cats grouped by IRIS stage	127

## LIST OF FIGURES

### Chapter 1

Figure 1.1	Immunofluorescence of glomerular $\alpha$ -enolase	9
Figure 1.2	Biopsy from a cat hyperinoculated with CRFK lysates	12
Figure 1.3	Immunohistochemistry for $\alpha$ -enolase from a renal biopsy	14

### Chapter 3

Figure 3.1	Graph of categorical histologic variables	45
Figure 3.2	Relative frequencies of 4 different patterns of interstitial inflammation	48
Figure 3.3	Relative frequencies of 4 different patterns of cortical scarring	49
Figure 3.4	Fibrointimal hyperplasia of an arcuate artery, cat, kidney	52
Figure 3.5	Thrombotic microangiopathy, glomerulus, kidney, cat	55
Figure 3.6	Scarring in chronic kidney disease, kidney, cat	57

### Chapter 4

Figure 4.1	Calcium x phosphorus product (CPP) is correlated to disease severity	83
Figure 4.2	Serum gastrin levels of CKD cats	83
Figure 4.3	Gastric glandular atrophy and fibrosis scores	85
Figure 4.4	Gastric fibrosis and mineralization in stomach of cats with CKD	87
Figure 4.5	Gastric mineralization scores	88

### Chapter 5

Figure 5.1	Alpha-enolase western blot with cat serum	105
Figure 5.2	Mean absorbance for $\alpha$ -enolase ELISA	107
Figure 5.3	%ELISA values for $\alpha$ -enolase	107
Figure 5.4	Mean absorbance for $\alpha$ -enolase ELISA by IRIS stage	107
Figure 5.5	%ELISA for $\alpha$ -enolase by IRIS stage	107
Figure 5.6	Spearman correlation of mean absorbance and creatinine for CKD cats	109
Figure 5.7	Spearman correlation of %ELISA and serum creatinine for CKD cats	109
Figure 5.8	Mean absorbance for $\alpha$ -enolase ELISA grouped by western blot results	109
Figure 5.9	%ELISA for $\alpha$ -enolase grouped by western blot results	109
Figure 5.10	Mean absorbance for $\alpha$ -enolase excluding western blot negative cats	110
Figure 5.11	%ELISA for $\alpha$ -enolase by excluding western blot negative cats	110

### Chapter 6

Figure 6.1	Mean immunoreactivity scores for hepatocytes of healthy controls	121
Figure 6.2	Alpha-enolase immunohistochemistry of the liver	121
Figure 6.3	Mean immunoreactivity scores for glomeruli and tubules	123
Figure 6.4	Alpha-enolase immunohistochemistry of the kidney in a healthy control cat	124
Figure 6.5	Alpha-enolase immunohistochemistry of the kidney in a CKD cat	124
Figure 6.6	Mean immunoreactivity scores for glomeruli and tubules by IRIS stage	127

## **Chapter 7**

Figure 7.1	Western blots of renal cortical cytosolic and membrane fractions confirmed by GAPDH and Na-K-ATPase monoclonal antibody	139
Figure 7.2	Western blot of CKD cytosolic fractions	139
Figure 7.3	Western blot of CKD membrane fractions from CKD cats	140
Figure 7.4	Prevalence of membranous expression of $\alpha$ -enolase by IRIS stage	140
Figure 7.5	Western blot of feline renal subcellular fractions with CKD IgG	142

## LIST OF PERTINENT PUBLICATIONS

McLeland S, Cianciolo R, Duncan C, et al. A Comparison of Biochemical and Histopathologic Staging in Cats with Chronic Kidney Disease. Vet Path E-pub 2014.

McLeland S, Lunn K, Duncan C, et al. Relationship Between Serum Creatinine, Serum Gastrin, Calcium-phosphorus Product and Uremic Gastropathy in Cats with Chronic Kidney Disease. J Vet Int Med 2014; 28(3):827-837.



## CHAPTER 1: LITERATURE REVIEW

The total production or output of a factory may fall for one of two reasons. The team of workers may become slack or may not have enough to do, like the nephrons in heart failure; or the team may have been seriously depleted in numbers owing to illness, the few remaining workers actually putting in overtime in an unsuccessful attempt to compensate for the absence of their fellows. The latter is the state of affairs in experimental renal failure, as our obliging rats have clearly demonstrated, and there is good reason to believe that it is the state of affairs also in chronic renal failure in the human subject.<sup>2</sup>

### **1.1 Feline chronic kidney disease**

#### *1.1.1 Prevalence of feline chronic kidney disease*

Chronic kidney disease (CKD) is associated with decreased survival and considerable morbidity in felines.<sup>5</sup> Reports on prevalence vary but it is the consensus that aged cats are particularly affected.<sup>6-8</sup> Within the general feline population prevalence of CKD is 1%-3%.<sup>9</sup> According to the State of Health Report issued by Banfield Pet Hospitals 160 per 10,000 feline patients seen annually have kidney disease which has increased in incidence 15% since 2007.<sup>10</sup> Lastly in a retrospective study of the co-prevalence of degenerative joint disease and CKD as many as 50% of study cats without and 68% of cats with degenerative joint disease had CKD.<sup>6</sup>

#### *1.1.2 Pathology of feline chronic kidney disease*

Chronic kidney disease is characterized by a reduction of structural and functional components resulting in retention of metabolic waste products, decreased urinary concentrating ability, and variable electrolyte and acid-base imbalances.<sup>5,7,8</sup> The most frequent morphologic diagnosis is chronic tubulointerstitial nephritis.<sup>7</sup> Other infrequent primary renal diseases that will cause renal dysfunction include of lymphosarcoma, amyloidosis, chronic pyelonephritis, and polycystic kidney disease.<sup>7</sup> CKD is progressive which in part is due to interstitial fibrosis--a common end

point that correlates with a decline of renal function.<sup>11-13</sup> The tubulointerstitium in particular appears to be the focus of renal injury in feline CKD. In addition to interstitial fibrosis, mononuclear inflammation and tubular atrophy are typical morphologic changes in chronic tubulointerstitial renal disease.<sup>14, 15</sup> In a histomorphologic study of felines in the United Kingdom interstitial fibrosis was the best histologic correlate to azotemia, hyperphosphatemia, and anemia in cats with CKD.<sup>12</sup> Additionally, fibrosis scores correlated with interstitial inflammation and glomerular obsolescence.<sup>12</sup> Primary glomerular lesions in cats with CKD are uncommon.<sup>7, 8, 12</sup>

### *1.1.3 Renal fibrosis*

Renal fibrosis, or scarring, is the accumulation of extracellular matrix which irreversibly replaces normal tissue.<sup>11, 16</sup> Interstitial fibroblasts, the culprit of fibroplasia, can be derived from resident fibroblasts, migration of pericytes, recruitment of mesenchymal cells from circulation, and transformation of tubular epithelial or endothelial cells.<sup>11</sup> Production of extracellular matrix by fibroblasts is regulated by various growth factors, leukocyte interactions, and physiologic stimuli.<sup>16, 17</sup> Transforming growth factor  $\beta$  (TGF- $\beta$ ) is an important renal pro-fibrotic mediator and is up-regulated in all mammalian chronic kidney diseases.<sup>16</sup> Pro-fibrotic effects include induction of various cells to a myofibroblast phenotype, a key event in initiation and progression of fibrosis; stimulation of extracellular matrix (ECM) gene transcription, and activation of other pro-fibrotic cytokines.<sup>18-21</sup>

The renin-angiotensin-aldosterone system (RAAS) is crucial for renal homeostasis and is up-regulated in CKD.<sup>16</sup> The individual members of the RAAS system have direct pro-fibrotic effects. Angiotensin, aldosterone and renin are capable of up-regulating TGF- $\beta$  expression along with other pro-inflammatory and pro-fibrotic mediators.<sup>16</sup> Expression of transglutaminase 2

(TG-2), an enzyme that stabilizes the extracellular matrix is associated with renal fibrosis in cats with CKD as well.<sup>22</sup>

A few other factors that contribute to renal injury and fibrosis include proteinuria, interstitial inflammation, and hypoxia. Protein can be directly toxic to tubular epithelial cells as well as contribute to epithelial to mesenchymal transition of tubular epithelial cells.<sup>16, 23, 24</sup> Inflammatory cells produce pro-fibrotic growth factors necessary for propagation of fibrosis.<sup>16</sup> Hypoxia promotes fibrogenesis by several mechanisms. A few of these mechanisms include epithelial to mesenchymal transition, induction of pro-fibrotic mediators by fibroblasts, decreased matrix turnover and increased matrix production.<sup>25, 26</sup>

In conclusion, there are numerous factors that contribute to renal fibrosis, a few which were discussed here. Fibrosis is considered irreversible, is a common end point of renal injury, and is progressive. The importance of understanding factors that contribute to initiation and propagation of fibrosis in the cat kidney could have preventative and therapeutic implications.

#### *1.1.4 Staging of feline chronic kidney disease*

The International Renal Interest Society was originally organized by veterinarians with an interest in nephrology at the 8<sup>th</sup> Annual Congress of the European Society of Veterinary Internal Medicine in Vienna, Austria in 1998. It is supported by Novartis Animal Health that provides financial and organizational assistance. The primary objective of this group was to establish a set of guidelines to aid the clinician in diagnosis and treatment of kidney disease in dogs and cats. Stages are determined by two serial serum creatinine concentrations measured in a stable patient. Stage I cats are not azotemic but at risk due to kidney abnormalities such as decreased urine specific gravity, renal proteinuria, or abnormal appearance on ultrasound or renal biopsy. Stage II cats have serum creatinine concentrations of 1.6-2.8 mg/dl, 2.8-5.0 mg/dl for Stage III,

and >5.0 mg/dl for Stage IV cats. In addition, renal disease is sub-staged based on presence of proteinuria and hypertension which increases the risk of additional organ damage.<sup>27</sup>

A recent study evaluating survival of CKD cats based on IRIS stage was reported.<sup>28</sup> Overall median survival for cats with kidney disease was 771 days from the time of diagnosis and survival was significantly less with increasing stage. For cats with serum creatinine concentrations of 2.3-2.8 mg/dl, which lies within the upper half of the defined Stage II by IRIS (i.e. Stage IIb), median survival was 1,511 days. Stage III cats had a median survival of 778 days while Stage IV cats median survival was only 103 days from the time of diagnosis. Clinicopathologic parameters were evaluated as risk factors for survival. Age at the time of diagnosis, albumin, blood urea nitrogen (BUN), creatinine, calcium, bicarbonate, potassium, and hematocrit were not predictive of survival. Hyperphosphatemia was the only variable identified as a risk factor. For every unit increase in phosphorus the risk for death increased 11.8% in cats with CKD.<sup>28</sup> These data and IRIS scoring for cats with kidney disease can aid the clinician in communicating potential risks and prognosis to pet owners.

## **1.2 Uremic gastropathy**

### *1.2.1 The uremic syndrome*

Uremia, a clinical syndrome of chronic kidney disease, is due to retention of toxic metabolic byproducts.<sup>15</sup> It manifests clinically in a variety of signs including weight loss, vomiting, inappetance, and anorexia.<sup>9, 29-31</sup> Clinical symptoms are thought to be related to gastrointestinal lesions and the central effects of metabolic waste products.<sup>32</sup> Toxins of uremia include products of protein catabolism and numerous other low, medium and large molecular weight proteins.<sup>15</sup> Theories on the mechanisms of injury include small molecular weight proteins acting on plasma membrane adenyl cyclase of gastric epithelial cells, generation of ammonia by gastric bacteria,

and altered blood flow with resultant local tissue hypoxia.<sup>33-35</sup> Treatment in feline uremia is typically symptomatic and largely based on pathology in other species.

### *1.2.2 Pathology of uremic gastropathy*

Uremic gastritis was first described in 1934 from autopsies in 135 uremic human patients; lesions varied from mild edema to hemorrhage, ulceration, and necrosis.<sup>36</sup> In humans complications of uremia such as gastritis, ulceration, and hemorrhage are common.<sup>37</sup> A descriptive study of gastric pathology in a small group of uremic dogs revealed marked lesions.<sup>33</sup> Half of the uremic dogs (n=2) had grossly identifiable lesion of the gastric mucosa in the fundus and body characterized by hemorrhage and ulceration.<sup>33</sup> The cardia, antrum, and pylorus were spared.<sup>33</sup> Histologically all uremic dogs were affected by lesions in the lamina propria, gastric glands, and submucosal vessels. Vascular lesions of degeneration, necrosis, and mineralization were present with variable severity in all uremic dogs. In addition, granular mineralization was present in the mucosa of uremic dogs.<sup>33</sup> In a more recent study of gastric histopathologic features in uremic dogs, common lesions included edema, mineralization, glandular atrophy and vasculopathy.<sup>38</sup> In this study lesions were present in 79% of dogs. Of the dogs, 14% had evidence of gastric mucosal necrosis.<sup>38</sup> Similar histopathologic studies have not been done in cats despite the high prevalence of renal disease in this species. Studies of toxin ingestion such as Easter lily and melamine and cyanuric acid which resulted in renal failure were not associated with gastric ulceration.<sup>39,40</sup>

### *1.2.2 Gastrin and uremic gastropathy*

Gastrin is a hormone that stimulates the production of hydrochloric acid by gastric parietal cells in response to stomach distension or the presence of proteins.<sup>41,42</sup> Its release is under negative feedback regulation and thus is not secreted in the presence of acid in health. In humans and

dogs, gastrin is excreted by the kidneys, and it is hypothesized that as renal function declines, hypergastrinemia develops, which could result in gastric hyperacidity.<sup>43</sup> Hyperacidity can result in local tissue injury in the stomach; however, this appears to be an inconsistent finding.<sup>44</sup> Additional factors that potentially contribute to gastric lesions are thought to be the result of delayed gastric emptying and *Helicobacter pylori* infection.<sup>45-47</sup> Gastric lesions have been reported in cats with hypergastrinemia due to gastrin-secreting tumors but the relationship of hypergastrinemia as an etiology for gastric lesions or gastrointestinal symptoms in feline CKD has not been evaluated.<sup>48</sup>

### **1.3 Alpha-enolase autoantibodies and kidney disease**

#### *1.3.1 Renal immunity*

Resident leukocytes of the kidney include dendritic cells, macrophages, and lesser number of lymphocytes and mast cells.<sup>49, 50</sup> Fibroblasts and dendritic cells are the most abundant cell type in the cortical and outer medullary interstitium.<sup>49</sup> Low molecular weight proteins passing through the glomerular filtration barrier concentrate in proximal tubules where they are reabsorbed. Some proteins pass through tubules into the interstitium and are taken up by resident dendritic cells. Interstitial dendritic cells can be exposed to 10-fold greater antigen levels in the kidney than any other tissue.<sup>50</sup> Dendritic cells are largely responsible for antigen processing and presenting to regional lymph nodes and thus are a key player in immune tolerance.<sup>50, 51</sup> Additional functions include regulation of effector cells and production of pro-inflammatory cytokines (e.g. TNF) during renal injury.<sup>50, 52-54</sup> Renal cortical macrophages are scarce but are associated with large vessels and are abundant in the renal pelvis.<sup>49</sup> Macrophages function in tissue repair by removal of apoptotic cellular debris and production of growth factors as well as controlling infectious agents via phagocytosis and production of pro-inflammatory cytokines (IL-

1 $\beta$ , IL-6, and TNF).<sup>52, 53, 55</sup> Resident lymphocytes are present in low numbers while mast cells contribute to inflammation in some glomerulonephritides.<sup>50</sup>

The intrinsic structural and functional properties of the kidney make it particularly susceptible to injury. The pattern of renal injury is largely influenced by the location and duration of the inflammatory stimulus.<sup>50</sup> For example, immune complex deposition in glomeruli results in glomerulonephritis while ischemic, toxic, and obstructive etiologies will result in tubulointerstitial injury.<sup>50</sup> These entities are not mutually exclusive and glomerulonephritis can lead to tubulointerstitial disease by various mechanisms such as injury to podocytes and other extracapillary components; ischemia secondary to post-glomerular capillary destruction; and tubular protein overload.<sup>13, 50, 56-59</sup>

Autoimmune diseases are characterized by an adaptive immune response to self-antigen. The inciting trigger or target of said response is not entirely eliminated and thus leads to chronic inflammation and ultimately tissue injury.<sup>60, 61</sup> Pathogenesis of autoimmunity, in general, is typical of any immune responses. Either directly cytotoxic by activation of T lymphocytes or indirectly via initiation of humoral immunity by B lymphocytes.<sup>60, 62</sup> Tolerance to self-antigens is established in the thymus by elimination of self-reactive T cells. However, peptides with low affinity binding to T cell receptors are not as effective at driving this negative selection process.<sup>60</sup> Auto-reactive antibodies just like any other antibody are capable of forming immune complexes in circulation or react directly to tissue specific antigens *in situ*.<sup>63</sup> The kidney is intrinsically susceptible to immune mediated injury by virtue of its structural composition. Immune complex deposition leads to complement fixation, leukocyte recruitment and inflammation of glomeruli and tubules.<sup>63-67</sup>

### 1.3.2 Alpha-enolase: a target for autoantibodies

Autoimmune disease can manifest systemically or be directed towards a specific organ. In systemic autoimmune diseases, multiple body systems are affected. Such is the case in systemic lupus erythematosus (SLE) in which several autoantibodies have been identified and typically target abundantly and ubiquitously expressed antigens.<sup>60, 68</sup> However, some autoantibodies can be non-pathogenic and auto-reactive antibodies are present in healthy individuals.<sup>3, 69-71</sup> The pathogenesis of antibody-mediated nephritis occurs by either deposition of circulating immune complexes or *in situ* binding of autoantibodies to self-antigen.<sup>3</sup> Ultimately immune complexes will activate complement and recruit inflammatory cells leading to inflammation and tissue injury.

Anti- $\alpha$ -enolase antibodies have been identified in a number of autoimmune diseases.<sup>72</sup> These antibodies were first described in patients with systemic rheumatic diseases a few decades ago.<sup>73</sup> Currently anti- $\alpha$ -enolase have been reported in patients suffering from systemic lupus erythematosus, mixed cryoglobulinemia, systemic sclerosis, Behcet's disease, and lymphocytic hypophysitis to name a few.<sup>74-79</sup> Conversely, anti- $\alpha$ -enolase antibodies can also be found in healthy individuals with reports of prevalence ranging from 0-6% which may raise doubt as to the significance of this particular autoantibody.<sup>70, 72, 74, 79-82</sup> However, in SLE and mixed cryoglobulinemia,  $\alpha$ -enolase antibodies were associated with active nephritis with declining antibody levels after therapeutic commencement.<sup>75-77, 83</sup> Furthermore, IgG and  $\alpha$ -enolase were co-localized within glomeruli of patients with membranous glomerulonephritis and lupus nephritis by immunofluorescence (Figure 1.1).<sup>1, 83</sup>



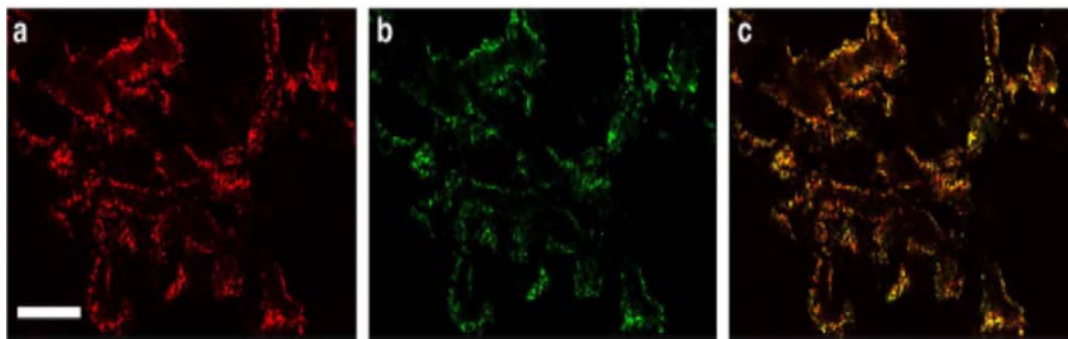


Figure 1.1 Immunofluorescence of glomerular  $\alpha$ -enolase (a) and IgG<sub>4</sub> (b) co-localized (merged, c) in membranous glomerulonephritis. Scale bar=20  $\mu$ m, x630. Adapted from “Direct characterization of target podocyte antigens and auto-antibodies in human membranous glomerulonephritis: Alfa-enolase and borderline antigens.” M. Bruschi, 2011, *J Proteomics*, 74(10), 2008-2017. Copyright by Elsevier. Adapted with permission. <sup>1</sup>

The reactivity of autoantibodies to target antigens may give additional clues to the variability of antibody pathogenicity in individuals. Patients with cancer-associated retinopathy syndrome, (CAR) a progressive retinal degenerative disease, develop anti-enolase antibodies. Epitope mapping of recombinant protein and anti- $\alpha$ -enolase sera from healthy and CAR patients revealed 3 common binding regions with an additional epitope unique to CAR patients.<sup>84</sup> In addition, antibodies in CAR sera had cytotoxic effects on *in vitro* retinal cells not observed in healthy controls. This suggests that not all autoantibodies are equivalent and that specific epitope recognition may confer pathogenicity.

In addition to autoimmune diseases,  $\alpha$ -enolase antibodies have been associated with few infectious diseases. Alpha-enolase antibodies were found in 99% of children that presented for *Streptococcus pneumoniae* otitis media.<sup>85</sup> Anti- $\alpha$ -enolase antibodies limit tissue invasion by *Streptococcus pyogenes* and is a major cell surface protein of group A *Streptococci*.<sup>86,87</sup> It is

likely that the homologous nature of  $\alpha$ -enolase between eukaryotes and prokaryotes contributes to the cross reactivity of antibodies via molecular mimicry.<sup>61, 68, 72, 85</sup>

### *1.3.3 Alpha-enolase autoantibodies in the cat*

Crandell Rees Feline Kidney (CRFK) cell lysate was established five decades ago as the first feline cell line to successfully be maintained in continuous culture.<sup>88</sup> CRFK cell lysates were derived from the renal cortex of a young domestic cat and morphologically described in culture as “epithelial-like”.<sup>88</sup> Designed for feline viral research, CRFK cells are susceptible to feline picornaviruses, reovirus, panleukopenia, and herpesvirus 1 which makes them ideal for the manufacturing of the core, prophylactic vaccine used routinely to immunize cats against feline herpesvirus 1 (rhinotracheitis), calicivirus, and panleukopenia virus (FVRCP).<sup>88-91</sup> Since the establishment of CRFK cells for replication of feline viruses other cell lines have been explored and utilized for research and vaccine purposes.<sup>89, 92</sup> Exclusion of all cellular constituents or proteins from the purification of viruses used in vaccines is improbable; therefore, cats may be exposed repeatedly to feline cellular antigens over the course of a lifetime from the administration of any parenteral vaccine that are developed in feline cell culture.

To determine if vaccine or the cell lysate could induce antibodies or renal injury, cats were hyperinoculated with FVRCP vaccine or CRFK cell lysates.<sup>91</sup> A total of 4 FVRCP vaccines or 11 lysate inocula at 10  $\mu$ g, 50  $\mu$ g, or 50  $\mu$ g with aluminum adjuvant were administered to a number of individual cats over 50 weeks. Serial serum samples were monitored for antibodies against CRFK or feline renal cell (FRC) lysates using tissues from specific pathogen free (SPF) cats. All cats that were hyperinoculated with cell lysates developed antibodies targeted against cell lysate (CRFK and FRC). Five of the 6 cats that were administered parenteral FVRCP vaccine developed antibodies against CRFK lysate with all

developing antibodies against FRC lysate antigen. Cats that were administered vaccine subcutaneously had significantly higher levels of antibodies than cats that were administered an intranasal vaccine. CRFK antigens recognized by vaccine induced antibodies were determined by immunoassays, affinity chromatography, and proteomics from cats administered FVRCP vaccination or CRFK lysates.<sup>93</sup> Sera from the majority (8/14) of cats from either inoculation group had anti- $\alpha$ -enolase antibodies. Post-inoculation sera from cats administered FVRCP vaccines parenterally had significantly greater amounts of CRFK and  $\alpha$ -enolase antibodies by enzyme-linked immunosorbent assay (ELISA).<sup>93</sup> In a separate study, azotemic cats with naturally occurring renal disease had significantly higher levels of  $\alpha$ -enolase antibodies than non-azotemic cats.<sup>94</sup>

Study cats that were hyperinoculated with either vaccine or cell lysates were biopsied. Two cats, 1 that received CRFK lysate and another parenteral FVRCP vaccine, developed mild interstitial inflammation by the end of the study.<sup>91</sup> A year later, cat's hyperinoculated with CRFK lysate were administered a booster and then biopsied 2 weeks later. Of these 6 cats, 3 developed interstitial nephritis (Figure 1.2).<sup>4</sup> Glomerular lesions or ultrastructural immune complexes were absent. Lesions present in the biopsies of these 3 cats are similar to the histologic changes encountered in feline CKD which includes interstitial mononuclear inflammation and tubular injury with relative sparing of glomeruli typical of chronic interstitial nephritis.<sup>7, 8, 15, 95</sup> This pattern of injury however is not specific to a particular cause but rather a common end result of multiple etiologies.<sup>15</sup> In a majority of cats with CKD and the 3 hyperinoculated cats with interstitial nephritis in the aforementioned study; primary glomerular lesions, or ultrastructural evidence of immune-complexes in the latter, were not present. Based on these observations an immune-complex mediated pathogenesis, such as with lupus nephritis,

is unlikely in the hyperinoculated cats. However, induction of auto-antibodies by hyperinoculation with parenteral vaccination or cell lysate; and the significant levels of  $\alpha$ -enolase antibodies in azotemic cats are suggestive of a role of these antibodies in feline renal disease and thus should be further investigated.

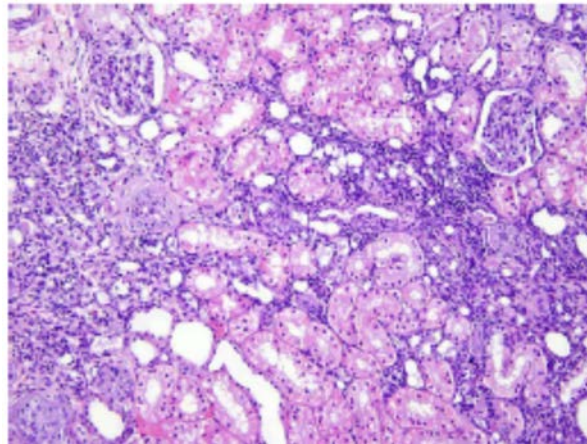


Figure 1.2 Biopsy from a cat hyperinoculated with CRFK lysates. Marked mononuclear interstitial inflammation with tubular loss. Hematoxylin and eosin, 20X. Adapted from “Interstitial nephritis in cats inoculated with Crandell Rees feline kidney cell lysates” M. Lappin, 2006, *J Feline Med Surg*, 8(5), 353-356. Copyright by SAGE publishing. Adapted with permission<sup>4</sup>

## 1.4 Alpha-enolase in health and disease

### 1.4.1 Alpha-enolase the glycolytic enzyme

Alpha-enolase (2-phospho-D-glycerate hydrolyase) is a metal-ion-activated enzyme that catalyzes the dehydration of 2-phospho-D-glycerate to phosphoenolpyruvate in the catabolic direction of the Emden Mayerhoff-Parnas glycolytic pathway.<sup>87, 96</sup> Enolase is capable of catalyzing the reverse reaction--hydrolysis of phosphoenolpyruvate--during gluconeogenesis (anabolic pathway). Six divalent metal ions can activate this enzyme; however magnesium is its natural cofactor.<sup>97, 98</sup>

An abundantly expressed cytosolic protein, enolase exists as 3 isoenzymes:  $\alpha$ -,  $\beta$ -, and  $\gamma$ -isoforms.<sup>99-102</sup> The  $\alpha$ -isoform is found in a variety of tissues,  $\beta$ -isoform is almost exclusively found in muscle, and  $\gamma$ -isoform is primary found in neural and neuroendocrine tissues. Three independent genetic loci encode for each individual isoenzyme.<sup>87, 99-103</sup> All enolase are made up of 2 identical subunits (dimer) and have a molecular weight of 82,000-100,000 Da.<sup>87</sup> The amino acid sequence of enolase is highly conserved across species.<sup>87</sup> Gene expression of enolase is variable depending on the pathophysiologic, metabolic, or developmental conditions of the cell and therefore not considered a housekeeping gene.<sup>104</sup> *ENO1* encodes for  $\alpha$ -enolase in addition to the DNA-binding tumor suppressor protein, c-myc binding protein (MBP-1). MBP-1 is shorter, 37 kDa as opposed to  $\alpha$ -enolase which is 48 kDa, and is mostly located within the nucleus.<sup>105</sup>

### 1.4.2 Alpha-enolase protein in disease

Alpha-enolase is not restricted to the cytoplasm as a glycolytic enzyme. This protein has been identified in the pathogenesis of several infectious, inflammatory, and neoplastic diseases.<sup>87</sup> Cardiac isoforms are altered during hypertrophy and subject to post-translation modifications in

diabetes.<sup>106, 107</sup> Alpha-enolase can be externalized on the cell surface as a marker for apoptosis or act as a plasminogen receptor on the cell membrane.<sup>108, 109</sup> It promotes tumor cell survival during anaerobic conditions and aids in tumor invasion.<sup>109</sup>

Up regulation in  $\alpha$ -enolase protein expression has been described in several diseases. Renal  $\alpha$ -enolase protein expression was assessed by immunohistochemistry utilizing an anti- $\alpha$ -enolase IgG1 monoclonal antibody purified from immunized BALB/c mice.<sup>3</sup> Renal biopsies from systemic lupus erythematosus (SLE) patients with lupus nephritis and healthy individuals were assessed for protein expression. In healthy controls, alpha-enolase was highly expressed in tubules but absent in glomeruli. In biopsies from patients with lupus nephritis tubular  $\alpha$ -enolase was greater than controls and glomerular expression was up regulated. Mesangial cells, parietal and visceral epithelial cells as well as cellular crescents in glomeruli expressed protein where it was otherwise absent in controls (Figure 1.3).<sup>3</sup>

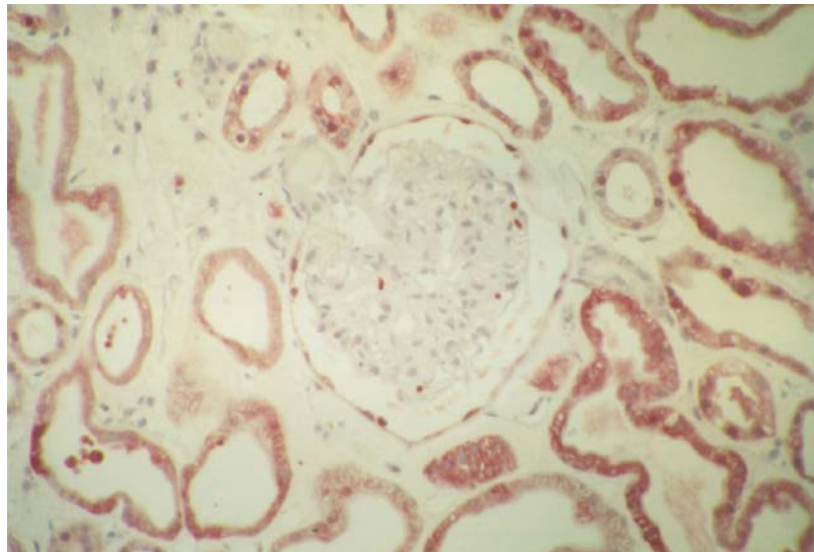


Figure 1.3 Immunohistochemistry for  $\alpha$ -enolase from a renal biopsy from a patient with systemic lupus erythematosus. High expression in tubules and glomeruli, monoclonal mouse  $\alpha$ -enolase antibody. Adapted from “The targets of nephritogenic antibodies in systemic autoimmune disorders” P. Migliorini, 2002, *Autoimmune Rev*,1(3),168-173. Copyright by Elsevier. Adapted with permission.<sup>3</sup>

In a separate immunohistochemical study of renal enolase expression in the tubules of renal adenocarcinoma it was shown that  $\alpha$ -enolase was preferentially expressed.<sup>110</sup> Alpha-enolase was strongly expressed in proximal tubules, collecting ducts, and distal tubules in healthy controls. Protein expression was not found in the loops of Henle. Gamma-enolase was localized to macula densa cells, occasionally in the collecting ducts, distal tubules and Bowman's capsule but not in the proximal tubules. In the medulla,  $\gamma$ -enolase was found in most of loops of Henle and collecting ducts but only a few distal tubules. Both isoforms were localized to the cytoplasm and occasionally the nucleus. Protein concentrations determined by immunoassay were greater for  $\alpha$ -enolase than  $\gamma$ -enolase. Levels of  $\gamma$ -enolase in the medulla were statistically higher than those in the cortex. Both isoforms were greater in renal cell carcinoma cells than controls.<sup>110</sup>

Alpha-enolase protein may also serve as a marker for physiologic stress.<sup>109</sup> Adverse environmental conditions such as elevated temperatures and glucose depletion may induce cellular synthesis of heat shock proteins (HSP) and glucose-regulated proteins (GRP), respectively. In addition endothelial cells exposed to hypoxic conditions *in vitro* can synthesize a distinct set of hypoxia-associated proteins (HAPS; Mr 34, 36, 39, 47, and 56 kDa).<sup>111, 112</sup> This appears unique to endothelial cells as primary cultures of mouse renal tubular epithelial cells did not up regulate any specific proteins during hypoxic conditions. However, a majority of renal tubular cells did not survive to the time point of maximal protein up regulation of other cell types ( $\geq 18$  hours). Endothelial cells appear to be tolerant of hypoxic conditions due to up regulation of HAPs while renal tubular epithelial cells are extremely sensitive.<sup>112</sup> Furthermore, the 47 kDa HAP protein from hypoxic endothelial lysates were isolated and sequenced. Significant identity was found with the glycolytic enzyme enolase (75% homology to human  $\alpha$ -enolase). This

suggests that  $\alpha$ -enolase can function as a hypoxic-associated protein aiding in the survival of endothelial cells during hypoxia.<sup>113</sup>

## **1.5 Membranous cellular localization of alpha-enolase**

### *1.5.1 Surface expression in autoimmune disease*

A feature of systemic autoimmune disorders is production of antibodies specific for antigens which are often highly conserved structures and are frequently enzymes.<sup>114</sup> Alpha-enolase antibodies are present in sera of patients with mixed cryoglobulinemia (MC), SLE, and systemic sclerosis.<sup>3, 74, 114</sup> In patients with SLE and MC the presence of antibodies invariably was associated with active nephritis. Alpha-enolase has been described as a multifunctional protein because of its variable cellular distribution and interaction with other cellular components.<sup>109</sup> In an experiment by Moscato et al. fractionated renal cortical cells were utilized to determine  $\alpha$ -enolase cellular location and assess the interaction of spontaneous and induced anti- $\alpha$ -enolase antibodies.<sup>114</sup> Mouse monoclonal antibodies and antibodies isolated from MC, SLE, and SSC patients bound to membranous  $\alpha$ -enolase by immunoprecipitation and inhibited binding of plasminogen. These data suggests a pathogenic role of anti- $\alpha$ -enolase antibodies in autoimmune disease by interfering with the function of membranous  $\alpha$ -enolase as a plasminogen receptor.

Systemic sclerosis is a connective tissue disorder characterized by excessive fibrosis of organs.<sup>115, 116</sup> A majority of individuals have detectable antinuclear autoantibodies.<sup>115</sup> These autoantibodies are capable of activating fibroblasts *in vitro*.<sup>116</sup> Indirect immunofluorescence with IgG from systemic sclerosis patients (antifibroblast antibodies, AFA) demonstrated significant reactivity to the plasma cell membrane of skin fibroblasts. Fibroblasts exposed to AFA IgG had a dose-dependent up-regulation of cell surface ICAM-1 expression and IL-6 production. In addition AFA IgG up-regulated cytokine gene expression (IL-1 $\alpha$ , IL-1 $\beta$ , and IL-



6). Alpha-enolase was identified as a major target of AFA IgG by immunoblot and ELISA.<sup>115</sup>

These findings show that  $\alpha$ -enolase is expressed on the cell surface of fibroblasts and act at some capacity in cell signaling which may contribute to the fibrotic phenotype in this disease.

### *1.5.2 Alpha-enolase: plasminogen receptor*

Plasminogen receptors are a heterogeneous group of proteins that contain a carboxyl-terminal lysine.<sup>3</sup> It is highly expressed and ubiquitously distributed on various cell types.<sup>3</sup> The importance of  $\alpha$ -enolase as a plasminogen receptor has been determined in several diseases. On the surface of leukocytes, neuronal and endothelial cells  $\alpha$ -enolase can function as a plasminogen receptor.<sup>109, 117-121</sup> Cell membrane expressed  $\alpha$ -enolase is structurally distinct from other enolases despite high sequence similarities which may explain its multifunctionality.<sup>122</sup> As a plasminogen receptor, activation of plasminogen is enhanced and plasmin is protected which ultimately promotes fibrinolysis and degradation of extracellular matrices.<sup>109</sup> In autoimmune disorders resulting in nephritis, such as previously discussed in lupus nephritis patients, autoantibodies target are known to target glomerular  $\alpha$ -enolase.<sup>3, 83</sup> It has been proposed that the mechanism of injury in this disorder is interference of  $\alpha$ -enolase that is functioning on the cell membrane as a plasminogen receptor. Blocking potential plasminogen binding sites would impair fibrinolysis promoting inflammation and tissue injury.<sup>3</sup> Therefore, membranous  $\alpha$ -enolase functioning as a plasminogen receptor could be blocked by autoantibodies and thus contribute to the pathogenesis of renal inflammation.

## REFERENCES

1. Bruschi M, Carnevali ML, Murtas C, et al. Direct characterization of target podocyte antigens and auto-antibodies in human membranous glomerulonephritis: Alfa-enolase and borderline antigens. *J Proteomics* 2011;74(10):2008-2017.
2. Platt R. Structural and functional adaptation in renal failure. *Br Med J* 1952;1(4773):1372-1377.
3. Migliorini P, Pratesi F, Bongiorno F, et al. The targets of nephritogenic antibodies in systemic autoimmune disorders. *Autoimmun Rev* 2002;1(3):168-173.
4. Lappin MR, Basaraba RJ, Jensen WA. Interstitial nephritis in cats inoculated with Crandell Rees feline kidney cell lysates. *J Feline Med Surg* 2006;8(5):353-356.
5. Elliott J, Barber PJ. Feline chronic renal failure: clinical findings in 80 cases diagnosed between 1992 and 1995. *J Small Anim Pract* 1998;39(2):78-85.
6. Marino CL, Lascelles BD, Vaden SL, et al. Prevalence and classification of chronic kidney disease in cats randomly selected from four age groups and in cats recruited for degenerative joint disease studies. *J Feline Med Surg* 2013.
7. DiBartola SP, Rutgers HC, Zack PM, et al. Clinicopathologic findings associated with chronic renal disease in cats: 74 cases (1973-1984). *J Am Vet Med Assoc* 1987;190(9):1196-1202.
8. Lulich J, Osborne C, O'Brien T, et al. Feline renal failure: questions, answers, questions. *Compendium on Continuing Education for the Practicing Veterinarian* 1992;14(2):26.
9. Bartges JW. Chronic kidney disease in dogs and cats. *Vet Clin North Am Small Anim Pract* 2012;42(4):669-692.
10. Banfield Pet Hospital. *State of Pet Health*. 2012. Accessed 5 February 2015. [www.stateofpethealth.com](http://www.stateofpethealth.com).
11. Hewitson TD. Renal tubulointerstitial fibrosis: common but never simple. *Am J Physiol Renal Physiol* 2009;296(6):F1239-1244.
12. Chakrabarti S, Syme HM, Brown CA, et al. Histomorphometry of feline chronic kidney disease and correlation with markers of renal dysfunction. *Vet Pathol* 2013;50(1):147-155.
13. Bohle A, Kressel G, Müller CA, et al. The pathogenesis of chronic renal failure. *Pathol Res Pract* 1989;185(4):421-440.
14. Lucke VM. Renal disease in the domestic cat. *J Pathol Bacteriol* 1968;95(1):67-91.

15. Maxie M, Newman S. Urinary system. In: Maxie M, ed. *Pathology of Domestic Animals*. Vol 2. 5 ed. Philadelphia: Elsevier Saunders; 2007:425-522.
16. Lawson J, Elliott J, Wheeler-Jones C, et al. Renal fibrosis in feline chronic kidney disease: Known mediators and mechanisms of injury. *Vet J* 2015;203(1):18-26.
17. Qi W, Chen X, Poronnik P, et al. The renal cortical fibroblast in renal tubulointerstitial fibrosis. *Int J Biochem Cell Biol* 2006;38(1):1-5.
18. Wu CF, Chiang WC, Lai CF, et al. Transforming growth factor  $\beta$ -1 stimulates profibrotic epithelial signaling to activate pericyte-myofibroblast transition in obstructive kidney fibrosis. *Am J Pathol* 2013;182(1):118-131.
19. Serini G, Bochaton-Piallat ML, Ropraz P, et al. The fibronectin domain ED-A is crucial for myofibroblastic phenotype induction by transforming growth factor-beta1. *J Cell Biol* 1998;142(3):873-881.
20. Border WA, Noble NA. Cytokines in kidney disease: the role of transforming growth factor-beta. *Am J Kidney Dis* 1993;22(1):105-113.
21. Grotendorst G. Connective tissue growth factor: A mediator of TGF-beta action on fibroblasts. *Cytokine and Growth Factor Reviews* 1997;8:9.
22. Sánchez-Lara AC, Elliott J, Syme HM, et al. Feline Chronic Kidney Disease Is Associated With Upregulation of Transglutaminase 2: A Collagen Cross-Linking Enzyme. *Vet Pathol* 2014.
23. Abbate M, Zoja C, Corna D, et al. In progressive nephropathies, overload of tubular cells with filtered proteins translates glomerular permeability dysfunction into cellular signals of interstitial inflammation. *J Am Soc Nephrol* 1998;9(7):1213-1224.
24. Rodríguez-Iturbe B, García García G. The role of tubulointerstitial inflammation in the progression of chronic renal failure. *Nephron Clin Pract* 2010;116(2):81-88.
25. Zell S, Schmitt R, Witting S, et al. Hypoxia Induces Mesenchymal Gene Expression in Renal Tubular Epithelial Cells: An in vitro Model of Kidney Transplant Fibrosis. *Nephron Extra* 2013;3(1):50-58.
26. Norman JT, Clark IM, Garcia PL. Hypoxia promotes fibrogenesis in human renal fibroblasts. *Kidney Int* 2000;58(6):2351-2366.
27. Novartis Animal Health Inc. IRIS staging CKD. <http://www.iris-kidney.com/guidelines/staging.shtml> (2013, accessed 1 April 2015).
28. Boyd LM, Langston C, Thompson K, et al. Survival in cats with naturally occurring chronic kidney disease (2000-2002). *J Vet Intern Med* 2008;22(5):1111-1117.

29. Polzin DJ. Chronic kidney disease in small animals. *Vet Clin North Am Small Anim Pract* 2011;41(1):15-30.
30. Roudebush P, Polzin DJ, Ross SJ, et al. Therapies for feline chronic kidney disease. What is the evidence? *J Feline Med Surg* 2009;11(3):195-210.
31. Polzin DJ, Osborne C, S R. Evidence-based management of chronic kidney disease. *Kirk's Current Veterinary Therapy XIV*. St. Louis, MO: Saunders Elsevier; 2009.
32. Zelnick EB, Goyal RK. Gastrointestinal Manifestations of Chronic Renal Failure. *Seminars in Nephrology* 1981;1:124-136.
33. Cheville N. Uremic Gastropathy in the Dog. *Veterinary Pathology* 1979;16:292-309.
34. Hamet P, Stouder DA, Ginn HE, et al. Studies of the elevated extracellular concentration of cyclic AMP in uremic man. *J Clin Invest* 1975;56(2):339-345.
35. Stanton ME, Bright RM. Gastroduodenal ulceration in dogs. Retrospective study of 43 cases and literature review. *J Vet Intern Med* 1989;3(4):238-244.
36. Jaffe R, Laing, DR. Changes of the Digestive Tract in Uremia. A Pathologic Anatomic Study. *JAMA Internal Medicine* 1934;53(6):851-864.
37. Lazarus H. *Gastrointestinal abnormalities*. Philadelphia: WB Saunders; 2000.
38. Peters RM, Goldstein RE, Erb HN, et al. Histopathologic Features of Canine Uremic Gastropathy: A Retrospective Study. *JVIM* 2005;19:315-320.
39. Cianciolo RE, Bischoff K, Ebel JG, et al. Clinicopathologic, histologic, and toxicologic findings in 70 cats inadvertently exposed to pet food contaminated with melamine and cyanuric acid. *J Am Vet Med Assoc* 2008;233(5):729-737.
40. Rumberiha WK, Francis JA, Fitzgerald SD, et al. A comprehensive study of Easter lily poisoning in cats. *J Vet Diagn Invest* 2004;16(6):527-541.
41. Edkins JS. The chemical mechanism of gastric secretion. *J Physiol* 1906;34(1-2):133-144.
42. Ferrand A, Wang TC. Gastrin and cancer: a review. *Cancer Lett* 2006;238(1):15-29.
43. Goldstein R, Marks S, Kass P, et al. Gastrin concentrations in plasma of cats with chronic renal failure. *JAVMA* 1998;213:826-828.
44. El Ghonaimy E, Barsoum R, Soliman M. Serum gastrin in chronic renal failure: morphological and physiological correlations. *Nephron* 1985;39:86-94.

45. Van Vlem B, Schoonjans R, Vanholder R, et al. Delayed gastric emptying in dyspeptic chronic hemodialysis patients. *Am J Kidney Dis* 2000;36(5):962-968.
46. Al-Mueilo SH. Gastroduodenal lesions and *Helicobacter pylori* infection in hemodialysis patients. *Saudi Med J* 2004;25(8):1010-1014.
47. El Ghonaimy E, Barsoum R, Soliman M, et al. Serum gastrin in chronic renal failure: morphological and physiological correlations. *Nephron* 1985;39(2):86-94.
48. Liptak J, Hunt G, Barrs V, et al. Gastroduodenal ulceration in cats: eight cases and a review of the literature. *Journal of Feline Medicine and Surgery* 2002;4:27-42.
49. Kaissling B, Le Hir M. Characterization and distribution of interstitial cell types in the renal cortex of rats. *Kidney Int* 1994;45(3):709-720.
50. Kurts C, Panzer U, Anders HJ, et al. The immune system and kidney disease: basic concepts and clinical implications. *Nat Rev Immunol* 2013;13(10):738-753.
51. Lukacs-Kornek V, Burgdorf S, Diehl L, et al. The kidney-renal lymph node-system contributes to cross-tolerance against innocuous circulating antigen. *J Immunol* 2008;180(2):706-715.
52. Geissmann F, Manz MG, Jung S, et al. Development of monocytes, macrophages, and dendritic cells. *Science* 2010;327(5966):656-661.
53. Nelson PJ, Rees AJ, Griffin MD, et al. The renal mononuclear phagocytic system. *J Am Soc Nephrol* 2012;23(2):194-203.
54. Dong X, Swaminathan S, Bachman LA, et al. Resident dendritic cells are the predominant TNF-secreting cell in early renal ischemia-reperfusion injury. *Kidney Int* 2007;71(7):619-628.
55. Gordon S. The macrophage. *Bioessays* 1995;17(11):977-986.
56. Bohle A, Strutz F, Müller GA. On the pathogenesis of chronic renal failure in primary glomerulopathies: a view from the interstitium. *Exp Nephrol* 1994;2(4):205-210.
57. Bohle A, Mackensen-Haen S, Wehrmann M. Significance of postglomerular capillaries in the pathogenesis of chronic renal failure. *Kidney Blood Press Res* 1996;19(3-4):191-195.
58. Kriz W, LeHir M. Pathways to nephron loss starting from glomerular diseases-insights from animal models. *Kidney Int* 2005;67(2):404-419.

59. Risdon RA, Sloper JC, De Wardener HE. Relationship between renal function and histological changes found in renal-biopsy specimens from patients with persistent glomerular nephritis. *Lancet* 1968;2(7564):363-366.
60. Janeway C, P T, M W, et al. *Autoimmune responses are directed against self antigens*. 5 ed. New York: Garland Science; 2001.
61. Cusick MF, Libbey JE, Fujinami RS. Molecular mimicry as a mechanism of autoimmune disease. *Clin Rev Allergy Immunol* 2012;42(1):102-111.
62. Sospedra M, Martin R. Molecular mimicry in multiple sclerosis. *Autoimmunity* 2006;39(1):3-8.
63. Migliorini P, Anzilotti C, Caponi L, et al. Autoantibodies and nephritis: Different roads may lead to Rome. *Molecular Autoimmunity* 2005:165-180.
64. Mezza LE, Seiler RJ, Smith CA, et al. Antitubular basement membrane autoantibody in a dog with chronic tubulointerstitial nephritis. *Vet Pathol* 1984;21(2):178-181.
65. Bannister KM, Ulich TR, Wilson CB. Induction, characterization, and cell transfer of autoimmune tubulointerstitial nephritis. *Kidney Int* 1987;32(5):642-651.
66. Rudofsky UH. Studies on the pathogenesis of experimental autoimmune renal tubulointerstitial disease in guinea-pigs. III. The role of adjuvants in the induction of disease. *Clin Exp Immunol* 1976;25(3):455-461.
67. Steblay RW, Rudofsky U. Renal tubular disease and autoantibodies against tubular basement membrane induced in guinea pigs. *J Immunol* 1971;107(2):589-594.
68. Gitlits VM, Toh BH, Sentry JW. Disease association, origin, and clinical relevance of autoantibodies to the glycolytic enzyme enolase. *J Investig Med* 2001;49(2):138-145.
69. Nagele EP, Han M, Acharya NK, et al. Natural IgG autoantibodies are abundant and ubiquitous in human sera, and their number is influenced by age, gender, and disease. *PLoS One* 2013;8(4):e60726.
70. Adamus G, Aptsiauri N, Guy J, et al. The occurrence of serum autoantibodies against enolase in cancer-associated retinopathy. *Clin Immunol Immunopathol* 1996;78(2):120-129.
71. Moodie FD, Leaker B, Cambridge G, et al. Alpha-enolase: a novel cytosolic autoantigen in ANCA positive vasculitis. *Kidney Int* 1993;43(3):675-681.
72. Terrier B, Degand N, Guilpain P, et al. Alpha-enolase: a target of antibodies in infectious and autoimmune diseases. *Autoimmun Rev* 2007;6(3):176-182.

73. Rattner JB, Martin L, Waisman DM, et al. Autoantibodies to the centrosome (centriole) react with determinants present in the glycolytic enzyme enolase. *J Immunol* 1991;146(7):2341-2344.
74. Pratesi F, Moscato S, Sabbatini A, et al. Autoantibodies specific for alpha-enolase in systemic autoimmune disorders. *J Rheumatol* 2000;27(1):109-115.
75. Migliorini P, Pratesi F, Moscato S, et al. Mechanisms of renal damage in mixed cryoglobulinaemia nephritis. *Nephrol Dial Transplant* 2001;16 Suppl 6:58-59.
76. Sabbatini A, Dolcher MP, Marchini B, et al. Alpha-enolase is a renal-specific antigen associated with kidney involvement in mixed cryoglobulinemia. *Clin Exp Rheumatol* 1997;15(6):655-658.
77. Pratesi F, Moscato S, Chimenti D, et al. Mechanism of renal damage in systemic autoimmune disorders. *J Chemother* 1998;10(2):167-168.
78. Lee JH, Cho SB, Bang D, et al. Human anti-alpha-enolase antibody in sera from patients with Behçet's disease and rheumatologic disorders. *Clin Exp Rheumatol* 2009;27(2 Suppl 53):S63-66.
79. Tanaka S, Tatsumi KI, Takano T, et al. Anti-alpha-enolase antibodies in pituitary disease. *Endocr J* 2003;50(6):697-702.
80. Roozendaal C, Zhao MH, Horst G, et al. Catalase and alpha-enolase: two novel granulocyte autoantigens in inflammatory bowel disease (IBD). *Clin Exp Immunol* 1998;112(1):10-16.
81. Ochi H, Horiuchi I, Araki N, et al. Proteomic analysis of human brain identifies alpha-enolase as a novel autoantigen in Hashimoto's encephalopathy. *FEBS Lett* 2002;528(1-3):197-202.
82. Wakui H, Imai H, Komatsuda A, et al. Circulating antibodies against alpha-enolase in patients with primary membranous nephropathy (MN). *Clin Exp Immunol* 1999;118(3):445-450.
83. Bruschi M, Sinico RA, Moroni G, et al. Glomerular autoimmune multicomponents of human lupus nephritis in vivo:  $\alpha$ -enolase and annexin AI. *J Am Soc Nephrol* 2014;25(11):2483-2498.
84. Adamus G, Amundson D, Seigel GM, et al. Anti-enolase-alpha autoantibodies in cancer-associated retinopathy: epitope mapping and cytotoxicity on retinal cells. *J Autoimmun* 1998;11(6):671-677.
85. Adrian PV, Bogaert D, Oprins M, et al. Development of antibodies against pneumococcal proteins alpha-enolase, immunoglobulin A1 protease, streptococcal lipoprotein rotamase

- A, and putative proteinase maturation protein A in relation to pneumococcal carriage and Otitis Media. *Vaccine* 2004;22(21-22):2737-2742.
86. Fontán PA, Pancholi V, Nociari MM, et al. Antibodies to streptococcal surface enolase react with human alpha-enolase: implications in poststreptococcal sequelae. *J Infect Dis* 2000;182(6):1712-1721.
  87. Pancholi V. Multifunctional alpha-enolase: its role in diseases. *Cell Mol Life Sci* 2001;58(7):902-920.
  88. Crandell RA, Fabricant CG, Nelson-Rees WA. Development, characterization, and viral susceptibility of a feline (*Felis catus*) renal cell line (CRFK). *In Vitro* 1973;9(3):176-185.
  89. Lee KM, Kniazeff AJ, Fabricant CG, et al. Utilization of various cell culture systems for propagation of certain feline viruses and canine herpesvirus. *Cornell Vet* 1969;59(4):538-547.
  90. Scott FW, Csiza CK, Gillespie JH. Feline viruses. IV. Isolation and characterization of feline panleukopenia virus in tissue culture and comparison of cytopathogenicity with feline picornavirus, herpesvirus, and reovirus. *Cornell Vet* 1970;60(2):165-182.
  91. Lappin MR, Jensen WA, Jensen TD, et al. Investigation of the induction of antibodies against Crandell-Rees feline kidney cell lysates and feline renal cell lysates after parenteral administration of vaccines against feline viral rhinotracheitis, calicivirus, and panleukopenia in cats. *Am J Vet Res* 2005;66(3):506-511.
  92. Yamamoto JK, Ackley CD, Zochlinski H, et al. Development of IL-2-independent feline lymphoid cell lines chronically infected with feline immunodeficiency virus: importance for diagnostic reagents and vaccines. *Intervirology* 1991;32(6):361-375.
  93. Whittemore JC, Hawley JR, Jensen WA, et al. Antibodies against Crandell Rees feline kidney (CRFK) cell line antigens, alpha-enolase, and annexin A2 in vaccinated and CRFK hyperinoculated cats. *J Vet Intern Med* 2010;24(2):306-313.
  94. Sonius C, Whittemore J, Hawley J, et al. Association Between Feline Antibody Responses to Alpha-Enolase and Azotemia in Privately-Owned Cats (poster). American College of Veterinary Internal Medicine Annual Forum, Denver CO; 2011.
  95. Minkus G, Reusch C, Horauf A, et al. Evaluation of renal biopsies in cats and dogs- histopathology in comparison with clinical data. *Journal of Small Animal Practice* 1994;35:8.
  96. Lohman K, Meyerhof O. Enzymatic transformation of phosphoglyceric acid into pyruvic and phosphoric acid. *Biochem Z* 1934;273:60-72.



97. Brewer JM, Collins KM. Studies of the role of catalytic and conformational metals in producing enzymatic activity in yeast enolase. *J Inorg Biochem* 1980;13(2):151-164.
98. Brewer JM, Ellis PD. <sup>31</sup>P-nmr studies of the effect of various metals on substrate binding to yeast enolase. *J Inorg Biochem* 1983;18(1):71-82.
99. Fletcher L, Rider CC, Taylor CB. Developmental changes in brain-specific enolase isoenzymes. *Biochem Soc Trans* 1976;4(6):1135-1136.
100. Fletcher L, Rider CC, Taylor CB. Enolase isoenzymes. III. Chromatographic and immunological characteristics of rat brain enolase. *Biochim Biophys Acta* 1976;452(1):245-252.
101. Rider CC, Taylor CB. Enolase isoenzymes in rat tissues. Electrophoretic, chromatographic, immunological and kinetic properties. *Biochim Biophys Acta* 1974;365(1):285-300.
102. Rider CC, Taylor CB. Enolase isoenzymes. II. Hybridization studies, developmental and phylogenetic aspects. *Biochim Biophys Acta* 1975;405(1):175-187.
103. Giallongo A, Oliva D, Cali L, et al. Structure of the human gene for alpha-enolase. *Eur J Biochem* 1990;190(3):567-573.
104. McAlister L, Holland MJ. Targeted deletion of a yeast enolase structural gene. Identification and isolation of yeast enolase isozymes. *J Biol Chem* 1982;257(12):7181-7188.
105. Subramanian A, Miller DM. Structural analysis of alpha-enolase. Mapping the functional domains involved in down-regulation of the c-myc protooncogene. *J Biol Chem* 2000;275(8):5958-5965.
106. Lu N, Zhang Y, Li H, et al. Oxidative and nitrative modifications of alpha-enolase in cardiac proteins from diabetic rats. *Free Radic Biol Med* 2010;48(7):873-881.
107. Zhu LA, Fang NY, Gao PJ, et al. Differential expression of alpha-enolase in the normal and pathological cardiac growth. *Exp Mol Pathol* 2009;87(1):27-31.
108. Ucker DS, Jain MR, Pattabiraman G, et al. Externalized glycolytic enzymes are novel, conserved, and early biomarkers of apoptosis. *J Biol Chem* 2012;287(13):10325-10343.
109. Díaz-Ramos A, Roig-Borrellas A, García-Melero A, et al.  $\alpha$ -Enolase, a multifunctional protein: its role on pathophysiological situations. *J Biomed Biotechnol* 2012;2012:1-12.
110. Haimoto H, Takashi M, Koshikawa T, et al. Enolase isozymes in renal tubules and renal cell carcinoma. *Am J Pathol* 1986;124(3):488-495.

111. Zimmerman LH, Levine RA, Farber HW. Hypoxia induces a specific set of stress proteins in cultured endothelial cells. *J Clin Invest* 1991;87(3):908-914.
112. Graven KK, Zimmerman LH, Dickson EW, et al. Endothelial cell hypoxia associated proteins are cell and stress specific. *J Cell Physiol* 1993;157(3):544-554.
113. Aaronson RM, Graven KK, Tucci M, et al. Non-neuronal enolase is an endothelial hypoxic stress protein. *J Biol Chem* 1995;270(46):27752-27757.
114. Moscato S, Pratesi F, Sabbatini A, et al. Surface expression of a glycolytic enzyme, alpha-enolase, recognized by autoantibodies in connective tissue disorders. *Eur J Immunol* 2000;30(12):3575-3584.
115. Terrier B, Tamby MC, Camoin L, et al. Antifibroblast antibodies from systemic sclerosis patients bind to {alpha}-enolase and are associated with interstitial lung disease. *Ann Rheum Dis* 2010;69(2):428-433.
116. Chizzolini C, Raschi E, Rezzonico R, et al. Autoantibodies to fibroblasts induce a proadhesive and proinflammatory fibroblast phenotype in patients with systemic sclerosis. *Arthritis Rheum* 2002;46(6):1602-1613.
117. Plow EF, Herren T, Redlitz A, et al. The cell biology of the plasminogen system. *FASEB J* 1995;9(10):939-945.
118. Redlitz A, Fowler BJ, Plow EF, et al. The role of an enolase-related molecule in plasminogen binding to cells. *Eur J Biochem* 1995;227(1-2):407-415.
119. Miles LA, Dahlberg CM, Plescia J, et al. Role of cell-surface lysines in plasminogen binding to cells: identification of alpha-enolase as a candidate plasminogen receptor. *Biochemistry* 1991;30(6):1682-1691.
120. López-Alemaný R, Longstaff C, Hawley S, et al. Inhibition of cell surface mediated plasminogen activation by a monoclonal antibody against alpha-Enolase. *Am J Hematol* 2003;72(4):234-242.
121. López-Alemaný R, Suelves M, Muñoz-Cánoves P. Plasmin generation dependent on alpha-enolase-type plasminogen receptor is required for myogenesis. *Thromb Haemost* 2003;90(4):724-733.
122. Kang HJ, Jung SK, Kim SJ, et al. Structure of human alpha-enolase (hENO1), a multifunctional glycolytic enzyme. *Acta Crystallogr D Biol Crystallogr* 2008;64(Pt 6):651-657.

## CHAPTER 2: RESEARCH OVERVIEW AND SPECIFIC AIMS

### 2.1 Research Overview

Chronic kidney disease (CKD) has been reported in 28-50% of cats and increases in prevalence with age.<sup>1-3</sup> It is characterized by a reduction of structural and functional components resulting in retention of metabolic waste products, decreased urinary concentrating ability, electrolyte and acid-base imbalances.<sup>3-5</sup> The most frequent morphologic diagnoses in cats with CKD are chronic tubulointerstitial nephritis and fibrosis; which are relatively non-specific lesions.<sup>4, 6, 7</sup> Fibrosis is considered a common end point of all kidney diseases which does little to aid the clinician in determining an inciting cause.<sup>8</sup> Frequently, CKD in cats is considered multifactorial resulting in progressive, irreversible kidney damage.<sup>5</sup> Etiologies that have been proposed to contribute to renal injury in cats include *Leptospira* species, feline morbillivirus, diet, age, and vaccines; however, definitively defining the etiopathogenesis of CKD has not been accomplished in this species.<sup>6, 9-12</sup>

The goal of this dissertation is twofold. First to better characterize renal pathology in feline CKD and associated gastric lesions histologically. These aims are covered in Chapters 3 and 4, respectively. The second goal of this dissertation is to evaluate the expression of renal  $\alpha$ -enolase and its potential role as a target for circulating autoantibodies in cats with CKD. These aims will be addressed in Chapters 5, 6, and 7.

### 2.2 Specific Aim 1 (Chapter 3: Histopathology of CKD IRIS stages)

Histologically tubulointerstitial nephritis is the most common diagnosis made in association with feline CKD.<sup>4</sup> This common lesion can be result of numerous renal insults however and is not indicative of any particular etiology.<sup>4, 6, 7</sup> The cause of CKD in cats frequently cannot be determined at the time of diagnosis and often renal injury is significant and irreversible.<sup>4, 5, 13</sup>

Staging feline CKD was established by the International Renal Interest Society (IRIS) based on measurement of serum creatinine concentrations and further sub-staged by the presence of hypertension and proteinuria.<sup>14, 15</sup> These clinicopathologic parameters are useful for diagnosing, staging, and prognosticating but give few clues as to the distribution and pattern of injury within the kidney at individual stages. Therefore it is difficult to determine which stages are characterized by irreversible lesions and at which stage interventional therapies should be targeted.

The objective of aim 1 is to characterize and quantify interstitial, tubular, glomerular and vascular lesions in the kidney of cats with CKD and assess the association between these histopathologic changes and clinical IRIS stage and sub-stage. **The hypothesis for this aim is that histopathologic lesions in the kidneys of cats with CKD will vary between clinical IRIS stages.** Renal tissue from cats at various IRIS stages were systematically evaluated and scored on defined histopathologic criteria by two pathologists. Histologic scores and clinicopathologic data are compared between groups. Young and geriatric, non-azotemic cats are included as controls.

### **2.3 Specific Aim 2 (Chapter 4: Uremic gastropathy)**

Uremia is a consequence of renal insufficiency with retention of metabolic waste products manifesting in clinical symptoms which can include weight loss, vomiting, inappetance and anorexia.<sup>16-19</sup> Such clinical presentations are often thought to be the result of gastric hyperacidity secondary to hypergastrinemia and gastric pathology.<sup>20, 21</sup> However, while this pathogenesis may hold true in human patients with uremia little has been described as to the presence or contribution of gastric lesions to clinical symptoms in feline patients suffering from renal

disease.<sup>22</sup> While hypergastrinemia has been shown to be associated with severity of feline CKD, the presence of gastric lesions have not assessed.<sup>20</sup>

The objectives of aim 2 is to evaluate the type and prevalence of histopathologic lesions in the stomach of cats with CKD, and to determine whether the degree of azotemia, calcium-phosphorus products and serum gastrin concentrations correlate with gastric pathology. **The hypothesis for aim 2 is that uremic gastropathy is an uncommon finding in cats with CKD.** In this chapter, gastric and renal tissues from cats at various stages, or severity, of renal disease and healthy controls are systematically evaluated and scored on defined histopathologic criteria by two pathologists. In addition, histologic scores are compared to clinicopathologic parameters such as serum creatinine, calcium-phosphorus product, and gastrin concentrations.

#### **2.4 Specific Aim 3 (Chapter 5: Alpha-enolase antibodies in serum)**

Core vaccines routinely administered to cats and the cell lysates used in vaccine production have been associated with development of antibodies against these lysates and renal disease experimentally.<sup>12, 23</sup> Crandell Rees feline kidney (CRFK) cell line originated from renal cortical tissue of a young, healthy domestic cat.<sup>24</sup> Established cell cultures were described morphologically as “epithelial-like” and are used for production of the core feline herpesvirus 1, calicivirus, and panleukopenia (FVRCP) vaccine.<sup>23-26</sup> Inevitably these cell contaminants are included in the vaccine therefore exposing cats to feline cellular proteins repeatedly over a lifetime.<sup>23</sup> An immunodominant protein,  $\alpha$ -enolase, was identified as a target antigen for vaccine and CRFK lysate induced antibodies in cats that were administered repeated boosters.<sup>27</sup>

Anti- $\alpha$ -enolase antibodies present in sera are associated with a myriad of infectious, autoimmune, inflammatory, and degenerative diseases.<sup>28-30</sup> Of particular interest, podocyte  $\alpha$ -

enolase has been found to be the target of auto-antibodies in membranous glomerulonephritis and lupus nephritis.<sup>31,32</sup> While the presence of autoantibodies to this particular protein has been defined in numerous disease states, the genesis of antibody production is largely undefined in human patients.<sup>29</sup>

The objective of this dissertation chapter is to identify and quantitate anti- $\alpha$ -enolase antibodies in cats with naturally occurring CKD. Additionally, to identify possible endogenous proteins targeted by autoantibodies. **The hypothesis for aim 3 is that anti- $\alpha$ -enolase antibodies will be present in sera of cats with naturally occurring CKD and that these antibodies will bind to endogenous feline renal  $\alpha$ -enolase protein.** Anti- $\alpha$ -enolase antibodies are assessed by western blot immunoassay and quantitated by an enzyme-linked immunosorbent assay (ELISA) against recombinant  $\alpha$ -enolase protein. Additionally, immunoglobulin is extracted from sera by a traditional immunoprecipitation assay from azotemic and non-azotemic cats with or without  $\alpha$ -enolase antibody confirmed by western immunoblot. This immunoglobulin is then used to target and identify specific endogenous renal antigens by gel electrophoresis and mass spectrometry, respectively. Serum from cats with naturally occurring CKD at IRIS stages II-IV and healthy, non-azotemic young cats have been included in this study. The healthy, laboratory reared control cats have not been administered parenteral vaccines containing viruses grown on cells. Vaccine histories of CKD cats will be recorded when available.

## 2.5 Specific Aim 4 (Chapter 6: Renal $\alpha$ -enolase protein expression)

Originally characterized as a cytoplasmic, glycolytic enzyme,  $\alpha$ -enolase has been shown to have multiple functions as well as variable cellular expression.<sup>33-35</sup> This protein is ubiquitously expressed but most concentrated in the thymus and kidney.<sup>36</sup> In the kidney  $\alpha$ -enolase is localized to the cytoplasm of renal proximal tubules, collecting ducts, and distal tubules.<sup>30, 37</sup> In human patients with lupus nephritis, an autoimmune disease associated with the presence of autoantibodies in sera,  $\alpha$ -enolase protein expression is altered. In biopsies from lupus nephritis patient's  $\alpha$ -enolase is overexpressed in tubules and glomeruli in comparison to healthy controls.<sup>30</sup> Similar descriptive studies of  $\alpha$ -enolase protein expression have not been explored in cats with or without CKD.

The objective of aim 4 is to semi-quantitate  $\alpha$ -enolase protein expression within tissues of cats in health and with CKD. **The hypothesis for aim 4 is that tubular and glomerular  $\alpha$ -enolase will be overexpressed in cats with CKD.** In order to test this hypothesis, immunohistochemistry utilizing a mouse monoclonal antibody will be optimized and validated. Kidney and liver tissue from cats with CKD and healthy, non-azotemic controls are included in this study. Thymic tissue from a young cat will be used to optimize and validate this assay.

## 2.6 Specific Aim 5 (Chapter 7: Cellular expression and antigenicity of renal proteins)

Autoimmune disease is characterized by dysregulation of the immune system and loss of self-tolerance.<sup>38</sup> Targets of autoantibodies are frequently conserved, abundantly expressed proteins.<sup>34</sup> Examples include topoisomerase in systemic sclerosis, insulin in type I diabetes, and  $\alpha$ -enolase in systemic lupus erythematosus.<sup>34, 38-40</sup> Anti- $\alpha$ -enolase antibodies can be induced experimentally in cats with feline panleukopenia, herpesvirus 1, and calicivirus containing viral vaccines.<sup>23, 27</sup> These vaccines (FVRCP) are routinely administered to cats and can contain cell

lysate contaminates (CRFK) that originated from cat renal cortical tissue.<sup>23, 24</sup> Feline renal derived cell lysates—CRKF lysates—not only can induce production of antibodies to  $\alpha$ -enolase but led to interstitial nephritis in a subset of cats.<sup>12, 27</sup> Furthermore, client owned cats with azotemia were more likely to have anti- $\alpha$ -enolase antibodies than non-azotemic client owned cats (Chelsea Sonius, unpublished work).<sup>41</sup> Cellular expression of  $\alpha$ -enolase is not restricted to the cytosol with membranous  $\alpha$ -enolase targeted by autoantibodies in autoimmune disease as well as alternative, non-glycolytic functions.<sup>34</sup>

The objective of this chapter is to localize cellular expression of  $\alpha$ -enolase in renal tissue homogenates from cats with CKD. **The hypothesis for aim 5 is that  $\alpha$ -enolase will be present in both cytosolic and membranous fractions in cats with CKD.** Identification of  $\alpha$ -enolase protein in subcellular fractions of whole renal tissue homogenate from cats with CKD and young healthy controls will be achieved by differential centrifugation (herein referred to as subcellular fractionation) and western immunoblot with mouse monoclonal  $\alpha$ -enolase antibody.



## REFERENCES

1. Marino CL, Lascelles BD, Vaden SL, et al. Prevalence and classification of chronic kidney disease in cats randomly selected from four age groups and in cats recruited for degenerative joint disease studies. *J Feline Med Surg* 2013.
2. Bartlett PC, Van Buren JW, Bartlett AD, et al. Case-control study of risk factors associated with feline and canine chronic kidney disease. *Vet Med Int* 2010;2010.
3. Lulich J, Osborne C, O'Brien T, et al. Feline renal failure: questions, answers, questions. *Compendium on Continuing Education for the Practicing Veterinarian* 1992;14(2):26.
4. DiBartola SP, Rutgers HC, Zack PM, et al. Clinicopathologic findings associated with chronic renal disease in cats: 74 cases (1973-1984). *J Am Vet Med Assoc* 1987;190(9):1196-1202.
5. Elliott J, Barber PJ. Feline chronic renal failure: clinical findings in 80 cases diagnosed between 1992 and 1995. *J Small Anim Pract* 1998;39(2):78-85.
6. Lawler DF, Evans RH, Chase K, et al. The aging feline kidney: a model mortality antagonist? *J Feline Med Surg* 2006;8(6):363-371.
7. Chakrabarti S, Syme HM, Brown CA, et al. Histomorphometry of feline chronic kidney disease and correlation with markers of renal dysfunction. *Vet Pathol* 2013;50(1):147-155.
8. Prunotto M, Ghiggeri G, Bruschi M, et al. Renal fibrosis and proteomics: current knowledge and still key open questions for proteomic investigation. *J Proteomics* 2011;74(10):1855-1870.
9. Rodriguez J, Blais MC, Lapointe C, et al. Serologic and urinary PCR survey of leptospirosis in healthy cats and in cats with kidney disease. *J Vet Intern Med* 2014;28(2):284-293.
10. Woo PC, Lau SK, Wong BH, et al. Feline morbillivirus, a previously undescribed paramyxovirus associated with tubulointerstitial nephritis in domestic cats. *Proc Natl Acad Sci U S A* 2012;109(14):5435-5440.
11. Hughes KL, Slater MR, Geller S, et al. Diet and lifestyle variables as risk factors for chronic renal failure in pet cats. *Prev Vet Med* 2002;55(1):1-15.
12. Lappin MR, Basaraba RJ, Jensen WA. Interstitial nephritis in cats inoculated with Crandell Rees feline kidney cell lysates. *J Feline Med Surg* 2006;8(5):353-356.

13. Maxie M, Newman S. Urinary system. In: Maxie M, ed. *Pathology of Domestic Animals*. Vol 2. 5 ed. Philadelphia: Elsevier Saunders; 2007:425-522.
14. Novartis Animal Health Inc. IRIS staging CKD. <http://www.iris-kidney.com/guidelines/staging.shtml> (2013, accessed 1 April 2015).
15. Polzin DJ. Evidence-based step-wise approach to managing chronic kidney disease in dogs and cats. *J Vet Emerg Crit Care (San Antonio)* 2013;23(2):205-215.
16. Roudebush P, Polzin DJ, Ross SJ, et al. Therapies for feline chronic kidney disease. What is the evidence? *J Feline Med Surg* 2009;11(3):195-210.
17. Bartges JW. Chronic kidney disease in dogs and cats. *Vet Clin North Am Small Anim Pract* 2012;42(4):669-692, vi.
18. Polzin DJ, Osborne C, S R. Evidence-based management of chronic kidney disease. *Kirk's Current Veterinary Therapy XIV*. St. Louis, MO: Saunders Elsevier; 2009.
19. Polzin DJ. Chronic kidney disease in small animals. *Vet Clin North Am Small Anim Pract* 2011;41(1):15-30.
20. Goldstein R, Marks S, Kass P, et al. Gastrin concentrations in plasma of cats with chronic renal failure. *JAVMA* 1998;213:826-828.
21. Jaffe R, Laing, DR. Changes of the Digestive Tract in Uremia. A Pathologic Anatomic Study. *JAMA Internal Medicine* 1934;53(6):851-864.
22. Lazarus H. *Gastrointestinal abnormalities*. Philadelphia: WB Saunders; 2000.
23. Lappin MR, Jensen WA, Jensen TD, et al. Investigation of the induction of antibodies against Crandell-Rees feline kidney cell lysates and feline renal cell lysates after parenteral administration of vaccines against feline viral rhinotracheitis, calicivirus, and panleukopenia in cats. *Am J Vet Res* 2005;66(3):506-511.
24. Crandell RA, Fabricant CG, Nelson-Rees WA. Development, characterization, and viral susceptibility of a feline (*Felis catus*) renal cell line (CRFK). *In Vitro* 1973;9(3):176-185.
25. Lee KM, Kniazeff AJ, Fabricant CG, et al. Utilization of various cell culture systems for propagation of certain feline viruses and canine herpesvirus. *Cornell Vet* 1969;59(4):538-547.
26. Scott FW, Csiza CK, Gillespie JH. Feline viruses. IV. Isolation and characterization of feline panleukopenia virus in tissue culture and comparison of cytopathogenicity with feline picornavirus, herpesvirus, and reovirus. *Cornell Vet* 1970;60(2):165-182.

27. Whittemore JC, Hawley JR, Jensen WA, et al. Antibodies against Crandell Rees feline kidney (CRFK) cell line antigens, alpha-enolase, and annexin A2 in vaccinated and CRFK hyperinoculated cats. *J Vet Intern Med* 2010;24(2):306-313.
28. Terrier B, Degand N, Guilpain P, et al. Alpha-enolase: a target of antibodies in infectious and autoimmune diseases. *Autoimmun Rev* 2007;6(3):176-182.
29. Gitlits VM, Toh BH, Sentry JW. Disease association, origin, and clinical relevance of autoantibodies to the glycolytic enzyme enolase. *J Investig Med* 2001;49(2):138-145.
30. Migliorini P, Pratesi F, Bongiorno F, et al. The targets of nephritogenic antibodies in systemic autoimmune disorders. *Autoimmun Rev* 2002;1(3):168-173.
31. Bruschi M, Sinico RA, Moroni G, et al. Glomerular autoimmune multicomponents of human lupus nephritis in vivo:  $\alpha$ -enolase and annexin AI. *J Am Soc Nephrol* 2014;25(11):2483-2498.
32. Bruschi M, Carnevali ML, Murtas C, et al. Direct characterization of target podocyte antigens and auto-antibodies in human membranous glomerulonephritis: Alfa-enolase and borderline antigens. *J Proteomics* 2011;74(10):2008-2017.
33. Pancholi V. Multifunctional alpha-enolase: its role in diseases. *Cell Mol Life Sci* 2001;58(7):902-920.
34. Moscato S, Pratesi F, Sabbatini A, et al. Surface expression of a glycolytic enzyme, alpha-enolase, recognized by autoantibodies in connective tissue disorders. *Eur J Immunol* 2000;30(12):3575-3584.
35. Díaz-Ramos A, Roig-Borrellas A, García-Melero A, et al.  $\alpha$ -Enolase, a multifunctional protein: its role on pathophysiological situations. *J Biomed Biotechnol* 2012;2012:156795.
36. Sabbatini A, Dolcher MP, Marchini B, et al. Alpha-enolase is a renal-specific antigen associated with kidney involvement in mixed cryoglobulinemia. *Clin Exp Rheumatol* 1997;15(6):655-658.
37. Haimoto H, Takashi M, Koshikawa T, et al. Enolase isozymes in renal tubules and renal cell carcinoma. *Am J Pathol* 1986;124(3):488-495.
38. Janeway C, P T, M W, et al. *Autoimmune responses are directed against self antigens*. 5 ed. New York: Garland Science; 2001.
39. Terrier B, Tamby MC, Camoin L, et al. Antifibroblast antibodies from systemic sclerosis patients bind to {alpha}-enolase and are associated with interstitial lung disease. *Ann Rheum Dis* 2010;69(2):428-433.

40. Pratesi F, Moscato S, Sabbatini A, et al. Autoantibodies specific for alpha-enolase in systemic autoimmune disorders. *J Rheumatol* 2000;27(1):109-115.
41. Sonius C, Whittemore J, Hawley J, et al. Association Between Feline Antibody Responses to Alpha-Enolase and Azotemia in Privately-Owned Cats (poster). American College of Veterinary Internal Medicine Annual Forum, Denver CO; 2011.

## CHAPTER 3: A COMPARISON OF BIOCHEMICAL AND HISTOPATHOLOGIC STAGING IN CATS WITH CHRONIC KIDNEY DISEASE

### 3.1 Chapter Summary

Chronic kidney disease (CKD) is prevalent in elderly cats. Frequently, a diagnosis is made in later stages of disease by which time many renal lesions are irreversible. As such, little headway has been made in identifying an etiology and preventing this common disease. The aim of this study was to evaluate the presence and severity of both reversible and irreversible histopathologic changes in the kidneys of cats at each stage of CKD and in addition, to determine if lesion prevalence and character was different between stages. A total of 46 cats with CKD were classified according to the International Renal Interest Society (IRIS) as: Stage I (3 cats), Stage II (16 cats), Stage III (14 cats), and Stage IV (13 cats). Eleven young, non-azotemic and 10 geriatric, non-azotemic cats were included as controls. The severity of tubular degeneration, interstitial inflammation, fibrosis, and glomerulosclerosis was significantly greater in later stages of CKD compared to early stages of disease. Proteinuria was associated with increased severity of tubular degeneration, inflammation, fibrosis, tubular epithelial single cell necrosis and decreased normal parenchyma. Presence of hyperplastic arteriolosclerosis, fibrointimal hyperplasia, or other vascular lesions was not found to be significantly different between hypertensive and normotensive cats. The greater prevalence and severity of irreversible lesions in Stage III and IV CKD implies that therapeutic interventions should be targeted at earlier stages of disease.

### 3.2 Introduction

Chronic kidney disease (CKD) affects as many as 50% of elderly cats, and prevalence increases with age.<sup>1,2</sup> The etiology of CKD in cats is unknown. In humans, the leading cause for end stage renal failure is type 2 diabetes mellitus and hypertension.<sup>3</sup> However, diabetic

nephropathy has not been identified in cats and renal lesions in diabetic cats were no different than those in non-diabetic cats.<sup>4</sup> The most frequent morphologic diagnosis in cats with CKD is chronic tubulointerstitial nephritis and fibrosis; which are relatively non-specific lesions.<sup>5-7</sup> Therefore, feline CKD is currently considered to be the consequence of a variety of etiologies that lead to a final common pathway of irreversible, progressive, kidney damage.<sup>8</sup> This damage culminates in reduction of glomerular filtration rate which, when severe, results in retention of metabolic byproducts such as creatinine and blood urea nitrogen. Eventually, uremia may develop and manifest as gastrointestinal, cardiovascular, pulmonary, neuromuscular, or hematologic diseases.<sup>8,9</sup>

CKD is categorized into disease stages established by the International Renal Interest Society (IRIS) based on serum creatinine measurements.<sup>10,11</sup> Clinical progression, or stage, is associated with decreased survival.<sup>12</sup> Clinicopathologic data are useful for diagnosing, staging, and prognosticating but gives few clues as to the distribution and pattern of injury within the kidney. Therefore it is difficult to determine which stages are characterized by irreversible lesions and at which stage interventional therapies should be targeted. In a previous study, renal fibrosis in cats with CKD from the United Kingdom correlated with clinicopathologic derangements such as azotemia, hyperphosphatemia, and anemia.<sup>7</sup> Renal scarring encompasses interstitial fibrosis, which is an increase in extracellular matrix, as well as glomerulosclerosis and tubular atrophy.<sup>13-16</sup> Collectively, these changes imply a loss of function and are considered, at least to date, irreversible.<sup>15,16</sup> However, not all injury leads to irreversible damage. Replication and repair can lead to a return of normal function. Inflammation, edema and tubular epithelial damage have the potential to resolve (i.e. reversible). Interest in these types of morphologic responses guided the design of this study. The aim of the current study was to further explore the

relationship between clinical parameters and renal pathology by characterizing and quantifying a wide variety of interstitial, tubular, glomerular and vascular lesions (both reversible and irreversible) in the kidney of cats with CKD from the United States and assessing the correlation between these histopathologic changes and clinical IRIS stage and substage.

### **3.3 Materials and Methods**

#### *3.3.1 Case Selection*

Cats necropsied at Colorado State University Diagnostic Medical Center between 2000 and 2013 with a history of CKD, appropriate clinicopathologic data necessary for IRIS staging, and adequate tissue available for histologic review were included in this study. Exclusion criteria included renal neoplasia, ureteral or urethral obstruction, or pyelonephritis. Non-azotemic geriatric cats were humanely euthanized with client consent for health problems unrelated to renal disease. Young non-azotemic cats were euthanized at a local humane society, according to humane society guidelines and protocols. Study samples were obtained from these cats after euthanasia, and no cats were euthanized for the purpose of this study. Age was estimated by surrender history and/or dental assessment.

#### *3.3.2 Clinicopathologic Data*

Using the IRIS staging scheme, patients (designated CKD cats) were assigned a Stage of I to IV based on clinical evaluation of the cat's medical history by a board-certified internist. Clinical evaluation for IRIS stage determination took into account 2 or more serum creatinine levels no less than 48 hours apart, clinical history, fluid therapy, body condition score and fluctuation in weight and muscle mass over the course of the disease. Patients assigned to Stage I had a urine specific gravity (USG) < 1.035, serum creatinine less than 1.6 mg/dl, as well as other evidence of renal abnormalities such as abnormal imaging (radiograph and/or ultrasound), and/or proteinuria.

Stages II, III, and IV were defined by creatinine measuring 1.6-2.8 mg/dl, 2.9-5.0 mg/dl and >5.0 mg/dl, respectively. Non-azotemic control cats had no clinical evidence or history of renal disease, USG >1.035, and creatinine  $\leq$  1.6 mg/dl. Control cats were divided into either non-azotemic geriatric controls (GC) if they were  $\geq$ 7 years of age or non-azotemic young controls (YC) if they were <4 years of age.

Substaging according to proteinuria and elevation of systemic blood pressure was determined based on data availability. Urine samples were collected via cystocentesis during routine examination and submitted to the Clinical Pathology Laboratory at Colorado State University Diagnostic Medical Center. Quantification of urine protein was determined by urine protein to creatinine ratio (UPC) measurement and only CKD cats in which UPC data were available were included in this portion of the analysis. GC cats were confirmed to have no urinary protein by the sulfosalicylic acid precipitation test. Hypertension was determined by repeated mean systolic blood pressure measurements of greater than 160 mm Hg, prior clinical diagnosis of hypertension, or evidence of hypertensive therapy (e.g. amlodipine) in the medical record; only cats with blood pressure data available were included in this portion of the analysis.

### *3.3.3 Histopathology*

Tissues were preserved in 10% neutral buffered formalin, routinely processed, and embedded in paraffin. Sections of kidney cut at 3  $\mu$ m and stained with hematoxylin and eosin, periodic acid-Schiff-hematoxylin to assess basement membranes of tubules and blood vessels, and Masson's trichrome for assessment of fibrosis. Tissues were evaluated for a range of histologic lesions by two pathologists. The scoring schematic for dichotomous and semi-quantitative histologic variables is outlined in Table 3.1. Additionally, continuous variables included global glomerulosclerosis and frequency of tubular epithelial single cell necrosis. Global



glomerulosclerosis was determined by examining 50 randomly distributed glomeruli per kidney to determine the proportion in which >75% of the capillary tuft was effaced by extracellular matrix. When present, specific glomerular lesions (e.g. glomerulonephritis or focal segmental glomerulosclerosis) were noted. As renal lesions can be unilateral, if both kidneys were available, each was scored separately for the following variables: percent normal parenchyma, interstitial cortical scarring, medullary scarring, interstitial inflammation, tubular epithelial single cell necrosis, and globally sclerotic glomeruli. Scarring was defined as a percentage of cortex or medulla occupied by trichrome-confirmed collagenous matrix, in conjunction with fibroplasia, parenchymal collapse due to tubular atrophy and loss and glomerulosclerosis.<sup>13,14</sup> Vasculature was assessed for degenerative changes, specifically arteriosclerosis. Evaluation of arteriosclerotic lesions included: concentric medial smooth muscle hyperplasia (hyperplastic arteriosclerosis); or segmental or circumferential intimal proliferation with disruption of the internal elastic lamina (fibrointimal hyperplasia). Other vascular lesions (eg fibrinoid vascular necrosis, arteritis) were recorded if present.

Table 3.1 Scoring schematic for dichotomous and semi-quantitative histologic variables.

Categorical variables	Score	Dichotomous variables <sup>a</sup>	Score
<b>Tubules</b>		<b>Tubules</b>	
% Tubular degeneration		Tubular lipid	1
No tubular degeneration	0	Normal	1
Focal, scattered tubular degeneration	1	Degenerative	1
Multifocal to coalescing degeneration	2	Atrophied	1
Entire nephron units affected	3	Lipid casts	1
		RBC casts	1
<b>Interstitial</b>		Cellular casts	1
% Inflammation		Intraluminal crystals	1
No inflammation	0	Dilation	1
<25% of the interstitium is affected by some degree of inflammation	1	Cysts	1
25-50%	2	Tubular necrosis	1
51-75%	3	Basement membrane mineralization	1
>75%	4		
<b>Pattern of inflammation</b>		<b>Interstitial</b>	
No inflammation	0	Inflammation	
Stripe d/Linear	1	Lymphocytes	1
Patchy/Multifocal	2	Plasma cells	1
Regionally extensive	3	Macrophages	1
Coalescing/Diffuse	4	Other	1
<b>% Cortical scarring</b>		Edema	1
None	0	Lipid	1
<25% of cortex affected by scarring	1		
25-50%	2	Glomerular	
51-75%	3	Bowman's capsule mineralization	1
>75%	4	Lesions, other	1
<b>% Medullary scarring</b>			
None	0	Vessels	
<25% of medulla affected by scarring	1	Fibrotic hyperplasia	1
25-50%	2	Hyperplastic arteriosclerosis	1
51-75%	3	Lesions, other	1
>75%	4		
<b>Pattern of scarring</b>		<b>Other</b>	
No fibrosis	0	Papillary necrosis	1
Stripe d/Linear	1	Collecting duct mineral	1
Patchy/Multifocal	2		
Regionally extensive	3		
Coalescing/Diffuse	4		
<b>Other</b>			
<b>% Overall normal parenchyma</b>			
<25% of the renal parenchyma is normal	1		
25-50%	2		
51-75%	3		
>75%	4		

<sup>a</sup>Dichotomous variables without lesions were assigned a score of '2'

### *3.3.4 Statistical Analysis*

A univariate approach was used to determine if histologic variables differed between non-azotemic cats and those with CKD. Serum creatinine, IRIS stage, and proteinuria status were designated as independent variables. For semi-quantitative outcome variables (e.g. pattern of interstitial scarring) medians were reported and data were converted into ‘ranks’ for linear regression analysis. For variables with multiple measurements from the same individual (i.e. both kidneys available for review) repeated measures were taken into account for regression analyses. Similarly, for continuous variables, differences in means among groups were determined by linear regression after assumptions for normality were confirmed. Fisher’s exact test was used for dichotomous variables and odds ratios were calculated with 95% confidence interval. Statistical significance for all analyses was set at  $p \leq 0.05$  and  $p \leq 0.0125$  for pairwise comparison to account for multiple comparisons. Statistical calculations were performed by SAS v9.3 (SAS Institute Inc., Cary, NC, USA).

## **3.4 Results**

### *3.4.1 Signalment*

Of 331 CKD cats necropsied between 2000 and 2013, a total of 46 CKD cats had sufficient clinical data and tissue for evaluation. Age, sex, and cause of death are outlined in Table 3.2. There was no statistically significant difference among groups with regards to gender or breed. Two CKD cats included in this study died of natural causes while the remaining cats were humanely euthanized. Those euthanized for poor quality of life or acute decompensation of CKD (21/46) were typically in later stages of the disease (Stage II, n=2; Stage III, n=7; and Stage IV, n=12).

Table 3.2 Signalment, cause of death, and clinicopathologic data for controls and CKD cats by stage.

	Young Controls (n=11)	Geriatric Controls (n=10)	Stage 1 (n=3)	Stage 2 (n=16)	Stage 3 (n=14)	Stage 4 (n=13)
Age (years) <sup>a</sup>	3 (1-4)	13 (10-16)	11 (9-15)	15 (8-21)	14 (5-19)	11 (5-18)
Cause of death/Euthanasia						
Kidney disease	0	0	0	2	7	12
Non-renal disease	0	10	3	14	7	1
	1.16	1.23	1.38	2.12	4.31	8.18
Creatinine <sup>b</sup>	(0.8-1.5)	(0.9-1.5)	(1.35-1.4)	(1.5-2.7)	(2.95-9.1)	(6.0-12.65)
	1.067	1.054	1.031	1.018	1.015	1.011
USG <sup>c</sup>	(1.049-1.084)	(1.044-1.067)	(1.025-1.035)	(1.012-1.032)	(1.010-1.020)	(1.007-1.015)
Proteinuria						
Stage <sup>d</sup>	n=11	n=10	n=1	n=13	n=7	n=12
UPC <0.2	11 (100)	10 (100)	1 (100)	11 (85)	1 (14)	3 (25)
UPC 0.2-0.4	0	0	0	2 (15)	5 (72)	1 (8)
UPC >0.4	0	0	0	0	1 (14)	8 (67)
Hypertensive <sup>e</sup>	n/d <sup>f</sup>	n/d	1 (100)	6 (50)	2 (22)	4 (36)

<sup>a</sup>Mean age in years (range)

<sup>b</sup>Average of two serum creatinine measurements taken prior to euthanasia in CKD cats (range of creatinine for each group)

<sup>c</sup>Mean (range)

<sup>d</sup>Number of cats with proteinuria per group (percentage of cats with available UPC data); Non-proteinuric <0.2, Borderline proteinuric 0.2-0.4, and Proteinuric >0.4

<sup>e</sup>Number of hypertensive cats per stage (percentage of hypertensive cats with available systolic blood pressure)

<sup>f</sup>Not measured (n/d)

Twenty-five cats were euthanized for reasons not directly related to kidney disease, including: neoplasia (n=9); gastrointestinal disease, liver disease, or pancreatitis (n=5); and cardiopulmonary disease (n=4) which included congestive heart failure, thromboembolism, or pulmonary disease. The remaining CKD cats were euthanized for a variety of metabolic or neurologic illnesses (n=7). Five of the 10 GC cats were euthanized for non-renal neoplasia; 4 were euthanized for cardiopulmonary disease and 1 for pancreatitis.

### 3.4.2 Histopathology

Statistically significant variables are outlined in Tables 3.3 and 3.4 for all CKD stages. The salient features of each stage are described below, with special attention being paid to the lesions deemed to have pathophysiologic relevance. Results for categorical variables for each group are summarized in Figure 3.1.

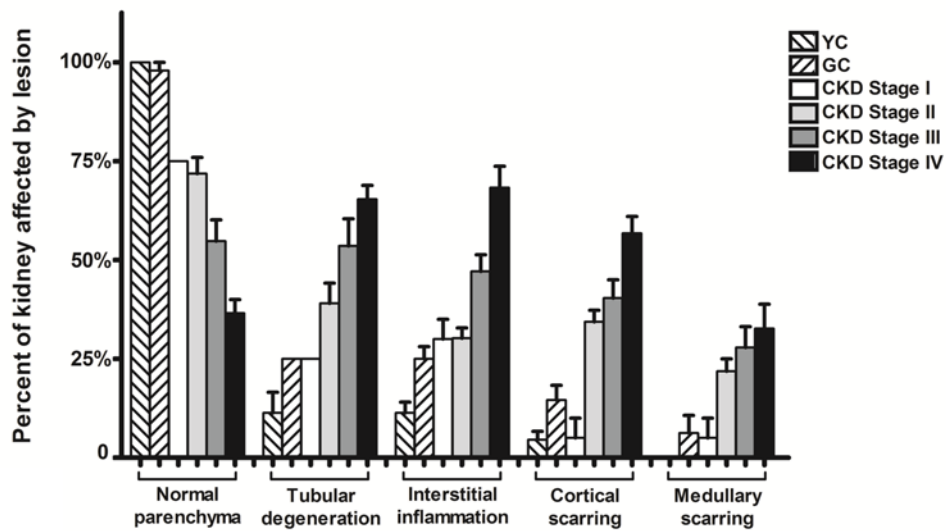


Figure 3.1 Graph of categorical histologic variables by group (YC=young controls; GC=geriatric controls) or chronic kidney disease (CKD) stage. Columns represent mean percentage of tissue affected by histologic lesion while bars represent the standard error of the mean.

Table 3.3 Dichotomous and continuous histologic variables with statistical significance. For each stage either means for continuous variable or total number of lesion incidence for dichotomous variables are given along with p-values. Bolded p-values indicate statistical significance.

	Interstitial compartment <sup>a</sup>		Tubular compartment <sup>b</sup>				Glomerular compartment <sup>c</sup>			Vascular <sup>d</sup>		
	Lymphocytes <sup>e</sup>	Lipid	Dead epithelial cell count <sup>f</sup>	Lipid: atrophic tubules	Cellular casts	Dilation	Cysts	Crystals	Glomerular lesions	Sclerosis <sup>f</sup>	BC thickening <sup>g</sup>	Hyperplastic arteriosclerosis
Stage I (n=3)	3	1	1.4	2	0	0	0	0	0	1.4	2	0
vs YC	0.26	0.67	0.6247	0.54	n/a <sup>h</sup>	n/a	n/a	n/a	n/a	< <b>0.0001</b>	0.033	n/a
vs GC	1	0.23	<b>0.0007</b>	0.56	0.53	n/a	n/a	1	n/a	0.7923	1	1
vs Stage II	1	0.15	< <b>0.0001</b>	0.3	0.26	0.0578	0.53	0.26	1	<b>0.0011</b>	1	0.53
vs Stage III	n/a	0.12	< <b>0.0001</b>	0.46	0.029	0.015	0.23	0.23	0.5	< <b>0.0001</b>	1	0.21
vs Stage IV	n/a	0.025	< <b>0.0001</b>	0.35	0.018	<b>0.0018</b>	0.018	0.06	0.063	< <b>0.0001</b>	1	1
Stage II (n=16)	15	13	11.0	15	7	11	5	7	3	8.4	12	5
vs YC	0.027	<b>0.0006</b>	< <b>0.0001</b>	<b>0.0025</b>	0.02	<b>0.0003</b>	0.059	0.022	0.25	< <b>0.0001</b>	<b>0.0002</b>	0.059
vs GC	1	<b>0.0048</b>	0.4092	<b>0.005</b>	0.68	<b>0.0007</b>	0.12	0.4	0.26	<b>0.0027</b>	0.23	0.35
vs Stage I	1	0.15	< <b>0.0001</b>	0.3	0.26	0.0578	0.53	0.26	1	<b>0.0011</b>	1	0.53
vs Stage III	1	1	0.2134	0.59	0.072	0.4	0.46	1	0.42	<b>0.0034</b>	0.44	0.27
vs Stage IV	1	0.23	<b>0.002</b>	1	0.05	0.048	<b>0.008</b>	0.26	<b>0.009</b>	< <b>0.0001</b>	0.69	0.7
Stage III (n=14)	14	12	15.0	12	11	12	7	7	5	15.7	8	8
vs YC	<b>0.0087</b>	<b>0.0003</b>	< <b>0.0001</b>	0.017	<b>0.0001</b>	< <b>0.0001</b>	<b>0.0078</b>	<b>0.0078</b>	0.046	< <b>0.0001</b>	<b>0.0029</b>	<b>0.0029</b>
vs GC	0.42	<b>0.0019</b>	0.0709	0.03	0.035	< <b>0.0001</b>	0.019	0.21	0.05	< <b>0.0001</b>	1	0.033
vs Stage I	n/a	0.12	< <b>0.0001</b>	0.46	0.029	0.015	0.23	0.23	0.5	< <b>0.0001</b>	1	0.21
vs Stage II	1	1	0.2134	0.59	0.072	0.4	0.46	1	0.42	<b>0.0034</b>	0.44	0.27
vs Stage IV	n/a	0.48	0.1341	1	1	0.48	0.1	0.44	0.13	<b>0.0117</b>	1	0.12
Stage IV (n=13)	13	13	19.9	12	11	13	11	9	9	25.7	8	3
vs YC	<b>0.011</b>	< <b>0.0001</b>	< <b>0.0001</b>	<b>0.0078</b>	< <b>0.0001</b>	< <b>0.0001</b>	< <b>0.0001</b>	0.006	<b>0.0006</b>	< <b>0.0001</b>	<b>0.002</b>	0.22
vs GC	0.43	<b>0.0005</b>	<b>0.001</b>	0.02	0.013	< <b>0.0001</b>	< <b>0.0001</b>	0.036	<b>0.002</b>	< <b>0.0001</b>	0.69	0.6
vs Stage I	n/a	0.025	< <b>0.0001</b>	0.35	0.018	0.0018	0.018	0.06	0.063	< <b>0.0001</b>	0.063	1
vs Stage II	1	0.23	<b>0.002</b>	1	0.05	0.048	<b>0.008</b>	0.26	<b>0.009</b>	< <b>0.0001</b>	0.69	0.7
vs Stage III	n/a	0.48	0.1341	1	1	0.48	0.1	0.44	0.13	<b>0.0117</b>	1	0.12
GC (n=10)	9	3	9	4	3	0	0	2	0	1.9	5	1
YC (n=11)	6	1	1	4	0	0	0	0	0	0.3	0	0

Table 3.4 Categorical histologic variables with statistical significance. For each stage the median, mean, and range for each variable are given along with p-values. Bolded p-values indicate statistical significance when compared to other groups by linear regression of ranks.

	Interstitial compartment			Tubular compartment	Other
	% Inflammation	% Cortical scar	% Medullary scar	% Degeneration	% Normal
Stage I (n=3)	1 (1.2, 1-2) <sup>a</sup>	0 (0.2, 0-1)	0 (0.2, 0-1)	1 (1, 1-1)	3 (3, 3-3)
vs YC	<b>0.0041</b>	0.9307	0.3074	0.253	n/a <sup>b</sup>
vs GC	0.4082	0.1105	0.9585	1	<b>&lt;0.0001</b>
vs Stage II	0.9429	<b>&lt;0.0001</b>	<b>0.0069</b>	0.1545	0.818
vs Stage III	<b>0.0123</b>	<b>&lt;0.0001</b>	<b>0.0039</b>	<b>0.0069</b>	<b>0.003</b>
vs Stage IV	<b>&lt;0.0001</b>	<b>&lt;0.0001</b>	<b>0.0032</b>	<b>0.0001</b>	<b>&lt;0.0001</b>
Stage II (n=16)	1 (1.2, 1-3)	1 (1.4, 1-3)	1 (0.9, 0-2)	1.5 (1.6, 0-3)	3 (2.9, 1-4)
vs YC	<b>&lt;0.0001</b>	<b>&lt;0.0001</b>	<b>&lt;0.0001</b>	<b>&lt;0.0001</b>	<b>&lt;0.0001</b>
vs GC	0.2136	<b>&lt;0.0001</b>	<b>0.0005</b>	<b>0.0263</b>	<b>&lt;0.0001</b>
vs Stage I	0.9429	<b>&lt;0.0001</b>	<b>0.0069</b>	0.1545	0.818
vs Stage III	<b>&lt;0.0001</b>	0.4513	0.7564	<b>0.0247</b>	<b>0.0404</b>
vs Stage IV	<b>&lt;0.0001</b>	<b>0.0001</b>	0.5705	<b>&lt;0.0001</b>	<b>&lt;0.0001</b>
Stage III (n=14)	2 (1.9, 0-4)	1 (1.6, 0-4)	1 (1.1, 0-4)	2.5 (2.1, 0-3)	2 (2.2, 1-4)
vs YC	<b>&lt;0.0001</b>	<b>&lt;0.0001</b>	<b>&lt;0.0001</b>	<b>&lt;0.0001</b>	<b>&lt;0.0001</b>
vs GC	<b>&lt;0.0001</b>	<b>&lt;0.0001</b>	<b>&lt;0.0001</b>	<b>&lt;0.0001</b>	<b>&lt;0.0001</b>
vs Stage I	<b>0.0123</b>	<b>&lt;0.0001</b>	<b>0.0039</b>	<b>0.0069</b>	<b>0.003</b>
vs Stage II	<b>&lt;0.0001</b>	0.4513	0.7564	<b>0.0247</b>	<b>0.0404</b>
vs Stage IV	<b>0.0259</b>	<b>0.008</b>	0.7795	0.062	<b>0.0062</b>
Stage IV (n=13)	3 (2.7, 1-4)	2 (2.3, 1-4)	1 (1.3, 0-4)	3 (2.6, 2-3)	1.5 (1.5, 0-3)
vs YC	<b>&lt;0.0001</b>	<b>&lt;0.0001</b>	<b>&lt;0.0001</b>	<b>&lt;0.0001</b>	<b>&lt;0.0001</b>
vs GC	<b>&lt;0.0001</b>	<b>&lt;0.0001</b>	<b>0.0003</b>	<b>&lt;0.0001</b>	<b>&lt;0.0001</b>
vs Stage I	<b>&lt;0.0001</b>	<b>&lt;0.0001</b>	<b>0.0032</b>	<b>0.0001</b>	<b>&lt;0.0001</b>
vs Stage II	<b>&lt;0.0001</b>	<b>0.0001</b>	0.5705	<b>&lt;0.0001</b>	<b>&lt;0.0001</b>
vs Stage III	<b>0.0259</b>	<b>0.008</b>	0.7795	0.062	<b>0.0062</b>
GC (n=10)	1 (1, 0-2)	1 (0.6, 0-1)	0 (0.3, 0-2)	1 (1, 1-1)	4 (3.9, 3-4)
YC (n=11)	0 (0.5, 0-1)	0 (0.2, 0-1)	0 (0, 0-0)	0 (0.5, 0-2)	4 (4, 4-4)
<sup>a</sup> Data presented as median score (mean, range)					
<sup>b</sup> Could not be determined					

### 3.4.2.1 CKD Stage I

Three cats were classified as Stage I having a serum creatinine of  $<1.6\text{mg/dL}$ ,  $\text{USG} \leq 1.035$ , as well as abnormal kidneys on gross examination. All three cats were scored as having 50-75% normal parenchyma remaining and this score was significantly less than that of GC cats ( $p < 0.0001$ ). In comparison with other CKD stages, Stage I cats had a significantly greater percent of normal parenchyma than Stages III and IV ( $p = 0.003$  and  $< 0.0001$ , respectively). No significant difference was found between Stage I and II. Interstitial inflammation, which was comprised exclusively of lymphocytes, affected  $< 25\%$  of the section (median, 1; range, 1-2) in Stage I cats. Inflammation at this stage was significantly greater than YC ( $p = 0.0041$ ) cats but significantly less than Stages III and IV ( $p = 0.0123$  and  $< 0.0001$ , respectively). Moreover, inflammatory infiltrates had a regionally extensive distribution in all cats within this group (Figure 3.2). Frequency of this pattern was only significantly different when Stage I cats were compared to YC and GC control cats ( $p = 0.0057$  and  $0.0263$ , respectively). No difference in pattern of inflammation was found when Stage I cats were compared to other stages.

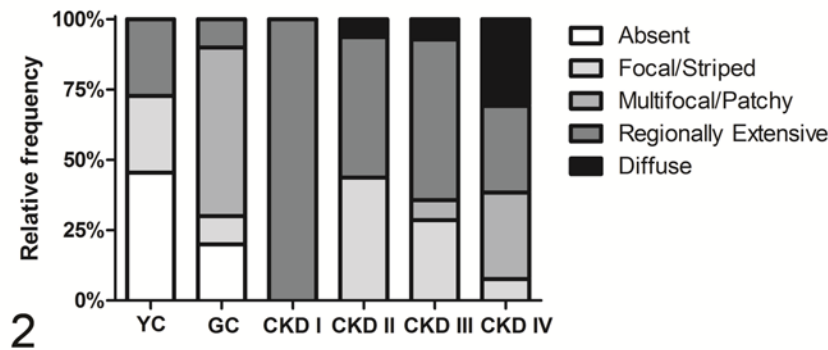


Figure 3.2 Relative frequencies of 4 different patterns of interstitial inflammation for each CKD stage I-IV or control group (YC=young controls; GC=geriatric controls).



Cortical and medullary scarring was nearly absent in Stage 1 cats (median 0; range 0-1), with one cat having a multifocal pattern of scarring occupying less than 25% of the section. Severity of cortical scarring within this group was significantly less than that observed in Stages II, III, and IV ( $p < 0.0001$  for all 3 stages). Likewise, medullary scarring was significantly less than other CKD stages (Stage II,  $p = 0.0069$ ; Stage III,  $p = 0.0039$ ; and Stage IV,  $p = 0.0032$ ). The pattern of scarring was found to be significantly different from all other CKD stages (versus Stage II,  $p = 0.0488$ ; Stage III,  $p = 0.0446$ ; and Stage IV,  $p = 0.0016$ ; Figure 3.3).

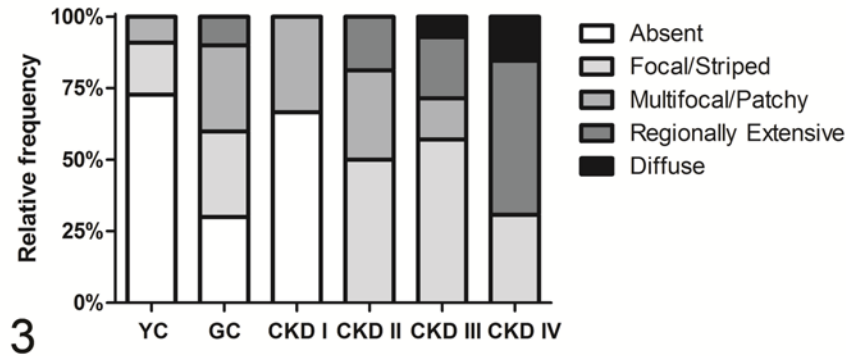


Figure 3.3. Relative frequencies of 4 different patterns of cortical scarring for each CKD stage I-IV or control group (YC=young controls; GC=geriatric controls).

Median score (1; range, 1-1) for tubular degeneration in Stage I cats was consistent with mild, focal to scattered cortical tubular degeneration. This change was statistically different from Stages III and IV ( $p = 0.0069$  and  $p = 0.0001$ , respectively). Dead tubular epithelial cells were infrequent (mean  $\pm$  standard deviation [SD],  $1.4 \pm 1.7$ ) and occurred significantly less than in GC cats ( $p = 0.0007$ ) and CKD cats in Stage II, III, and IV ( $p < 0.0001$ ). Tubular dilation was not present at this stage and this was statistically different from Stage IV ( $p = 0.0018$ ).

Glomerular lesions and mineralization of Bowman's capsule were not present within cats at this stage of kidney disease. Global glomerulosclerosis was statistically more frequent in Stage I cats (mean  $\pm$  SD,  $1.4 \pm 2.2$ ) than in YC ( $p < 0.0001$ ) but less frequent than CKD Stages II-IV (Stage II,  $p = 0.0011$ ; Stage III and IV,  $p < 0.0001$ ). Global glomerulosclerosis occurred more frequently in GC cats compared to Stage I but the difference was not statistically significant.

Vascular lesions and papillary necrosis were absent in this stage while collecting duct mineral was present in a single cat. No statistical significance was found when comparing these lesions with other groups.

#### *3.4.2.2 Stage II*

A total of 16 cats were classified as CKD Stage II. Similar to Stage I, Stage II cats had a median score for normal parenchyma that corresponded to 51-75% remaining in the examined sections (median, 3; range, 1-4). This was significantly less than control groups (YC and GC,  $p < 0.0001$ ) but significantly greater than later stages (Stage III,  $p = 0.0404$ ; Stage IV,  $p < 0.0001$ ). Interstitial inflammation affected  $< 25\%$  of the kidney in Stage II cats (median, 1; range, 1-3) which consisted mostly of lymphocytes and plasma cells, and less frequently macrophages and granulocytes (neutrophils or eosinophils). Severity of inflammation was significantly greater in Stage II compared to YC cats ( $p < 0.0001$ ) but significantly less than later stages (versus Stage III and IV,  $p < 0.0001$ ). Regionally extensive interstitial inflammation was the most common distribution in Stage II cats. Statistical significance between groups was only found when compared to YC cats ( $p = 0.0125$ ).

Cortical (median, 1; range, 1-3) and medullary scarring (median, 1; range, 0-2) was significantly greater in Stage II cats than either control group ( $p < 0.0001$ ) or Stage I cats ( $p < 0.0001$ ). No difference in the severity of scarring was found when Stage II cats were

compared to Stage III cats, but scarring of the cortex was significantly less when compared to Stage IV cats ( $p=0.0001$ ). The pattern of scarring was significantly different from YC ( $p<0.0001$ ), Stage I ( $p=0.0488$ ), and Stage IV ( $p=0.037$ ). No difference in the distribution of scarring between Stage II and III were found. Interstitial lipid was present in a majority of cats in this stage, however, statistical significance was only found when comparing Stage II with control groups (YC,  $p=0.0006$ ; GC,  $p=0.0048$ ).

Stage II cats had a median score of 1.5 (range, 0-3) for tubular degeneration which was consistent with mild to moderate degeneration. Cortical tubular degeneration in Stage II was significantly greater than control groups (YC,  $p<0.0001$ ; GC,  $p=0.0263$ ). Similar to Stage I, Stage II cats have significantly less tubular degeneration than later stages (Stage III,  $p=0.0247$ ; Stage IV,  $p<0.0001$ ). Dead tubular epithelial cells (mean  $\pm$  SD,  $11.0 \pm 7.0$ ) were significantly more frequent than in YC and Stage I cats ( $p<0.0001$ ), but were similar to the frequency observed in GC. Tubular epithelial cell lipid accumulation was a common finding within Stage II cats, similar to the other CKD cats. Nearly half of Stage II cats had cellular casts (7/16) or intraluminal crystals (7/16), less frequently lipid casts (6/16). Statistical significance among groups was not found for these variables. Tubular dilation occurred frequently (11/16), and this was significantly greater than either control group (YC;  $p=0.0003$ ; GC,  $p=0.0007$ ). Tubular basement membrane mineralization or coagulative necrosis was not seen at this stage.

Three cats in Stage II had glomerular lesions. A single cat had moderate cystic glomerular atrophy and another had mesangial expansion. The remaining cat had multiple glomerular changes including focal glomerular hypercellularity and remodeling of the glomerular basement membrane, consistent with a membranoproliferative glomerulonephritis pattern as well as focal segmental glomerulosclerosis (FSGS). Bowman's capsule thickening

with or without parietal cell hypertrophy was present in a majority of cats (12/16) and this was significantly greater than YC cats ( $p=0.0002$ ). Global glomerulosclerosis was significantly greater in Stage II cats (mean  $\pm$  SD,  $8.4 \pm 6.6$ ) compared to controls (YC,  $p<0.0001$ ; GC,  $p=0.0027$ ) and Stage I cats ( $p=0.0011$ ); but significantly less than later stages (Stage III,  $p=0.0034$ ; Stage IV,  $p<0.0001$ ).

Vascular lesions identified in Stage II cats consisted of fibrointimal hyperplasia in 9 cats (Figure 3.4), hyperplastic arteriolosclerosis in 5, hyalinosis in 2, and torturous vessels in regions of scarring in 2. Statistical significance of the frequency of vascular lesions was not present when comparing Stage II cats with other groups. Lastly, the incidence of collecting duct mineral ( $n=8$ ) or papillary necrosis ( $n=3$ ) was not significantly different between Stage II cats and any other group.

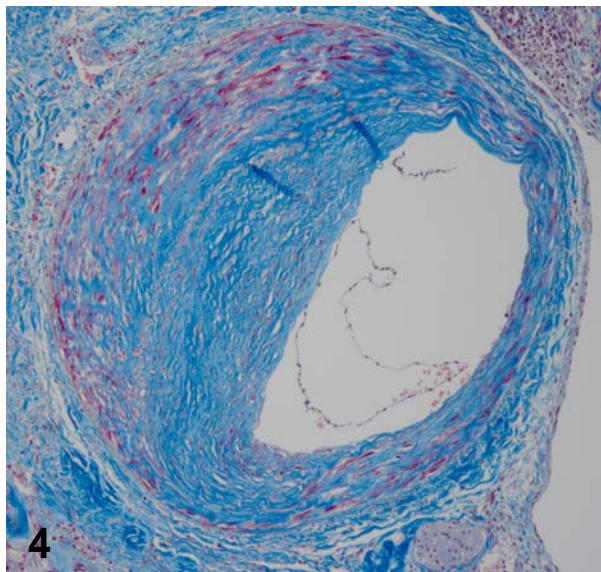


Figure 3.4. Fibrointimal hyperplasia of an arcuate artery, cat, kidney. Masson's trichrome stain.

### 3.4.2.3 Stage III

A total of 14 cats were classified as Stage III. There was significantly less normal renal parenchyma in Stage III cats, equating to approximately 25-50% of the section (median, 2; range, 1-4) compared to earlier stages (Stage I,  $p=0.003$ ; Stage II,  $p=0.0404$ ) and controls (YC and GC,  $p<0.0001$ ). Stage III cats had significantly more normal parenchyma than Stage IV cats ( $p=0.0062$ ). Severity of interstitial inflammation in Stage III cats was significantly different when compared to controls and each CKD stage. With a median score of 2 (range, 0-4), Stage III cats were more severely affected by inflammation than controls (YC and GC,  $p<0.0001$ ) and early CKD stages (Stage I,  $p=0.0123$ ; Stage II,  $p<0.0001$ ) but was less when compared to Stage IV cats ( $p=0.0259$ ). All cats in Stage III had interstitial lymphocytic infiltrates while half had plasma cells, macrophages, and granulocytes. Over half of cats in this stage had regionally extensive inflammation (8/14). Frequency of inflammatory patterns was only significantly different from controls (versus GC,  $p=0.0351$  and YC,  $p=0.0027$ ).

Renal scarring was not as severe as inflammation in Stage III cats. Similar to Stage II cats, median scores for cortical and medullary scarring were 1 (range 0-4, for both variables) corresponding to <25% of the tissue. Scarring was significantly greater in Stage III cats than controls (YC and GC,  $p<0.0001$ , cortical and medullary) and Stage I ( $p<0.0001$  and  $p=0.0039$  cortical and medullary, respectively). Severity of cortical scarring in Stage III cats was significantly less than Stage IV ( $p=0.008$ ) with no difference found when compared to Stage II. The most frequent scarring pattern in Stage III cats was focal to striped (8/14). Statistical significance was found when compared to YC ( $p<0.0001$ ) and Stage I ( $p=0.0446$ ). Interstitial lipid was a common finding and occurred with significantly greater frequency than in control cats (YC,  $p=0.0003$ ; GC,  $p=0.0019$ ).

The median score (2.5; range, 0-3) of tubular degeneration in Stage III cats was consistent with moderate to severe degeneration. These cats were affected by tubular degeneration significantly more than controls (YC and GC,  $p < 0.0001$ ) and early CKD stages (Stage I,  $p = 0.0069$ ; Stage II,  $p = 0.0247$ ). Although compared to Stage IV cats, a significant difference was not found. Dead tubular epithelial cells were significantly greater in Stage III cats (mean  $\pm$  SD,  $15.0 \pm 9.7$ ) compared to only YC controls ( $p < 0.0001$ ) and Stage I cats ( $p < 0.0001$ ). Cellular casts were present in 11 Stage III cats which was significantly greater than YC cats ( $p = 0.0001$ ). Tubular epithelial cell lipid accumulation was common, as was the presence of lipid casts (9/14) but neither lesion was significantly different from other groups. Tubular dilation was another frequent finding (12/14) with statistical significance when comparing Stage III with controls ( $p < 0.0001$ ). Tubular cysts and intraluminal crystals affected half of Stage III cats and were significantly greater than YC cats for both variables ( $p = 0.0078$ ).

Five of 14 cats in Stage III had glomerular lesions that included one or more of the following: FSGS, thrombotic microangiopathy, MPGN pattern, basement membrane remodeling, mesangial expansion, mesangiolysis, and/or glomerular hypertrophy. A single cat with focal thrombotic microangiopathy was a unique finding in this study (Figure 3.5); specifically, there was prominent glomerular endothelial hypertrophy that obscured capillary lumina and duplication of glomerular basement membranes in multiple glomeruli. The mean number of globally sclerotic glomeruli in Stage III cats was 15.7 (SD,  $\pm 11.4$ ) which was significantly different from all other groups (YC, GC, Stage I  $p < 0.0001$ ; Stage II,  $p = 0.0034$ ; Stage IV,  $p = 0.0117$ ). Over half of the Stage III cats had glomeruli with thickened Bowman's capsules and parietal cell hypertrophy (8/14). Incidence of this lesion was significantly different from YC cats ( $p = 0.0029$ ).

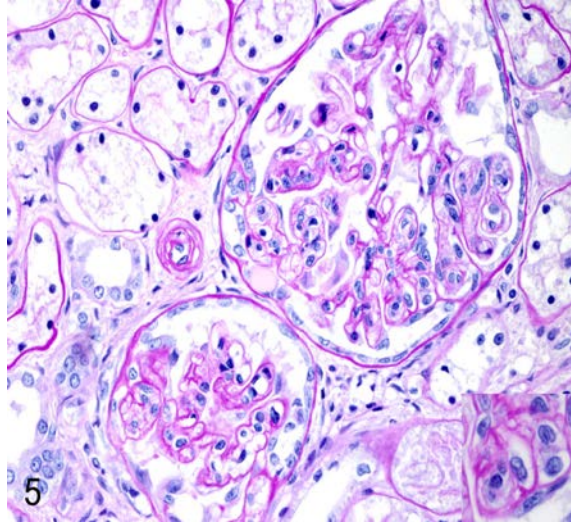


Figure 3.5. Thrombotic microangiopathy, glomerulus, kidney, cat. Endothelial cells are swollen and frequently obscure the capillary lumen (inset). Periodic acid-Schiff and hematoxylin.

Vascular lesions identified in Stage III cats consisted of fibrointimal hyperplasia (9/14), hyperplastic arteriolosclerosis (8/14), and a single case each of hyalinosis and torturous vessels in regions of scarring. The frequency of hyperplastic arteriolosclerosis was significantly greater in Stage III cats when compared to YC cats ( $p=0.0029$ ). Lastly, the frequency of collecting duct mineral (6/14) or papillary necrosis (1/14) was not significantly different between Stage III cats and any other group.

#### 3.4.2.4 Stage IV

A total of 13 cats were classified as Stage IV. Normal renal parenchyma was significantly less in Stage IV cats than all other groups (median, 1.5; range, 0-3; versus YC, GC, Stage I, Stage II,  $p<0.0001$ ; Stage III,  $p=0.0062$ ). Interstitial inflammation was the most severe in Stage IV cats affecting 50-75% of the section examined (median, 3; range, 1-4) which was significantly different from controls (YC and GC,  $p<0.0001$ ) and other CKD stages (Stage I,  $p<0.0001$ ; Stage II,  $p<0.0001$ ; Stage III,  $p=0.0259$ ). Populations of inflammatory cells in a majority of cases were

composed of lymphocytes (13/13) and plasma cells (9/13) with macrophages and / or granulocytes being present in 5 cats. Pattern of inflammation was variable. Statistically significant differences between the frequency of inflammatory patterns was found when comparing Stage IV to controls (YC,  $p < 0.0001$ ; GC,  $p = 0.0028$ ) but not with other CKD stages.

The median score for cortical scarring was greater than that in the medulla for Stage IV cats (cortical median, 2; range, 1-4; medullary median, 1; range, 0-4). Cortical scarring was significantly greater in this late stage compared to controls (YC,  $p < 0.0001$ ; GC,  $p < 0.0001$ ) and all CKD stages (Stage I,  $p < 0.0001$ ; Stage II,  $p = 0.0001$ ; Stage III,  $p = 0.008$ ; Figure 3.6).

Medullary scarring was only significantly different from controls (YC,  $p < 0.0001$ ; GC,  $p = 0.0003$ ) and Stage I cats ( $p = 0.0032$ ). The majority of Stage IV cats were affected by regionally extensive scarring (7/13). Frequency of scarring patterns was significantly different when Stage IV cats were compared to controls (YC,  $p < 0.0001$ ; GC,  $p = 0.0011$ ) and early stages of CKD (Stage I,  $p = 0.0016$ ; Stage II,  $p = 0.037$ ). Interstitial lipid was present in all Stage IV cats with statistically significant difference in incidence when compared to controls (YC,  $p < 0.0001$ ; GC,  $p = 0.0005$ ) but no other stage.



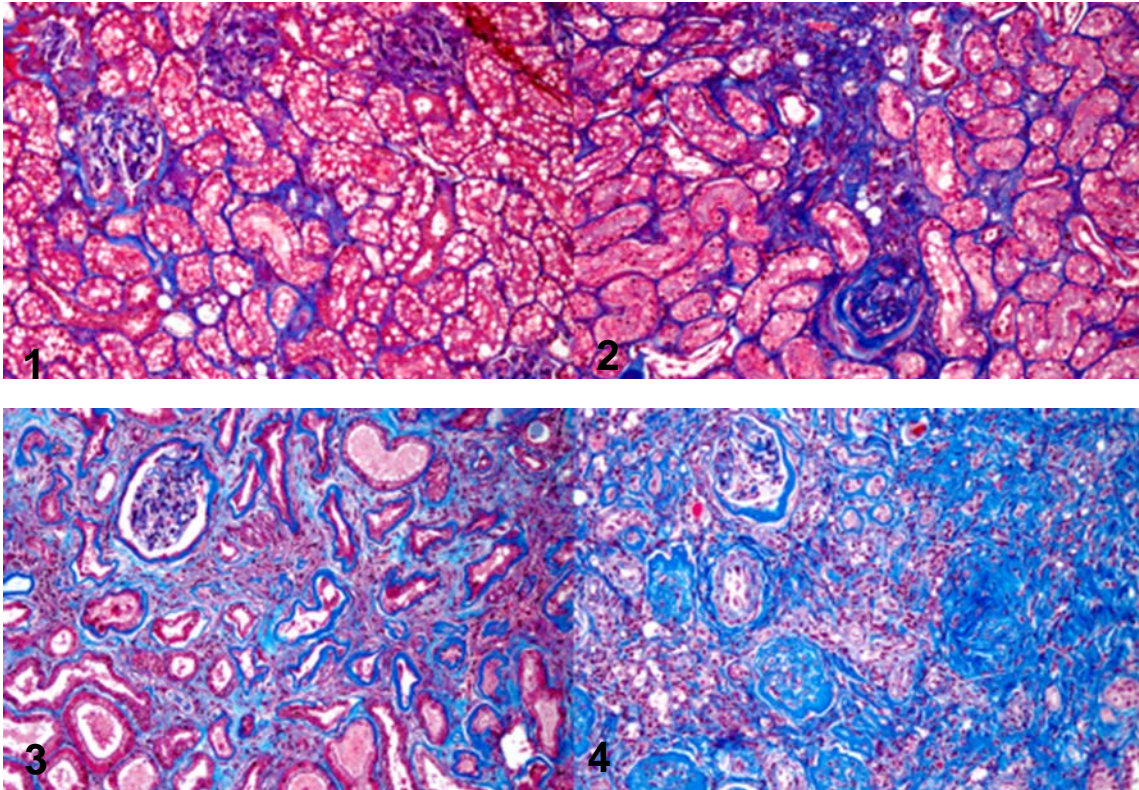


Figure 3.6 Scarring in chronic kidney disease, kidney, cat. Figure 3.6.1 Cortical scarring score of '1' with minimal tubular atrophy and interstitial expansion by increased matrix. Masson's trichrome stain. Figure 3.6.2 Scarring score of '2' with increased interstitial fibrosis, periglomerular fibrosis, and tubular atrophy. Masson's trichrome stain. Figure 3.6.3 Score of '3' with at least 50% of the tissue affected by interstitial fibrosis, tubular atrophy, and glomerulosclerosis (not present in image). Masson's trichrome stain. Figure 3.6.4 Score of '4' with a majority of the cortical parenchyma replaced by fibrosis, tubular atrophy and loss; and glomerulosclerosis. Masson's trichrome stain.

Tubular degeneration in Stage IV cats was marked affecting entire nephrons (median, 3; range, 2-3). Percent of tissue affected was significantly greater in Stage IV CKD than controls (YC and GC,  $p < 0.0001$ ) and earlier stages of CKD (Stage I,  $p = 0.0001$ ; Stage II,  $p < 0.0001$ ). Similarly mean individual dead tubular epithelial cells were significantly greater than controls (mean  $\pm$  SD,  $19.9 \pm 10.8$ ; YC,  $p < 0.0001$ ; GC,  $p = 0.001$ ) and early CKD stages (Stage I,  $p < 0.0001$ ; Stage II,  $p = 0.002$ ). Lipid within tubular epithelial cells was present in a majority of

Stage IV cats. However, lipid in tubular epithelium was common among all groups. Cellular casts were more frequent in Stage IV compared to YC cats (11/13,  $p < 0.0001$ ). Tubular dilation (13/13) and cysts (11/13) occurred more frequently in Stage IV cats than controls (YC and GC,  $p < 0.0001$ ). Stage IV cats were more likely to have tubular dilation than Stage I cats ( $p = 0.0018$ ) and more likely to have tubular cysts than Stage II cats ( $p = 0.008$ ). Intraluminal crystals were a common finding (9/13) but not statistically different from other groups. Likewise no significant difference was found in prevalence of tubular basement membrane mineralization (3/13) or tubular coagulative necrosis (0/13) when Stage IV cats were compared with other groups.

The majority of Stage IV cats in this study (10/13) had some degree of glomerular lesion. Lesions affecting glomeruli in this stage included one or more of the following: FSGS, glomerular hypertrophy, mesangial expansion, endothelial hypertrophy, MPGN pattern, and cystic glomerular hypertrophy. The prevalence of glomerular lesions at this stage was significantly more than that seen in controls (YC,  $p = 0.0006$ ; GC,  $p = 0.002$ ) and Stage II ( $p = 0.009$ ). Mean global glomerulosclerosis was greater in Stage IV than any other group (mean  $\pm$  SD,  $25.7 \pm 13.8$ ; versus YC, GC, Stage I, Stage II  $p < 0.0001$ ; Stage III,  $p = 0.0117$ ). Mineralization (2/13) and thickening of Bowman's capsule with or without parietal cell hypertrophy (8/13) were present in Stage IV cats.

Stage IV kidneys frequently contained vascular fibrointimal hyperplasia (8/13) but infrequently were affected by hyperplastic arteriolosclerosis (3/13). A total of 5 Stage IV cats had vascular lesions which consisted of a single case of tunica media mineralization, hyalinosis, fibrinoid necrotizing arteritis, endothelial swelling, and diffuse torturous vasculature. The cat with mineralization of the tunica media had concurrent Bowman's capsule and tubular basement membrane mineralization. Prevalence of vasculature lesions was not significantly different in

Stage IV cats from controls or other stages. Finally, frequency of collecting duct mineral (7/13) or papillary necrosis (2/13) was not significantly different between Stage IV cats and any other group.

### *3.4.3 Clinicopathologic Data*

Clinicopathologic data for each group is summarized in Table 2. Analysis of the relationship between histologic lesions and serum creatinine did not reveal any major differences from what was observed when analysis of the relationship between histologic variables and individual IRIS stages was performed (data not shown). A total of 33 cats out of 46 included in this study had UPC measurements available for analysis. Nine CKD cats (Stage III: 1 cat, Stage IV: 8 cats) were proteinuric (UPC >0.4). Eight CKD cats (Stage II: 2 cat; Stage III: 5 cats, Stage IV: 1 cat) were classified as borderline proteinuric (UPC 0.2-0.4) and 16 CKD cats were non-proteinuric (Stage I, n=1; Stage II, n=11; Stage III, n=1; Stage IV, n=3). All control cats (YC and GC) were non-proteinuric. Non-proteinuric cats (n=37) were more likely to have a greater percent of normal parenchyma than either borderline proteinuric cats (p=0.0014) or proteinuric cats (p<0.0001). Interstitial inflammation and cortical scarring were significantly greater in proteinuric cats than borderline (p=0.0402 and p=0.0052, respectively) and non-proteinuric cats (p≤0.0001). Medullary scarring in contrast was only significantly different between non-proteinuric and borderline proteinuric cats (p=0.0006). Inflammatory constituents were not significantly different between groups. Tubular degeneration was significantly less frequent in all non-proteinuric cats when compared to borderline (p=0.0003) and proteinuric (p<0.0001) cats. Frequency of cellular and lipid casts were significantly less in non-proteinuric cats than borderline (p=0.028) and proteinuric cats (p=0.0162 and p=0.05, respectively). The presence of lipid vacuoles in normal tubules was significantly greater in non-proteinuric cats than borderline

( $p=0.0014$ ) and proteinuric cats ( $p<0.001$ ). Incidence of tubular crystals in non-proteinuric cats was significantly less than either borderline ( $p=0.031$ ) or proteinuric cats ( $p=0.0046$ ). Tubular dilation and cysts were significantly less likely to occur in non-proteinuric cats than borderline cats ( $p=0.017$  and  $p=0.0299$ , respectively), however, cysts were more likely to occur in proteinuric cats when compared to non-proteinuric cats ( $p=0.0029$ ). Dead tubular epithelial cells were significantly greater in borderline proteinuric ( $p=0.0009$ ) and proteinuric cats ( $p=0.0081$ ) when compared to non-proteinuric cats.

Glomerular lesions occurred more frequently in proteinuric cats than both non-proteinuric cats ( $p=0.0004$ ) and borderline proteinuric cats ( $p=0.018$ ). In contrast global glomerulosclerosis was only significantly different when comparing non-proteinuric cats to proteinuric cats ( $p=0.007$ ). Bowman's capsule mineralization was significantly worse in borderline proteinuric cats compared to non-proteinuric cats ( $p<0.0001$ ; mineral was not seen in all groups, therefore, significance could not be determined). No significance difference in the occurrence of vascular lesion was found between non-proteinuric, proteinuric and borderline proteinuric cats.

A total of 33/46 CKD cats had blood pressure data available for analysis; Stage I ( $n=1$ ), Stage II ( $n=12$ ), Stage III ( $n=9$ ), and Stage IV ( $n=11$ ). All 10 GC cats had available systolic blood pressures and were normotensive. Conversely, no information in regards to blood pressure was available for YC cats. The single Stage I cat with available blood pressure was hypertensive. Half of Stage II ( $n=6$ ), 2 Stage III, and 4 Stage IV cats with available blood pressure data were hypertensive. Hypertension was more likely to occur in cats with CKD than GC cats ( $p=0.03$ ). Presence of hyperplastic arteriolosclerosis, fibrointimal hyperplasia, or other vascular lesions was not found to be significantly different between hypertensive and normotensive cats.

### 3.5 Discussion

While progress has been made in better categorizing stages of feline CKD and the associated prognosis and treatment recommendations, a great deal is still unknown about the etiopathogenesis of such a common disease.<sup>17</sup> Clinicopathologic data is useful for diagnosing, staging, and prognosticating but gives few clues about the distribution and pattern of injury within the kidney. Therefore, it is difficult to determine which stages are characterized by irreversible lesions and at which stage therapeutic interventions should be targeted. In an attempt to bridge clinical parameters with renal pathology, reversible and irreversible histologic lesions affecting all renal compartments were identified for each stage of CKD. This study showed that reversible lesions were present throughout the stages of CKD while irreversible lesions were more prevalent in later stages than early stages of CKD.

Histologic variables that were significantly different among stages affected the interstitial, tubular, and glomerular compartments. Overall, earlier stages of CKD (i.e. Stages I and II) retained a greater proportion of normal parenchyma in comparison to later stages (i.e. Stages III and IV). Within the interstitial compartment the severity of inflammation was similar in earlier stages and significantly less than later stages. Lymphocytes were the most common constituent of inflammation at any stage and a regionally extensive pattern was most frequent. Lipid within the interstitium was frequently associated with interstitial inflammation and scarring while edema was rare. Cortical scarring was prevalent in the final stages of CKD (Stage IV), but was mild in cats in Stages II and III. Tubular degeneration was significantly greater in later stages when compared to earlier stages, although the degree of degeneration was similar between individual later stages (i.e. Stages III and IV). Tubular lipid was a frequent finding in normal and atrophic tubules. Single epithelial cell necrosis was significantly less in the earliest stage of

disease (Stage I) than all other stages, however, coagulative necrosis was rare.

Glomerulosclerosis progressively worsened with CKD stage while other glomerular lesions were uncommon. Vascular lesions did not differ among IRIS stages.

Normal parenchyma unaffected by degeneration, atrophy, inflammation, or fibrosis was significantly less in later stages of CKD (i.e. Stage III and IV) compared to earlier stage (Stages I and II) but similar between Stages I and II. Interestingly, as little as 25-50% of the parenchyma was affected in the earlier stages of CKD implying that even mild degree of lesions could have functional significance. This is in contrast to the dogma that at least 75% of functional mass must be lost before clinical evidence of renal disease is evident.<sup>18-21</sup> The determination of the functional consequence of histologic lesions involving only  $\leq 50\%$  of the renal tissue was based on serum creatinine levels as an estimate of renal function, as is commonly used in clinical practice. Other functional tests such as glomerular filtration rates which have been demonstrated to decline with 75% or greater surgical reduction in renal mass in cats were not measured in this study.<sup>21-24</sup> Reasons for this contradiction may include uncertainty of the relationship between histologic assessment of normal parenchyma and functional renal mass and potential variation in whether the most or least severe renal lesions were sampled for histopathology in the 11/46 cases that were collected retrospectively in a unilateral manner.

Percent tubular degeneration was significantly greater in later stages than earlier stages of disease, but was not different between controls and Stage I. This could be a result of small sample size for Stage I. In fact the only histologic lesions significantly different between geriatric controls and Stage I CKD cats were percent normal parenchyma and tubular epithelial single cell necrosis with the latter being greater in geriatric controls. When comparing all CKD stages there was an obvious upward trend of tubular epithelial single cell necrosis with each

stage although statistical significance was not reached between stages. Lastly, the authors acknowledge that the methods used would not differentiate single cell necrosis and include apoptosis.

Interstitial fibrosis and scarring, confirmed by Masson's trichrome stain, was statistically greater in Stage IV compared to all other stages. Cats in Stage IV were most likely to have 25-50% of their kidneys affected by scarring in comparison to  $\leq 25\%$  scarring in other stages. Interstitial fibrosis did not increase significantly between cats in IRIS Stage II and III. This is in contrast to a previous study (which did not evaluate tissues stained with trichrome) where interstitial fibrosis was the lesion that best correlated with severity of azotemia.<sup>7</sup> This suggests that additional pathologic processes other than fibrosis are involved in disease progression, and implies that initiation of any potential anti-fibrotic therapies in CKD cats should occur prior to Stage IV when irreversible fibrosis is most severe.

While mean percentage of tissue affected by interstitial inflammation increased between stages II-IV, histologic scores for inflammation were typically greater than scarring scores for each stage. This would be compatible with inflammation preceding and inducing fibrosis.<sup>15</sup> However, patterns of scarring did not parallel that of interstitial inflammation and a significant progression in scarring patterns from focal to regional to diffuse with increasing IRIS stage was not found. This suggests that instigators of fibrosis other than inflammation may be players in the progression of CKD and should be identified and evaluated as potential therapeutic targets.

Glomerulonephropathies, with the exception of FSGS, were infrequently diagnosed by light microscopy (4/46). Due to the retrospective nature of this study tissues were not available for ultrastructural evaluation. However our results were similar to previously published work on

feline renal disease where glomerular disease was uncommon with a reported prevalence of 8-15%.<sup>2, 5, 6, 25</sup> In the present study the most common glomerular changes were global glomerulosclerosis and FSGS. Global glomerulosclerosis was the only histologic variable in this study that precipitously increased with IRIS stage progression. Interestingly, glomerulosclerosis was more severe in non-azotemic geriatric cats than Stage I CKD cats. This suggests that although global glomerulosclerosis appears to be a feature of aging, it can be considered pathologic in certain scenarios.<sup>26</sup> Additional studies on non-azotemic geriatric cats are needed to better characterize normal renal aging changes.

Focal segmental glomerulosclerosis is a poorly characterized entity in veterinary medicine.<sup>27, 28</sup> Histologic features are one or more glomeruli with segmental consolidation of capillary tufts with replacement by increased extracellular matrix, cellularity, or both.<sup>29, 30</sup> Clinically, proteinuria is a hallmark of FSGS and typically is accompanied by variable degrees of hypoalbuminemia, hypercholesterolemia, and edema (nephrotic syndrome) in human patients.<sup>29</sup> Etiologies for FSGS are classified as either primary (idiopathic or genetic) or secondary (adaptive) the latter encompasses drug-induced or viral-associated causes.<sup>29, 30</sup> In humans, distinct histologic variants of FSGS have been identified, based on location and character of the lesion within the glomerular tuft, and have been found to relate to specific therapeutic responses and prognostic outcomes. For example, the variant perihilar FSGS is defined by sclerosis at the vascular pole and often seen in secondary, adaptive FSGS. Individuals with perihilar variant of FSGS typically have nephrotic syndrome less frequently with a milder degree of proteinuria than other variants.<sup>30</sup> Aging, advanced renal disease and obesity are three examples of conditions that are associated with adaptive FSGS.<sup>29, 30</sup>



In the current study, 8 cats with CKD had histologic evidence of FSGS. Urinalysis and UPC measurements were available for 6 of the 8 cats. Although none of the cats suffered from nephrotic syndrome, 5/6 were proteinuric with only 2/6 within nephrotic range (UPC > 2.0). A single cat was hypoalbuminemic but proteinuric status was not available for this cat. However, hypoalbuminemia in this cat was most likely due to pleural effusion from severe mediastinitis secondary to complications from an esophageal feeding tube rather than glomerular disease. While *Leishmania* infection in dogs has been associated with chronic glomerulosclerosis, other primary or secondary etiologies for FSGS in veterinary medicine have not been reported.<sup>31</sup> Viral infections (e.g. parvovirus or feline immunodeficiency virus) were not suspected clinically. None of the cats in the current study were treated with any FSGS-associated drugs. While these 8 cats may have had primary FSGS, that is typically a diagnosis of exclusion. A more plausible explanation would be that these lesions were secondary to adaptive changes due to the loss of functional renal mass in these cats. Loss of functional glomeruli leads to hyperfiltration of the remaining glomeruli which can result in podocyte injury and eventually sclerosis. In support of this theory, perihilar pattern of segmental sclerosis was identified in 4 of the 8 cats with FSGS in this study. Based on histopathology and clinicopathologic data it seems most likely that FSGS in these 8 cats were likely secondary, or adaptive, to loss of renal mass.

In the present study, proteinuria was an uncommon finding and typically present in later stages of disease. Despite the infrequency of proteinuria in CKD cats, an association with increased severity of tubular degeneration, inflammation, fibrosis, tubular epithelial single cell necrosis and decreased normal parenchyma was detected. Similarly, positive correlations between severity of proteinuria and tubular epithelial injury, interstitial inflammation and fibrosis have been found in humans.<sup>32</sup> Protein exposure to tubular epithelial cells perpetuates renal

injury by direct damage to these cells or indirectly through production of proinflammatory and profibrotic cytokines.<sup>32-34</sup>

Cats with glomerular lesions had an average UPC greater ( $1.3 \pm 1.8$ ) than those cats without glomerular lesions ( $0.2 \pm 0.1$ ), however, a  $UPC > 2$  was only present in 3 cats. These were late stage (Stage III: n=1, Stage IV: n=2) and glomerular lesions were marked (e.g. MPGN pattern and TMA). A  $UPC > 2$  typically indicates glomerular disease while tubular reabsorption defects are suspected if  $< 2$ .<sup>35</sup> These data suggest that proteinuria in study cats is unlikely a result of primary glomerular disease in a majority of cases and is more likely tubular in origin. In this study, proteinuria was more common in late stage cats implying that it is a consequence rather than an initiator of disease.

Mineralization of Bowman's capsule and tubular basement membranes was more frequent in cats with more severe renal disease (i.e. Stages III and IV) than those with milder disease (Stages I and II). While calcium-phosphorus products (CPP) were not evaluated in the current study, mineralization may be the result of an increased CPP secondary to late--stage renal disease.<sup>36, 37</sup>

A novel glomerular lesion identified in this report was thrombotic microangiopathy (TMA). This cat presented for acute onset of ataxia and blindness. Systolic blood pressure was 190 mm Hg at presentation with severe proteinuria (UPC 4.8) and a creatinine of 3.2 mg/dL. Histologically, scattered glomeruli had endothelial swelling with occlusion of capillary lumina which is a characteristic feature of the TMA variant glomerular endotheliosis.<sup>38, 39</sup> Endotheliosis diminishes filtration and thus decreases overall glomerular filtration rate (GFR) in affected individuals.<sup>38</sup> Endotheliosis is often seen in women due to pre-eclampsia with clinical

hypertension and proteinuria. Although, unrelated to pregnancy in the cat reported here, confirmed hypertension may have resulted in endothelial injury with endotheliosis. The relationship of this to feline CKD is unknown.

Vascular lesions other than fibrointimal hyperplasia and hyperplastic arteriolosclerosis were uncommon. Fibrointimal hyperplasia appeared as segmental to circumferential thickening of the tunica intima accompanied by a discontinuous internal elastic lamina. It was present in over half of all CKD cats as well as in young normal cats, and did not differ among stages of CKD. Fibrointimal hyperplasia has been associated with hypertension but is indistinguishable from similar lesions in aging, normotensive human patients.<sup>40, 41</sup> Ultimately, vascular lesions associated with hypertension may lead to glomerular damage, sclerosis, tubular atrophy, and interstitial fibrosis.<sup>42</sup> In the present study, however, hypertensive cats were not more likely to be affected by fibrointimal hyperplasia than normotensive cats. In a study evaluating lesions in the aging feline kidney, vascular lesions were infrequent (6/600 cats), although lesion detection may have been limited in that study by the absence of histochemical stains.<sup>6</sup> In a recent study assessing renal histologic lesions in diabetic cats, vascular lesions were infrequent, with only 4 cats affected by arterial hypertrophy and a single cat with vascular thickening and splitting.<sup>4</sup> Lesions were not significantly different between those cats with or without diabetes mellitus.<sup>4</sup> Lastly, in the present study fibrointimal hyperplasia was prevalent in young, non-azotemic cats (6/11). From these data, the relationship of this vascular lesion to feline kidney disease is uncertain.

Hyperplastic arteriolosclerosis, a feature of systemic hypertension thought to be due to microvascular injury, was found in 48% of normotensive cats with CKD. This is in contrast to a previous report of 3% in normotensive CKD cats.<sup>7</sup> The reason for this discrepancy is not clear,

but may indicate that systemic blood pressure does not adequately represent local renal hemodynamics in cats. For example, in a previous study, cats with CKD had significantly higher renal vascular resistance than cats without CKD, despite no difference in systemic blood pressure between groups, as well as no correlation between systemic blood pressure and renal arterial resistance indices.<sup>43</sup> In contrast, in humans, indices of vascular resistance (RI) are associated with the severity and progression of CKD and RI correlates with systemic blood pressure. The reason for the difference between species is unclear but increased RI may be a more accurate measurement of local renal hemodynamics in cats.

Irregularly-sized lipid vacuoles were frequent within tubular epithelium and free within the interstitium of CKD cats in this study. Interstitial lipid is thought to originate from tubular lipid after rupture of basement membranes and cell lysis.<sup>44</sup> The role of tubular lipidoses in feline CKD has not been determined. Given that many different lipids have identical histologic appearances, it is unclear whether the larger lipid vacuoles and lipid casts are simply due to coalescence of smaller vacuoles from normal feline tubules or if they are composed of different types of lipids.

## REFERENCES

1. Marino CL, Lascelles BD, Vaden SL, et al. Prevalence and classification of chronic kidney disease in cats randomly selected from four age groups and in cats recruited for degenerative joint disease studies. *J Feline Med Surg* 2013.
2. Lulich J, Osborne C, O'Brien T, et al. Feline renal failure: questions, answers, questions. *Compendium on Continuing Education for the Practicing Veterinarian* 1992;14(2):26.
3. Atkins RC. The epidemiology of chronic kidney disease. *Kidney Int Suppl* 2005(94):S14-18.
4. Zini E, Benali S, Coppola L, et al. Renal Morphology in Cats With Diabetes Mellitus. *Vet Pathol* 2014.
5. DiBartola SP, Rutgers HC, Zack PM, et al. Clinicopathologic findings associated with chronic renal disease in cats: 74 cases (1973-1984). *J Am Vet Med Assoc* 1987;190(9):1196-1202.
6. Lawler DF, Evans RH, Chase K, et al. The aging feline kidney: a model mortality antagonist? *J Feline Med Surg* 2006;8(6):363-371.
7. Chakrabarti S, Syme HM, Brown CA, et al. Histomorphometry of feline chronic kidney disease and correlation with markers of renal dysfunction. *Vet Pathol* 2013;50(1):147-155.
8. Elliott J, Barber PJ. Feline chronic renal failure: clinical findings in 80 cases diagnosed between 1992 and 1995. *J Small Anim Pract* 1998;39(2):78-85.
9. Polzin DJ. Chronic kidney disease in small animals. *Vet Clin North Am Small Anim Pract* 2011;41(1):15-30.
10. Polzin DJ. Evidence-based step-wise approach to managing chronic kidney disease in dogs and cats. *J Vet Emerg Crit Care (San Antonio)* 2013;23(2):205-215.
11. Novartis Animal Health Inc. IRIS staging CKD. <http://www.iris-kidney.com/guidelines/staging.shtml> (2013, accessed 1 April 2015).
12. Boyd LM, Langston C, Thompson K, et al. Survival in cats with naturally occurring chronic kidney disease (2000-2002). *J Vet Intern Med* 2008;22(5):1111-1117.
13. Farris AB, Adams CD, Brousides N, et al. Morphometric and visual evaluation of fibrosis in renal biopsies. *J Am Soc Nephrol* 2011;22(1):176-186.
14. Hewitson TD, Darby IA, Bisucci T, et al. Evolution of tubulointerstitial fibrosis in experimental renal infection and scarring. *J Am Soc Nephrol* 1998;9(4):632-642.

15. Hewitson TD. Renal tubulointerstitial fibrosis: common but never simple. *Am J Physiol Renal Physiol* 2009;296(6):F1239-1244.
16. Nadasdy T, Sedmak D. Acute and Chronic Tubulointerstitial Nephritis. In: Jennette JC, Olson JL, Schwartz MM, et al., eds. *Heptinstall's Pathology of the Kidney*. Vol II. 6th ed. Philadelphia, PA: Lippincott Williams & Wilkins; 2007:1083-1137.
17. White JD, Malik R, Norris JM. Feline chronic kidney disease: can we move from treatment to prevention? *Vet J* 2011;190(3):317-322.
18. Linnetz EH, Graves TK. Glomerular filtration rate in general small animal practice. *Compend Contin Educ Vet* 2010;32(10):E1-5; quiz E6.
19. Miyamoto K. Use of plasma clearance of iohexol for estimating glomerular filtration rate in cats. *Am J Vet Res* 2001;62(4):572-575.
20. Brown SA, Crowell WA, Brown CA, et al. Pathophysiology and management of progressive renal disease. *Vet J* 1997;154(2):93-109.
21. Brown SA, Brown CA. Single-nephron adaptations to partial renal ablation in cats. *Am J Physiol* 1995;269(5 Pt 2):R1002-1008.
22. Brenner BM. Nephron adaptation to renal injury or ablation. *Am J Physiol* 1985;249(3 Pt 2):F324-337.
23. Adams LG, Polzin DJ, Osborne CA, et al. Influence of dietary protein/calorie intake on renal morphology and function in cats with 5/6 nephrectomy. *Lab Invest* 1994;70(3):347-357.
24. Ross LA, Finco DR. Relationship of selected clinical renal function tests to glomerular filtration rate and renal blood flow in cats. *Am J Vet Res* 1981;42(10):1704-1710.
25. Minkus G, Reusch C, Horauf A, et al. Evaluation of renal biopsies in cats and dogs-histopathology in comparison with clinical data. *Journal of Small Animal Practice* 1994;35:465-472.
26. Zhou XJ, Rakheja D, Yu X, et al. The aging kidney. *Kidney Int* 2008;74(6):710-720.
27. Aresu L, Zanatta R, Luciani L, et al. Severe renal failure in a dog resembling human focal segmental glomerulosclerosis. *J Comp Pathol* 2010;143(2-3):190-194.
28. Wimberly HC, Antonovych TT, Lewis RM. Focal glomerulosclerosis-like disease with nephrotic syndrome in a horse. *Vet Pathol* 1981;18(5):692-694.
29. D'Agati VD, Kaskel FJ, Falk RJ. Focal segmental glomerulosclerosis. *N Engl J Med* 2011;365(25):2398-2411.

30. Thomas DB, Franceschini N, Hogan SL, et al. Clinical and pathologic characteristics of focal segmental glomerulosclerosis pathologic variants. *Kidney Int* 2006;69(5):920-926.
31. Aresu L, Benali S, Ferro S, et al. Light and electron microscopic analysis of consecutive renal biopsy specimens from leishmania-seropositive dogs. *Vet Pathol* 2013;50(5):753-760.
32. Hill GS, Delahousse M, Nochy D, et al. Proteinuria and tubulointerstitial lesions in lupus nephritis. *Kidney Int* 2001;60(5):1893-1903.
33. Benigni A, Remuzzi G. How renal cytokines and growth factors contribute to renal disease progression. *Am J Kidney Dis* 2001;37(1 Suppl 2):S21-24.
34. Perico N, Codreanu I, Schieppati A, et al. Pathophysiology of disease progression in proteinuric nephropathies. *Kidney Int Suppl* 2005(94):S79-82.
35. Harley L, Langston C. Proteinuria in dogs and cats. *Can Vet J* 2012;53(6):631-638.
36. McLeland SM, Lunn KF, Duncan CG, et al. Relationship among serum creatinine, serum gastrin, calcium-phosphorus product, and uremic gastropathy in cats with chronic kidney disease. *J Vet Intern Med* 2014;28(3):827-837.
37. Llach F, Velasquez Forero F. Secondary hyperparathyroidism in chronic renal failure: pathogenic and clinical aspects. *Am J Kidney Dis* 2001;38(5 Suppl 5):S20-33.
38. Stillman IE, Karumanchi SA. The glomerular injury of preeclampsia. *J Am Soc Nephrol* 2007;18(8):2281-2284.
39. Moake JL. Thrombotic microangiopathies. *N Engl J Med* 2002;347(8):589-600.
40. Jain M. Hypertensive renal disease: Histological aspects. *Clinical Queries: Nephrology* 2013;2:6.
41. Martin JE, Sheaff MT. Renal ageing. *J Pathol* 2007;211(2):198-205.
42. Marín R, Gorostidi M, Fernández-Vega F, et al. Systemic and glomerular hypertension and progression of chronic renal disease: the dilemma of nephrosclerosis. *Kidney Int Suppl* 2005(99):S52-56.
43. Novellas R, Ruiz de Gopegui R, Espada Y. Assessment of renal vascular resistance and blood pressure in dogs and cats with renal disease. *Vet Rec* 2010;166(20):618-623.
44. Lucke VM. Renal disease in the domestic cat. *J Pathol Bacteriol* 1968;95(1):67-91.

## CHAPTER 4: RELATIONSHIP BETWEEN SERUM CREATININE, SERUM GASTRIN, CALCIUM-PHOSPHORUS PRODUCT AND UREMIC GASTROPATHY IN CATS WITH CHRONIC KIDNEY DISEASE

### 4.1 Chapter Summary

Chronic kidney disease (CKD) in cats is associated with gastrointestinal signs commonly attributed to uremic gastropathy. Consequently, patients are often treated with antacids and gastrointestinal protectants. This therapeutic regime is based on documented gastric lesions in uremic humans and dogs; however the incidence of uremic gastropathy in cats is unknown. The objective of this study was to determine the prevalence and characterize gastric lesions in cats with CKD. In addition, histologic lesions were compared with serum creatinine, calcium-phosphorus product (CPP) and serum gastrin concentrations. A total of 37 CKD cats and 12 non-azotemic control cats were evaluated. Gastric ulceration, hemorrhage, edema, and vascular injury, were not observed in cats with CKD. The most significant gastric lesions in CKD cats were fibrosis and mineralization. Sixteen CKD cats (43%) had evidence of gastric fibrosis of varying severity and 14 CKD cats (38%) had gastric mineralization. Cats with CKD were more likely to have gastric fibrosis and mineralization than non-azotemic controls ( $p=0.005$  and  $p=0.021$ , respectively). Only cats with moderate and severe azotemia had gastric mineralization. CPP was correlated to disease severity; severely azotemic CKD cats had significantly greater CPP when compared to non-azotemic controls, and to mildly and moderately azotemic cats ( $p<0.05$ ). Gastrin concentrations were significantly greater in CKD cats when compared to non-azotemic controls ( $p=0.003$ ) but elevated concentrations were not associated with gastric ulceration.



## 4.2 Introduction

Chronic kidney disease (CKD) is a common clinical problem that affects a significant proportion of aged cats.<sup>1</sup> Progression of CKD typically results in uremia, a syndrome that manifests clinically as a variety of signs, including weight loss, vomiting, inappetance, and anorexia.<sup>1-4</sup> These clinical signs are frequently ascribed to uremic gastritis, a condition attributed to the presence of uremic toxins and gastric hyperacidity secondary to hypergastrinemia.<sup>5</sup> However there are significant gaps in our understanding of the prevalence and pathogenesis of feline uremic gastrointestinal disease.

Uremic gastritis was first described in 1934 from autopsies in 135 uremic human patients; lesions varied from mild edema to hemorrhage, ulceration, and necrosis.<sup>6</sup> Although complications of uremia such as gastritis, ulceration, and hemorrhage are common in humans,<sup>7</sup> they appear to be less common and less severe in dogs.<sup>8</sup> In 1979 Cheville described vascular injury, calcification, mucosal edema, and necrosis in the stomachs of a small group of uremic dogs with renal amyloidosis and pyelonephritis.<sup>9</sup> In a more recent study, mucosal necrosis was found to occur less frequently, while mineralization, edema and vascular injury were frequently present in dogs with renal disease.<sup>8</sup> The prevalence of uremic gastritis has not been systematically evaluated in cats. A report of 70 cats with acute renal toxicity due to contamination of food with melamine and cyanuric acid indicated that a small percentage of animals had gastric mineralization, but ulceration was not observed.<sup>10</sup> In addition, an experimental study of Easter lily poisoning in cats reported an absence of gastric lesions in 10 cats that were examined by necropsy.<sup>11</sup> Finally, in a case series and literature review of gastric ulceration in cats, CKD was not found to be an underlying cause.<sup>12</sup>

Cats with CKD have been shown to have elevated concentrations of gastrin that increase with the severity of renal failure,<sup>5</sup> but the relationship between gastrin, gastric acid secretion, and gastric pathology has not been investigated. Gastrin is secreted by G cells in the gastric antrum and stimulates the secretion of gastric acid by the parietal cells. The presence of gastric acid results in negative feedback to decrease the secretion of gastrin. In humans and dogs, gastrin is excreted by the kidneys, and it is hypothesized that as renal function declines, hypergastrinemia develops, resulting in gastric hyperacidity.<sup>5</sup> Cats that have gastrin-secreting tumors with levels of hypergastrinemia similar to those found in cats with CKD have significant gastric pathology; however no study has shown this to be the case in cats with CKD.<sup>12</sup> Even in humans, the development of hyperacidity in association with CKD appears to be inconsistent, and may be related to the presence of *Helicobacter spp.* infection.<sup>13</sup> Thus there is very little available evidence on which to base recommendations for the use of acid-reducing medications such as H<sub>2</sub> blockers, proton pump inhibitors or sucralfate in cats with uremia.<sup>1-4</sup> The aims of this study were to evaluate the type and prevalence of histopathologic lesions in the stomach of cats with CKD, and to determine whether degree of azotemia, calcium-phosphorus products and serum gastrin concentrations are correlated with gastric pathology. A better understand of gastric pathology in CKD cats will facilitate the refinement of medical management strategies for gastrointestinal symptoms.

## **4.3 Material and Methods**

### *4.3.1 Animals*

Feline CKD patients necropsied at the Colorado State University Veterinary Teaching Hospital (CSU-VTH) between years 2009-2012 were prospectively included in the study. Inclusion criteria included historical and clinicopathological findings consistent with CKD, a complete

necropsy with evaluation of all major organs, and a serum biochemistry profile and urinalysis performed within 2 weeks of euthanasia or death. All owners signed the CSU-VTH consent form for euthanasia (when applicable) and educational necropsy; no cats were euthanized for the purpose of this study. Exclusion criteria included concurrent primary gastrointestinal disease, such as neoplasia, administration of non-steroidal anti-inflammatory drugs or glucocorticoids within two weeks prior to euthanasia and ureteral obstruction identified as a post-renal cause of azotemia. CKD cats were defined as those with creatinine over 1.6 mg/dL, a urine specific gravity (USG) of less than 1.035, and evidence of changes consistent with CKD on renal histopathology. Cats were grouped based on severity of azotemia as follows: mild (1.6-2.8 mg/dL), moderate (2.9-5.0 mg/dL), and severe (>5.0 mg/dL). Although this grouping is in accordance with IRIS Staging system,<sup>2</sup> staging could not officially be performed as two serum creatinine measurements during a clinically stable period were not available for all cats. Labwork performed when marked dehydration or clinical decompensation was noted in the medical record was not included in analysis. Information regarding administration of antacid medications and phosphate binders was recorded. Non-azotemic control cats were young, apparently healthy cats in good body condition and free of reported gastrointestinal disease that were euthanized at a local humane society, according to humane society guidelines and protocols. Study samples were obtained from these cats after euthanasia, and no cats were euthanized for the purpose of this study. Age was estimated by humane society staff based on surrender history and/or dental assessment. Non-azotemic status was defined as cats with urine specific gravity (USG) >1.035, creatinine <1.6 mg/dL and no evidence of CKD on renal histopathology.

#### *4.3.2 Clinicopathologic Data*

For the CKD cats, serum creatinine concentration, serum total calcium concentration, serum phosphorus concentration and USG values measured within 2 weeks of euthanasia were obtained from the medical record. Calcium x phosphorus product (CPP) was calculated as serum total calcium concentration multiplied by serum phosphorus concentration and expressed in  $\text{mg}^2/\text{dL}^2$ . For the non-azotemic control cats, serum creatinine, total calcium and phosphorus, serum gastrin, and USG were obtained on samples obtained immediately post-mortem via cardiac venipuncture and urinary bladder cystocentesis.

#### *4.3.3 Gastrin Assay*

For measurement of serum gastrin concentrations, serum left over from biochemical analysis was collected, stored at  $-80^{\circ}\text{C}$ , and shipped to Michigan State University for analysis. Circulating concentrations of gastrin were measured with a commercially available radioimmunoassay kit, with assay procedures performed according to the manufacturer's protocol (Gastrin [ $^{125}\text{I}$ ] Radioimmunoassay Kit, MP Biomedicals, Diagnostics Division, Orangeburg, NY 10692-1294). Synthetic human gastrin17-I standards were used to make the displacement curve, with the highest standard of 1000 ng/L. The manufacturer reported the following percent cross reactivity with related compounds: gastrin 17-I (100%), gastrin 17-II (77%), gastrin 34-I (42%), gastrin 5-17 (54%), cholecystokinin-PZ ( $<0.1\%$ ), and cholecystokinin-8 (10.9%). The manufacturer-reported sensitivity of detection was 3 ng/L. For intra-assay repeatability (10 replicates), the % coefficient of variation was 8.6% for a feline sample with a gastrin concentration of 45 ng/L. For inter-assay repeatability (10 replicates), the % coefficient of variation was 9.2% for a feline sample with a concentration of 54 ng/L. Three feline samples with higher concentrations of gastrin (461, 145, 124 ng/L) were diluted with 0 standard at rates of 1:2, 1:4, and 1:8. The

average recovery (observed/expected) at these dilutions was 121%, 130%, and 138%, respectively.

#### *4.3.4 Gross and Histopathologic Evaluation*

Complete necropsies were performed on all animals with evaluation of all major organs. Specifically, the stomach was incised along the lesser curvature from cardia to pylorus and grossly evaluated for the presence of edema, hemorrhage, ulceration or other visible abnormalities. Kidneys were cut longitudinally along the long axis (cranial to caudal pole).

##### *4.3.4.1 Gastric Histopathology*

Three full thickness cross-sections from five anatomic locations of the stomach (cardia, fundus, body, antrum, and pylorus) were sampled in a routine manner. Tissues were preserved in 10% neutral buffered formalin, paraffin embedded, and sectioned at 5 $\mu$ m. All sections were stained with standard hematoxylin and eosin histochemical stain and evaluated independently by 2 pathologist (SM and CD), blinded to clinical data. For final lesion score, discrepancies between the pathologists were resolved by joint review of tissues. Lesion description and scoring rationale are outlined in Table 4.1. All sections were systematically reviewed for the presence or absence of histologic changes consistent with uremic gastropathy as observed in dogs (i.e. amyloid, edema, vascular fibrinoid change, fibrosis and mineralization).<sup>8,9</sup> An overall qualitative score was given for mineralization in all gastric sections highlighted by Von Kossa stain. Evaluation of fibrosis utilizing Masson's trichrome was restricted to sections from the gastric body, and a semi-quantitative scoring scheme for fibrosis was adapted from WSAVA gastrointestinal evaluation guidelines.<sup>14,15</sup> Finally, sections from the gastric body were evaluated for the presence and character of superficial mucosal inflammation, ulceration and/or erosion, and presence of

lamina propria lymphoid nodules. Overall inflammatory infiltrates in the body, if present, were graded using a modification of previously published guidelines and visual scoring scale.<sup>14,16</sup>

#### *4.3.4.2 Renal Histopathology*

Renal sections from CKD and control cats were examined independently by two pathologists blinded to clinical and gastric findings for confirmation of CKD and lesion scoring. Descriptions of lesion scoring are outlined in Table 4.1. For final lesion score, discrepancies between the pathologists were resolved by joint review of tissues. Semi-quantitative analysis for the presence of amyloid (Congo red) and fibrosis (Masson's trichrome) in the kidney were given a score from 0-3 by each pathologist.

#### *4.3.5 Statistical Analysis*

Serum creatinine concentration, USG, CPP, serum gastrin concentration and gastric lesion scores were compared between non-azotemic control cats and CKD cats with mild, moderate, or severe azotemia using one-way analysis of variance (ANOVA) and Bonferroni's multiple comparison post hoc test with Prism software (Prism 5, GraphPad, La Jolla, CA). Scoring consensus between the two pathologists for each category was evaluated by Cohen's kappa coefficient with SAS software (SAS 9.1.3, SAS Institute Inc., Cary, NC). Comparison between individual groups (presence of gastric lesion scores in normal versus CKD cats, the CPP of CKD cats with gastric mineralization versus those without gastric mineralization, and cats receiving phosphate binders or antacids versus those who were not) was performed using a Mann-Whitney test with Prism software (Prism 5, GraphPad, La Jolla, CA). Statistical significance for all analyses was set at  $p \leq 0.05$ .

Table 4.1 Scoring system for gastric and renal lesions

Category	Score
Lesion Description	Score
<b>Stomach</b>	
<b>Amyloid</b>	
Absent	0
Rare	1
<50% of the section	2
>50% of the section	3
<b>Edema</b>	
Absent	0
Rare	1
<50% of the section affected	2
>50% of the section affected	3
<b>Vascular fibrinoid change</b>	
Absent	0
Rare, focal	1
Segmental to regionally extensive	2
Diffusely affecting a majority of vessels	3
<b>Mineralization</b>	
Absent	0
Scattered and/or patchy	1
Multifocal to coalescing	2
Diffuse/serpentine	3
<b>Fibrosis/Mucosal atrophy</b>	
Glands closely packed, separated by scant connective tissue	0
Mild increase in proprial connective tissue	1
Separation of glands and moderate thickening of lamina propria	2
Marked lamina propria connective tissue with loss of glands	3

Category	Score
Lesion Description	Score
<b>Stomach</b>	
<b>Superficial mucosal inflammation</b>	
No inflammation	0
<30% of lamina propria populated by leukocytes	1
30-60% of lamina propria affected	2
>60% of lamina propria infiltrated by leukocytes that aggregate and crowd glands	3
<b>Mucosal erosions or ulcerations</b>	
Yes	1
No	2
<b>Lymphoid nodules</b>	
Yes	1
No	2
<b>Kidney</b>	
<b>Amyloid</b>	
Absent	0
Rare	1
<50% of glomeruli affected	2
>50% affected and/or diffuse	3
<b>Interstitial Fibrosis</b>	
Absent	0
<25% of the section	1
25-50% of the section	2

## **4.4 Results**

### *4.4.1 Animals*

Fifty-nine cats with CKD were necropsied during this time period; 37 met the inclusion criteria for the study. Twenty-two were excluded for the following reasons: routine gastric samples not obtained (7), no laboratory testing near the time of euthanasia or marked dehydration/decompensation at time laboratory data was collected (7), intestinal neoplasia (6), autolysis (1) and FIV positive status (1). In total, 9 mildly azotemic cats, 9 moderately azotemic cats, 19 severely azotemic cats, and 12 non-azotemic controls were included in the study.

The mean age for CKD cats was 13.8 years, ranging from 5 to 21 years of age. There were 24 spayed females and 13 castrated male cats. All but two CKD cats were euthanized due to poor or declining quality of life. The remaining two cats died at home, and were kept cold and submitted for necropsy within 12 hours of death. Five of the CKD cats included in this study were receiving famotidine antacid therapy at the time of death (mild azotemia: 2 cats; moderate azotemia: 1 cat; severe azotemia 2 cats), while 9 were receiving oral aluminum hydroxide phosphate binder therapy (mild azotemia: 1 cat; moderate azotemia: 1 cat; severe azotemia 7 cats). Average estimated age of control cats was 2.7 years (range 0.8-4 years of age). There were 2 male intact and 1 female intact cats; 3 neutered male cats and 6 spayed female control cats. Control cats had no known history of renal disease, gastrointestinal disease or medication administration.

### *4.4.2 Clinicopathological Data*

Serum creatinine, USG, CPP and gastrin results for all groups are summarized in Table 4.2. As expected, when analyzed with a one-way ANOVA, serum creatinine values were significantly higher in severely azotemic CKD cats compared to mild and moderately azotemic groups



( $p < 0.05$ ), while non-azotemic control serum creatinine values were significantly lower than those of moderately and severely azotemic CKD cats ( $p < 0.05$ ). Urine specific gravity in non-azotemic control cats was significantly greater than USG in each CKD group ( $p < 0.05$ ) when analyzed using a one-way ANOVA. Calcium x phosphorus product was correlated to disease severity; when analyzed using a one-way ANOVA severely azotemic CKD cats had significantly greater CPP when compared to non-azotemic controls, mildly azotemic cats and moderately azotemic cats ( $p < 0.05$ ) (Figure 4.1). No change in statistical significance was noted when cats that had been administered phosphate binders were removed from analysis. The CPP of severely azotemic cats receiving phosphate binders was not significantly different from severely azotemic cats not receiving phosphate binders when compared with a Mann Whitney test. Although cats with gastric mineralization had higher CPP relative to cats without mineralization ( $114.6 \text{ mg}^2/\text{dL}^2$  and  $82.5 \text{ mg}^2/\text{dL}^2$  respectively) this difference was not statistically significant ( $p = 0.058$ ).

Circulating serum gastrin concentrations in cats with CKD were significantly higher than serum gastrin concentrations in control cats ( $p = 0.003$ ) when compared using a Mann Whitney test. When all groups were compared using a one-way ANOVA, cats with severe azotemia had significantly higher serum gastrin concentrations than the control group ( $p < 0.05$ , Figure 4.2). No change in statistical significance was noted when cats that had been administered antacids were removed from analysis. The median serum gastrin concentration of azotemic cats receiving antacids was not significantly different from the median serum gastrin concentration of those azotemic cats not receiving antacids when compared with a Mann Whitney test.

Table 4.2 Summary of clinicopathologic data in control and CKD cats

Parameter	Azotemia			
	Control (0.8-1.5 mg/dL)	Mild (1.6-2.8 mg/dL)	Moderate (2.9-5.0 mg/dL)	Severe (>5.0 mg/dL)
<b>Creatinine</b>				
n	12	9	9	19
Mean	1.2 mg/dL	2.2 mg/dL	3.9 mg/dL	9.1 mg/dL
Range	0.8-1.5 mg/dL	1.7-2.7 mg/dL	3.0-4.6 mg/dL	5.5-15.5 mg/dL
<b>Urine Specific Gravity</b>				
n	12	9	8	19
Mean	1.066	1.016	1.015	1.012
Range	1.048-1.084	1.009-1.036	1.012-1.020	1.007-1.017
<b>Ca (mg/dL)</b>				
n	12	8	8	18
Mean	9.18	10.86	11.31	10.86
Range	8.1-10.1	8.5-13.0	9.1-15.0	8.5-14.3
<b>Phos (mg/dL)</b>				
n	12	8	8	18
Mean	4.71	4.90	6.21	11.46
Range	3.7-6.0	3.6-8.6	2.7-10.0	3.4-20.2
<b>Ca (mg/dL) X Phos (mg/dL)</b>				
n	12	8	8	18
Mean	43.29	53.71	70.44	122.13
Range	34.02-58.80	32.30-92.90	29.43-119.60	32.98-208.19
<b>Gastrin (pg/ml)</b>				
n	9	3	5	15
Mean	46.22	143	73.6	148.73
Range	17-94	24-234	42-191	39-288

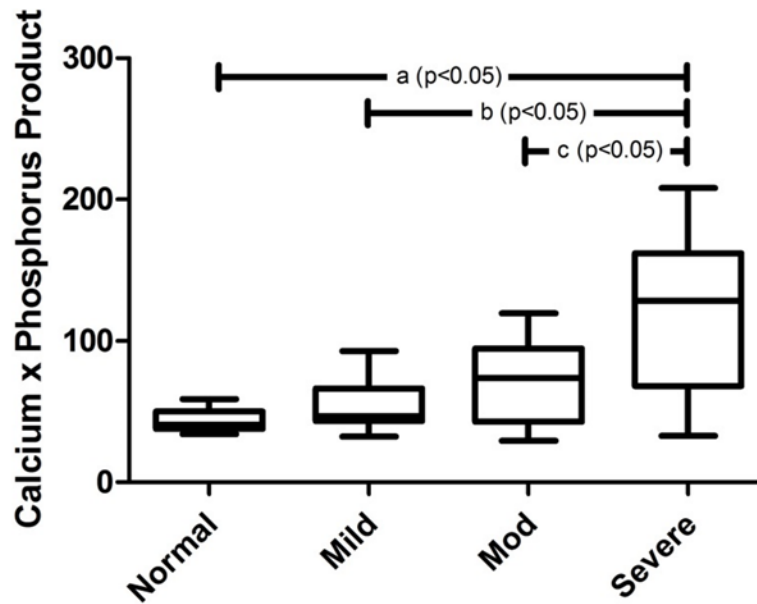


Figure 4.1 Calcium x phosphorus product (CPP) is correlated to disease severity. Severely azotemic CKD cats had significantly greater CPP when compared to non-azotemic controls (a), mildly azotemic cats (b) and moderately azotemic cats (c) when analyzed with a one way ANOVA with Bonferroni's post hoc analysis

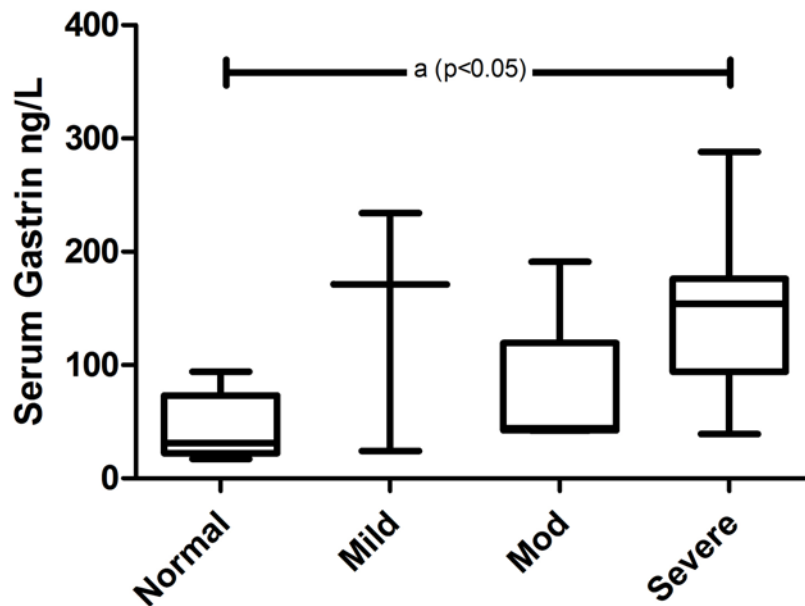


Figure 4.2 Serum gastrin levels are significantly elevated in severely azotemic CKD cats. Cats with severe azotemia had significantly higher serum gastrin concentrations when compared to non-azotemic controls (a) when analyzed with a one way ANOVA with Bonferroni's post hoc analysis ( $p < 0.05$ ).

#### 4.4.3 Histopathology

Inter-observer variation in histologic scoring was compared between pathologists, yielding an average kappa coefficient of 0.84 (range 0.78-0.91) for all gastric and renal histologic categories. Of the 37 CKD cats and 12 controls, three sections from each anatomic location (cardia, fundus, body, antrum, and pylorus) were evaluated with the exception of two CKD cats; only one section from the body was available for evaluation in these cases. Bilateral kidneys were available for evaluation on all study cats with the exception of one CKD cat that only had the right kidney available for histologic evaluation.

Gastric lesion scores in CKD and control cats are summarized in Table 4.3. No gross or histologic evidence of gastric mucosal ulcerations, hemorrhage, or edema were observed in either CKD or control gastric tissues. No histologic evidence of amyloid deposition, edema, or vascular fibrinoid change was observed in CKD or control gastric tissues. Gastric fibrosis occurred more frequently in CKD cats when compared to controls using a Mann Whitney test ( $p=0.005$ ). When all groups were compared using a one-way ANOVA, there was a statistically significant difference in the degree of fibrosis in severely azotemic CKD cats when compared to the non-azotemic control group ( $p<0.05$ , Figure 4.3). Fibrosis was absent in the stomachs of control cats while some degree of fibrosis occurred in 16/37 (43%) of CKD cats (Figure 4.4). Fibrosis was typically superficial, with variable expansion of the lamina propria, and minimal nesting of pit and glandular cells in severe cases. Three of nine mildly azotemic cats had a mild increase in superficial proprial fibrous connective tissue (Figure 4.4.2). A single mildly azotemic cat had moderate thickening of proprial fibrous connective tissue with separation of superficial glands (Figure 4.4.3). Two moderately azotemic CKD cats and 8 severely azotemic cats had mild

gastric fibrosis. One severely azotemic cat had moderate lamina propria fibrous thickening and one severely azotemic cat had marked lamina propria fibrous thickening.

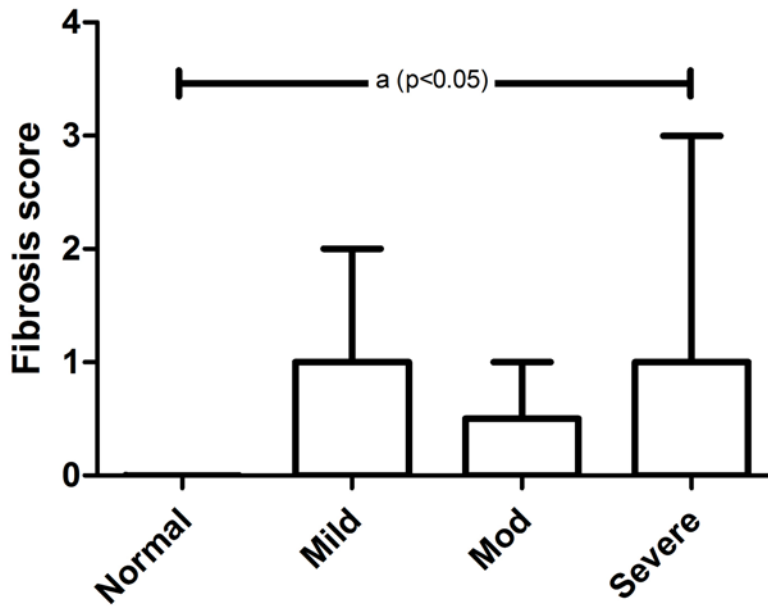


Figure 4.3 Gastric glandular atrophy and fibrosis occurred more frequently in CKD cats. Fibrosis scores in severely azotemic CKD cats were significantly increased when compared to the non-azotemic controls (a) using a one way ANOVA with Bonferroni's post hoc analysis ( $p<0.05$ ).

Table 4.3 Summary of gastric lesions in control and CKD cats.

Stomach Lesions	Azotemia			
	Controls (<1.6 mg/dL)	Mild (1.6-2.8 mg/dL)	Moderate (2.9-5.0 mg/dL)	Severe (>5.0 mg/dL)
Amyloid	0	0	0	0
Edema	0	0	0	0
Fibrosis <sup>a</sup>				
0	12	5	7	9
1	0	3	2	8
2	0	1	0	1
3	0	0	0	1
Average score	0	0.56	0.22	0.68
Mineralization <sup>b,c</sup>				
0	12	9	5	9
1	0	0	0	1
2	0	0	2	3
3	0	0	2	6
Average score	0	0	1.11	1.32
Vascular Fibrinoid change	0	0	0	0
Superficial mucosal inflammation <sup>d</sup>				
0	4	0	1	3
1	6	7	7	12
2	2	2	1	4
3	0	0	0	0
Average score	0.83	1.22	1	1.05
Mucosal erosion/ulceration	0	0	0	0
Lymphoid nodules <sup>e</sup>	8	7	6	8

<sup>a</sup>Fibrosis scores and <sup>b</sup>mineralization scores for severely azotemic group statistically greater than control group (p<0.05)

<sup>c</sup>Mineralization scores for severely azotemic group statistically greater than mildly azotemic group (p<0.05)

<sup>d,e</sup>No statistical difference between any group

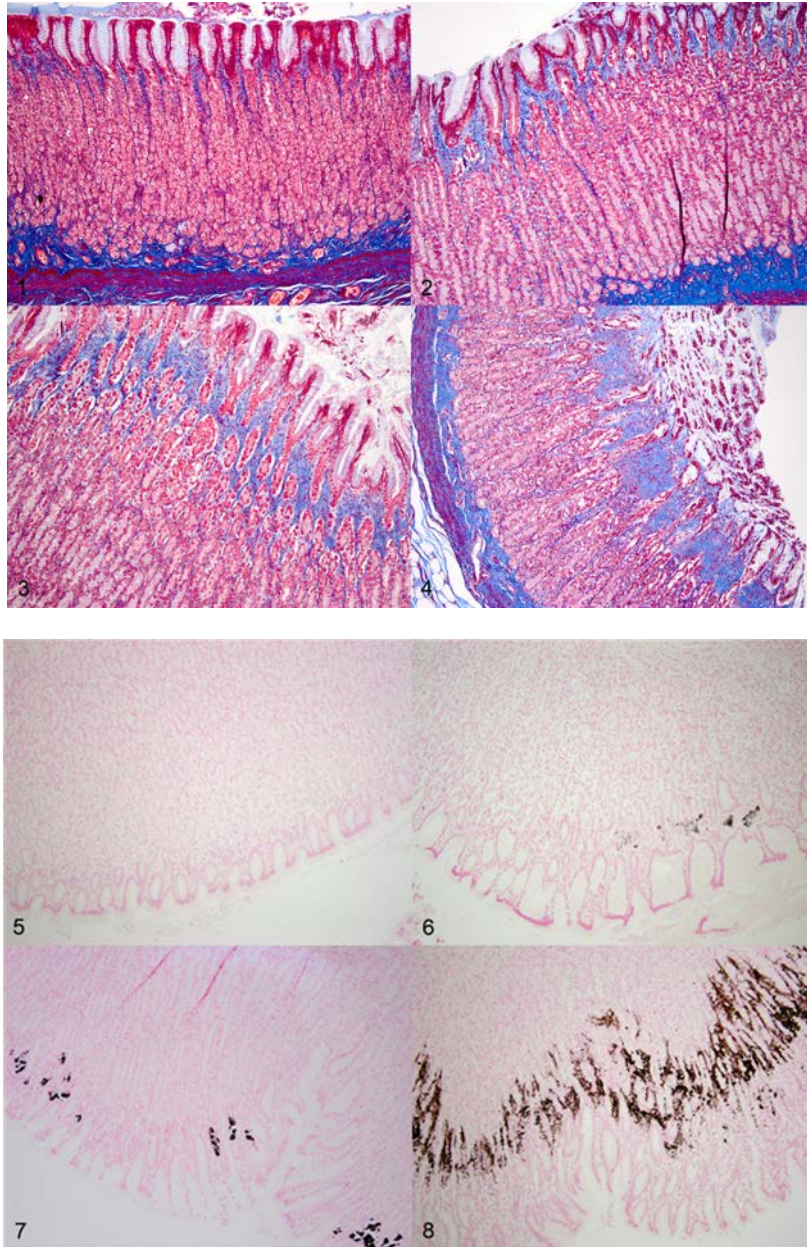


Figure 4.4 Representative examples of degrees of gastric fibrosis (1-4) and mineralization (5-8) detected in cats with chronic kidney disease (CKD) compared to non-azotemic controls. (1) Control cat stomach, body. Glands are tightly packed with minimal lamina propria connective tissue. Masson's trichrome. (2) Cat with CKD, body. Mild expansion of foveolae by lamina propria fibrous connective tissue. Masson's trichrome. (3) Cat with CKD, body. Moderate expansion of foveolae and gastric glands by lamina propria connective tissue. Masson's trichrome. (4) Cat with CKD, body. Marked separation and individualization of gastric glands by fibrous connective tissue. Masson's trichrome. (5) Control cat stomach, body. Absence of mineral within the mucosa. Von Kossa. (6) Cat with CKD, body. Mild, patchy mineralization. Von Kossa. (7) Cat with CKD, body. Moderate, multifocal to coalescing mineralization. Von Kossa. (8) Cat with CKD, body. Severe, diffuse, serpentine pattern of mineralization in the apical 1/2 to 1/3 of the mucosa. Von Kossa

Gastric mineralization was more likely to occur in cats with CKD than non-azotemic cats ( $p=0.0214$ ) when compared using a Mann Whitney test. When all groups were compared using a one-way ANOVA, gastric mineralization scores were significantly greater in cats with severe azotemia compared to non-azotemic and mildly azotemic cats ( $p<0.05$ , Figure 4.5). A total of 14 CKD cats (38%), all from the moderate and severe azotemia groups had gastric mineral of varying severity within the apical 1/3 to 1/2 of the mucosal lamina propria (Figure 4.4).

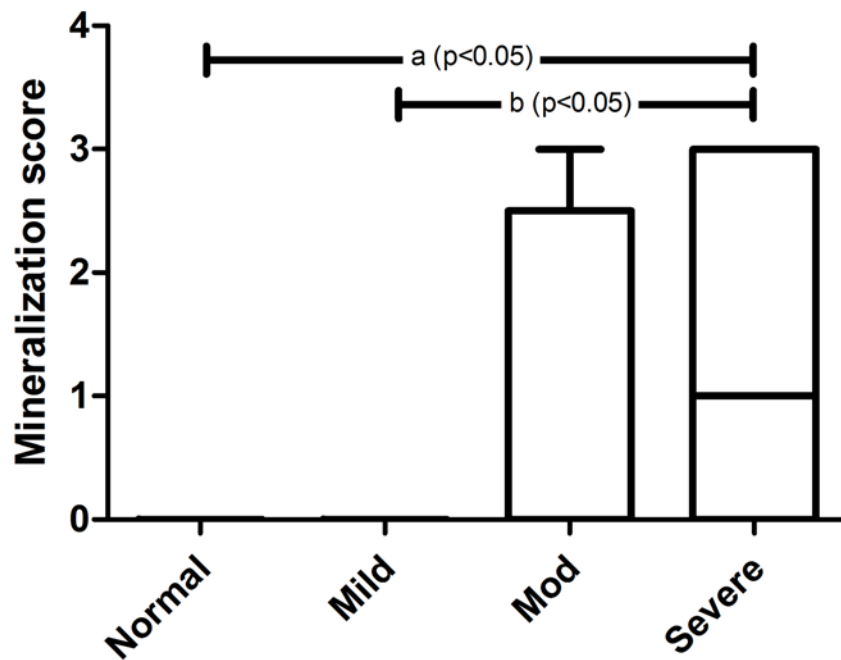


Figure 4.5 Gastric mineralization was present in moderately and severely azotemic CKD cats. Gastric mineralization scores were significantly greater in cats with severe azotemia when compared to non-azotemic and mildly azotemic cats using a one way ANOVA with Bonferroni's post hoc analysis ( $p<0.05$ ).



Within the gastric mucosa of 3 cats karyorrhectic debris was strictly associated with the presence of proprial mineral. Mineral was not found in sections of stomach from non-azotemic control or mildly azotemic CKD cats. Moderately azotemic cats had multifocal to coalescing (n=2) and diffuse (n=2) gastric mineral. Mineralization was evident in 10/19 cats (52%) of cats in the severe azotemia group. A single severely azotemic cat had mild, scattered gastric mucosal mineral. Diffuse, marked mucosal mineralization that formed a serpentine band across the mucosa was prominent in 6 cats with severe azotemia. The remaining 3 had multifocal to coalescing patches of mucosal mineral. In addition, 3 cats with gastric mineralization (moderate azotemia: 1 cat; severe azotemia: 2 cats) also had mineralization of gastric arteries and arterioles. One of these cats had vascular mineralization that was so severe that the tunica media and tunica intima of coronary arteries and the aorta were affected.

There was no statistically significant difference in inflammation scores between any groups. Lymphocytic aggregates forming nodules deep within the mucosal lamina propria with variable expansion were present in 21/37 (57%) CKD cats and 8/12 (67%) control cats. Follicles were not factored into presence or severity of inflammation in either group. Six control cats had mild inflammation and 2 had moderate inflammation, which was nearly exclusively lymphocytic in character. A single control cat had intraepithelial globular leukocytes present superficially. Severe inflammation was not detected in any control or CKD cat. Seven mildly azotemic cats had mild superficial inflammation which involved no more than 1/3 of the section. Two additional cats with mild azotemia had moderate inflammation involving 30-60% of the section. Leukocytic infiltrates primarily were mononuclear (lymphocytes with few plasma cells) while 5 cats had intraepithelial globular leukocytes that ranged from 0-6 per high-power field. The majority (7/9) of moderately azotemic cats had mild inflammation with only a single cat (1/9)

with moderate inflammation. Mononuclear inflammatory cells (predominantly lymphocytes with occasional macrophages and/or plasma cells) frequently aggregated around mineral when present in the moderately azotemic group of cats. Mild inflammation also predominated in cats with severe azotemia (12/19). An additional 4 cats with severe azotemia had moderate inflammation. Within the group of severely azotemic cats, infiltrates in addition to lymphocytes included frequent neutrophils and occasional eosinophils. In a single cat with severe azotemia, eosinophils were aggregated around mineral.

Renal lesions in the CKD group were consistent with those previously reported including interstitial fibrosis, interstitial nephritis, and tubular atrophy and glomerulosclerosis.<sup>17</sup> Frequency and severity of renal fibrosis in study cats are summarized in Table 4.4. The fibrosis score in CKD kidneys was significantly greater than that in controls ( $p < 0.001$ ) when compared using a Mann Whitney test. When groups were compared using a one-way ANOVA, renal fibrosis scores were significantly higher in all CKD groups in comparison to controls ( $p < 0.05$ ). Renal amyloidosis was not observed in either CKD or control groups.

Table 4.4 Summary of renal lesions in control and CKD cats.

Kidney Lesions	Azotemia								
	Control ( $< 1.6$ mg/dL)		Mild ( $1.6-2.8$ mg/dL)		Moderate ( $2.9-5.0$ mg/dL)		Severe ( $> 5.0$ mg/dL)		
	Kidney 1	Kidney 2	Kidney 1	Kidney 2	Kidney 1	Kidney 2	Kidney 1	Kidney 2	
Amyloid	0	0	0	0	0	0	0	0	0
Fibrosis <sup>a</sup>									
0	11	12	0	0	0	0	0	0	0
1	1	0	3	4	4	4	0	1	
2	0	0	4	5	3	4	17	12	
3	0	0	2	0	2	1	2	5	
Average score	0.08	0	1.89	1.56	1.78	1.67	2.11	2.22	

<sup>a</sup>Severity of renal fibrosis for all CKD groups were significantly greater than controls ( $p < 0.05$ )

## 4.5 Discussion

In this study CKD cats were more likely to have gastric mineralization, fibrosis, elevated CPP and increased serum gastrin levels than non-azotemic controls. Mineralization was only observed in cats with moderate and severe azotemia, and CPP increased significantly with degree of azotemia. Lesions in CKD cats were restricted to mucosal mineralization and fibrosis, while classic uremic gastropathy lesions such as gastric ulceration, amyloid deposition, edema, vascular fibrinoid change and hemorrhage were not observed in the cats examined. These findings are unique because no studies have previously reported the prospective and systematic evaluation of uremia-induced gastric lesions in cat with CKD. These findings also have important clinical implications as they suggest that gastrointestinal signs seen in CKD cats may be more likely to be the result of uremic toxins and centrally acting emetogens as opposed to pathology within the stomach.

Gastric mineralization was a common finding in cats with CKD in this study, as also reported in canines.<sup>8</sup> Thirty-eight per cent of stomachs evaluated from cats with CKD contained mineral within the mucosal lamina propria. Only cats with moderate and severe azotemia had mineralization, suggesting that worsening azotemia and associated derangements in calcium and phosphorus concentrations put the cats at risk for soft-tissue mineralization, specifically in the stomach. In this study, CPPs tended to be higher in those cats with gastric mineral (114.6) compared to those without mineralization (82.58), which approached statistical significance. In general, animals with a CPP exceeding 60-70 are at risk for soft tissue mineralization, although increased concentrations likely need to be present for weeks to months.<sup>18</sup> Development of gastric mineralization may vary depending on individual patient factors or variation in the timeframe of elevated plasma mineral concentrations (i.e. months versus days). The administration of

phosphate binders did not appear to affect the presence of gastric mineralization; however it is difficult to assess the efficacy of phosphate binder therapy from this study as duration of hyperphosphatemia, duration of therapy and individual trends in calcium and phosphorus during the course of treatment are not known for these patients. In addition relatively small numbers of cats were receiving phosphate-binder therapy (7/18 severely azotemic cats), which is consistent with a recent survey of medication practices in CKD cats in which 78.3% of cats with CKD were not receiving phosphate binders.<sup>19</sup> The extent to which gastric mineralization contributes to clinical signs of uremia is unclear and additional studies are needed to fully elucidate the pathophysiology of gastric mineralization in cats with CKD.

Fibrosis in the superficial mucosa of the gastric body was a common lesion in cats with CKD. Evaluation of fibrosis and atrophy was restricted to the body due to variability in glandular density and lamina propria connective tissue in other gastric regions.<sup>20</sup> Typically, atrophic gastritis is the result of chronic inflammation leading to loss of gastric glands and replacement by fibrosis; however significant amounts of inflammation were not seen in CKD cats in this study.<sup>21-23</sup> Disorders leading to atrophic gastritis in humans are predominantly *Helicobacter pylori* infections or autoimmune gastritis.<sup>21</sup> Conversely, atrophic gastritis in dogs and cats is not frequently reported and a causative relationship between *Helicobacter spp.* infection and disease is equivocal.<sup>20</sup> In a single study investigating non-inflammatory atrophy and/or fibrosis, 27% of vomiting dogs and 26% of clinically asymptomatic dogs had similar lesions.<sup>23</sup> Despite the statistically significant difference between controls and CKD cats, the role of azotemia and uremia in the pathogenesis of gastric fibrosis is unclear. A limitation of this study was that control cats were not aged matched; thus age variation between the two groups is one possible explanation for this difference. The amount of fibrous connective tissue normally found in

different locations of the cat stomach at different ages has not been established. Additionally, without corroborative pathologic evidence of edema, or other evidence of mucosal injury preceding the glandular loss and fibrosis, the interpretation that uremia leads to gastric fibrosis should be made with caution. Future studies evaluating cross sectional connective tissue density amongst similarly aged animals is necessary in order to draw further conclusions.

Median serum circulating gastrin concentrations were nearly three times greater in azotemic cats than non-azotemic cats. Hypergastrinemia in CKD cats reported here is similar to findings in previously published reports.<sup>5</sup> Gastrin signals the release of hydrochloric acid from parietal cells. Hypergastrinemia may lead to hyperacidity and potential chemical damage to the gastric mucosa. Despite this reasonable theory for the pathogenesis of uremic gastropathy, gastric ulceration was not found in CKD cats in this study, even when serum gastrin concentrations were markedly elevated. Hypergastrinemia may strictly be a consequence of renal disease. More than one third of plasma gastrin is extracted from circulation in a single pass through the kidney by renal cortical inactivation.<sup>24</sup> In one study in humans, hypergastrinemia correlated with loss of functional renal mass, but not the degree of uremia.<sup>24</sup> Gastrin concentrations did not necessarily correlate with severity of azotemia in the CKD cats in this study, although this has been documented in a previous study.<sup>5</sup> Alternatively, in concordance with the fibrotic changes found in this study, increased concentrations of gastrin may be the result of atrophic gastritis, with reduced gastric acid secretion failing to give appropriate negative feedback. The data presented here showed a significant difference in the presence and severity of fibrosis in cats with CKD in comparison to controls. However, it is difficult to determine the role of renal disease in development of gastric fibrosis based on this information. Appropriate morphometric density studies of parietal cells within the gastric mucosa and measurement of

gastric acid pH are needed to determine the exact role of hypergastrinemia in gastric pathology in cats with CKD.

Inflammation and lymphoid hyperplasia were similar in the stomachs of CKD and control cats. Therefore, their presence was likely unrelated to renal disease, or perhaps within normal limits of leukocyte constituents of the feline gastric mucosa. Studies characterizing leukocyte subpopulations within the superficial gastric mucosa have been performed in dogs, and standards for infiltrates within a defined unit have been described.<sup>14,15</sup> Similar studies have not been reported in cats.

In conclusion, cats with CKD appear more likely to have gastric fibrosis and mineralization, rather than uremic gastropathy lesions previously described in dogs and humans. Therefore, the administration of gastric protectants such as sucralfate may not be justified, unless obvious clinical evidence of gastrointestinal hemorrhage such as melena or hematemesis is appreciated. The notable frequency of gastric mineralization, presumably as a consequence of metastatic mineralization, may highlight the need for more aggressive control of hyperphosphatemia and renal secondary hyperparathyroidism in cats with CKD. Gastrointestinal symptoms in these animals may not necessarily be the result of gastric lesions, but perhaps the consequence of circulating uremic toxins interacting with the chemoreceptor trigger zone in the brain. Medical management of gastrointestinal symptoms with anti-emetic and anti-nausea drugs may therefore be more appropriate. Lastly, the exact role of hypergastrinemia in contributing to gastric hyperacidity and/or gastric lesions in cats with CKD is still unclear. Further studies to determine gastric acidity and parietal cell density in cats are needed in order to close this gap in our understanding of the etiopathogenesis of hypergastrinemia in feline uremia.

## REFERENCES

1. Bartges JW. Chronic kidney disease in dogs and cats. *Vet Clin North Am Small Anim Pract* 2012;42:669-692, vi.
2. Polzin DJ. Chronic kidney disease in small animals. *Vet Clin North Am Small Anim Pract* 2011;41:15-30.
3. Roudebush P, Polzin DJ, Ross SJ, et al. Therapies for feline chronic kidney disease. What is the evidence? *J Feline Med Surg* 2009;11:195-210.
4. Polzin DJ, Osborne C, Ross SJ. Evidence-based medicine of chronic kidney disease. In: Bonagura JD, Twedt DC, eds. *Kirk's Current Veterinary Therapy XIV*, 14th ed. St. Louis, MO: Saunders Elsevier; 2009:872-878.
5. Goldstein RE, Marks SL, Kass PH, et al. Gastrin concentrations in plasma of cats with chronic renal failure. *J Am Vet Med Assoc* 1998;213:826-828.
6. Jaffe R, Laing D. Changes in the digestive tract in uremia. A pathologic anatomic study. *Arch Int Med* 1934;53:851-864.
7. Lazarus H. Gastrointestinal abnormalities. In: Brenner BM, Rector FC, eds. *The kidney*. Philadelphia, PA: WB Saunders; 2000:1634-1659.
8. Peters RM, Goldstein RE, Erb HN, et al. Histopathologic features of canine uremic gastropathy: a retrospective study. *J Vet Intern Med* 2005;19:315-320.
9. Cheville NF. Uremic gastropathy in the dog. *Vet Pathol* 1979;16:292-309.
10. Cianciolo RE, Bischoff K, Ebel JG, et al. Clinicopathologic, histologic, and toxicologic findings in 70 cats inadvertently exposed to pet food contaminated with melamine and cyanuric acid. *J Am Vet Med Assoc* 2008;233:729-737.
11. Rumbleha WK, Francis JA, Fitzgerald SD, et al. A comprehensive study of Easter lily poisoning in cats. *J Vet Diagn Invest* 2004;16:527-541.
12. Liptak JM, Hunt GB, Barrs VR, et al. Gastroduodenal ulceration in cats: eight cases and a review of the literature. *J Feline Med Surg* 2002;4:27-42.
13. El Ghonaimy E, Barsoum R, Soliman M, et al. Serum gastrin in chronic renal failure: morphological and physiological correlations. *Nephron* 1985;39:86-94.
14. Day MJ, Bilzer T, Mansell J, et al. Histopathological standards for the diagnosis of gastrointestinal inflammation in endoscopic biopsy samples from the dog and cat: a report from the World Small Animal Veterinary Association Gastrointestinal Standardization Group. *J Comp Pathol* 2008;138 Suppl 1:S1-43.

15. Washabau RJ, Day MJ, Willard MD, et al. Endoscopic, biopsy, and histopathologic guidelines for the evaluation of gastrointestinal inflammation in companion animals. *J Vet Intern Med* 2010;24:10-26.
16. Price AB. The Sydney System: histological division. *J Gastroenterol Hepatol* 1991;6:209-222.
17. Chakrabarti S, Syme HM, Brown CA, et al. Histomorphometry of feline chronic kidney disease and correlation with markers of renal dysfunction. *Vet Pathol* 2013;50:147-155.
18. Landau D, Krymko H, Shalev H, et al. Transient severe metastatic calcification in acute renal failure. *Pediatr Nephrol* 2007;22:607-611.
19. Markovich JE, Freeman LM, Labato MA, et al. Survey of the dietary and medication practices of owners of cats with chronic kidney disease. *J Vet Intern Med* 2013;27:735.
20. Wilcock B. Histopathology. In: Washabau R, Day MJ, eds. *Canine and Feline Gastroenterology*, 1st ed. St. Louis, MO: Saunders Elsevier; 2013:333-341.
21. Ruge M, Pennelli G, Pilozzi E, et al. Gastritis: the histology report. *Dig Liver Dis* 2011;43 Suppl 4:S373-384.
22. Sullivan M, Yool DA. Gastric disease in the dog and cat. *Vet J* 1998;156:91-106.
23. van der Gaag I. The histological appearance of peroral gastric biopsies in clinically healthy and vomiting dogs. *Can J Vet Res* 1988;52:67-74.
24. Zelnick EB, Goyal RK. Gastrointestinal manifestations of chronic renal failure. *Seminars in Nephrology* 1981;1:124-136.



## CHAPTER 5: IDENTIFICATION AND QUANTIFICATION OF ANTI- $\alpha$ -ENOLASE ANTIBODIES IN SERA OF CATS WITH CHRONIC KIDNEY DISEASE AND IMMUNOPRECIPITATION OF ENDOGENOUS RENAL PROTEINS

### 5.1 Chapter Summary

Feline chronic kidney disease (CKD) is a leading cause of morbidity and mortality in aged cats. While progress has been made to better characterize and stage feline CKD little is known in regards to why CKD is so prevalent in this species or the underlying etiology. It has been shown that parenteral administration of vaccines against feline viral rhinotracheitis (feline herpesvirus 1), calicivirus, and panleukopenia (FVRCP) or cell lysates (CRFK) used to grow the viruses or CRFK lysates alone can induce autoantibodies that bind  $\alpha$ -enolase protein. In addition, a subset of these cats with antibodies against CRFK lysates developed interstitial nephritis. The focus of this study was to determine if cats with CKD have anti- $\alpha$ -enolase antibodies by western blot immunoassay and if antibody levels are associated with stage of disease or recent vaccination. Additionally, to determine if circulating antibodies target endogenous renal  $\alpha$ -enolase. Alpha-enolase antibodies were quantitated in cats with naturally-occurring CKD (n=29) and healthy, unvaccinated controls (n=8) by indirect enzyme-linked immunosorbent assay (ELISA). Cats with CKD had significantly greater levels of  $\alpha$ -enolase antibodies than controls ( $p < 0.0001$ ). Levels of  $\alpha$ -enolase antibodies between IRIS stages were not significantly different ( $p > 0.05$ ). A relationship between levels of antibodies and vaccination status could not be determined due to incomplete vaccine histories in a majority of study cats. Immunoglobulin present within the sera of CKD cats was capable of binding endogenous feline renal  $\alpha$ -enolase.

## 5.2 Introduction

Chronic kidney disease (CKD) is a significant healthy concern in geriatric cats affecting anywhere from 28-50% of felines.<sup>1,2</sup> Feline CKD is characterized clinicopathologically by increased concentrations of serum creatinine and blood urea nitrogen, decreased urinary concentrating ability with variable electrolyte and acid-base derangements.<sup>2,3</sup> Histologically, tubulointerstitial lesions predominate.<sup>3,4</sup> Tubulointerstitial lesions consist of interstitial fibrosis, inflammation, with tubular degeneration and atrophy.<sup>4,5</sup> Multifactorial etiologies are often cited in the genesis of CKD in cats, although little headway has been made in definitively defining the etiopathogenesis in this species.

Vaccines and the cell lines used in the production of viral vaccines have been associated with development of interstitial nephritis in cats.<sup>6</sup> Feline viral rhinotracheitis, calicivirus, and panleukopenia (FVRCP) vaccine is a core vaccine recommended by the American Feline Practitioners to be given every 3-4 weeks starting as early as 5 weeks until 16 weeks of age followed by every 1-3 years depending on risk.<sup>7</sup> Viruses included in some FVRCP vaccines are grown on cell cultures derived from feline renal tissues (Crandell Rees feline kidney, CRFK) that have been described as “epithelial-like”.<sup>8</sup> While the manufacturer’s attempt to exclude all cell lines during vaccine production some contamination is likely. Parenteral administration of FVRCP vaccines and CRFK lysates has been shown to induce an antibody response to CRFK and renal cell lysates. In a subset of cats that were hyperinoculated with CRFK lysate, interstitial nephritis was evident.<sup>6,9</sup> The majority of cats had significant amounts of vaccine induced antibodies that targeted  $\alpha$ -enolase.<sup>10</sup> It has yet to be determined what the effect of vaccinations over the course of a lifetime has on feline autoantibody levels or renal health.

Alpha-enolase autoantibodies have been implicated in a variety of autoimmune diseases with associated nephritis such as systemic lupus erythematosus (SLE), mixed cryoglobulinemia, rheumatoid arthritis, and Sjogren's syndrome.<sup>11-13</sup> Patients with SLE which go on to develop lupus nephritis had significant elevations in  $\alpha$ -enolase antibodies in serum that were associated with proteinuria and increased serum creatinine concentrations.<sup>14</sup> Alpha-enolase, a ubiquitous glycolytic enzyme, has been identified as a podocyte antigen which is the target for serum autoantibodies in lupus nephritis patients.<sup>14</sup> Alpha-enolase in the glomeruli of lupus nephritis patients is overexpressed when compared to patients without nephritis, however, the cause for up regulation is unclear.<sup>12</sup> A relationship between naturally occurring CKD in cats and the presence of renal specific autoantibodies has not been explored and is the aim of the current study.

### **5.3 Methods and Materials**

#### *5.3.1 Samples*

Cats with CKD presenting to Colorado State University Diagnostic Medical Center for necropsy from 2012 to 2014 that had an available serum sample were used for this study. Residual serum remaining from routine ante mortem biochemistry were collected and stored at -20°C until assays could be batched. Serum from 8 young ( $\leq 1.5$  years), laboratory reared, non-azotemic cats without previous history of vaccination or renal disease were included as controls. Parenteral FVRCP vaccination histories were collected from medical records for CKD cats when available.

#### *5.3.2 Clinicopathologic Data*

Using the IRIS staging scheme for CKD, study cats were assigned into a stage between II and IV based on elevated serum creatinine concentration, a urine specific gravity  $< 1.035$ , and clinical history consistent with CKD.<sup>15</sup> Cats with a normal serum creatinine concentration ( $< 1.6$  mg/dl),

which include IRIS Stage I, were not included. Stages II, III, and IV were defined by serum creatinine concentrations measuring 1.6-2.8 mg/dl, 2.9-5.0 mg/dl and >5.0 mg/dl, respectively. Non-azotemic control cats had no clinical evidence or history of renal disease, USG >1.035, and serum creatinine concentration  $\leq$  1.6 mg/dl.

### 5.3.3 Western blot Immunoassay

Optimized gel electrophoresis and western blot immunoassays were run similar to that previously described.<sup>10</sup> Alpha-enolase antigen was prepared as follows: 3 ug ENO1 recombinant protein (Abnova, Taiwan Corp) was mixed with lithium dodecyl sodium (LDS) sample buffer, reducing agent, denatured and loaded on a precast 10% Bis-Tris mini gel along with a molecular weight standard (Thermo Scientific). Gels were electrophoresed in 3-(N-Morpholino)-propanesulfonic acid running buffer at 200V for 50 minutes. Proteins were then transferred to a polyvinylidene difluorure (PVDF) membrane in transfer buffer with 20% methanol in a XCell II Blot Module (NuPage, Intitrogen, Carlsbad) at 25V for 90 minutes. Membranes were dried at room temperature and stored at -20°C.

When all samples had been collected membranes were thawed, moistened with methanol, rinsed in distilled water, and blocked with 1xNEH at room temperature with gentle rocking for 1 hour. Samples were loaded into Miniblotter 28 (Immunogenics) at an optimized dilution of 1:20 in TNTP-10% milk at room temperature with gentle rocking for 2 hours. Membranes were rinsed with PBS-Tween 80 for 5 minutes for a total of three washes then incubated with peroxidase labeled goat anti-cat IgG ( $\gamma$ ) secondary antibody (Kirkegaard and Perry Laboratories, Gaithersburg, MD) in a 1:25 dilution in TNTP-10% milk for 1 hour at room temperature with gentle rocking. Membranes were rinsed three times for 5 minutes in PBS-Tween 80. Protein bands were visualized by colorimetric horseradish peroxidase (HRP) detection with 3, 3'-

diaminobenzidine in 10% hydrogen peroxide buffer and analyzed by Quantity One (Bio-Rad) software.

#### *5.3.4 Enzyme-linked immunosorbent assay (ELISA)*

Optimized  $\alpha$ -enolase enzyme-linked immunosorbent assay (ELISA) was run on samples as previously described.<sup>10</sup> Briefly, each well of a 96-well plate (Immulon II, ThermoScientific, Waltham, MA) were incubated with 10 ng of recombinant  $\alpha$ -enolase in 100 microliters of 0.06 M carbonate buffer (pH 9.6) overnight at 4°C. Wells were washed with 0.05% Tween 20-PBS (PBS-TW) 3 times. Previously determined positive and negative controls and test samples were diluted 1:40 in PBS-TW at 400 microliters per well, loaded in triplicates, and incubated at 37°C for 30 minutes. Wells were washed 3 times in PBS-TW. Peroxidase labeled goat anti-cat IgG ( $\gamma$ ) secondary antibody (Kirkegaard and Perry Laboratories, Gaithersburg, MD) was diluted 1:100 in PBS-TW at 100 microliters per well, and incubated at 37°C for 30 minutes. Wells were washed with PBS-TW as previously described and 100 microliters per well of TMB (Kirkegaard and Perry Laboratories, Gaithersburg, MD) was incubated at room temperature (20°C) for 10 minutes. Color reaction was stopped with 100 microliters of 0.18M H<sub>2</sub>SO<sub>4</sub> per well. Optical density was read by an automatic plate reader at 450nm and results were reported as the mean absorbance of triplicates (Ascent Multiskan, ThermoScientific, Waltham, MA). The mean absorbance was converted to %ELISA by dividing the difference between the test sample mean absorbance and negative control mean absorbance by the difference between the positive and negative control mean absorbance and multiplying by 100.

#### *5.3.5 Immunoprecipitation (IP)*

Renal cortex from a non-azotemic, healthy cat was homogenized and desalted by acetone precipitation. Protein was quantified by BCA protein assay (ThermoScientific). A commercially

available classic immunoprecipitation kit (ThermoScientific) was used to complex purified immunoglobulin G from pooled  $\alpha$ -enolase positive serum of CKD cats and monoclonal mouse alpha-enolase antibody with feline renal tissue homogenate. Immunoglobulin from CKD cats was titrated at 2, 5, and 10  $\mu$ g with 500  $\mu$ g of renal protein. Alpha-enolase mouse monoclonal antibody was titrated at 1, 2, and 5  $\mu$ g and complexed with a total of 250 $\mu$ g of protein for each dilution. Homogenized renal tissue was pre-cleared according to the manufacturer's protocol and immune complexes were prepared by incubating at 4°C overnight. Immune complexes were captured on a Protein A/G agarose resin column and eluted off with sample elution buffer and heating. Immune complexes were run on a 10% Bis-Tris gel in LDS buffer for 50 minutes at 200V. Protein bands were visualized with SimpleBlue stain (Life Technologies), rinsed in dH<sub>2</sub>O and then 20% ethanol. Bands were excised, subject to trypsin digestion, and mass spectrometry at the Colorado State University Proteomics and Metabolomics Facility.

### *5.3.6 Mass Spectrometry*

Sample peptides were purified and concentrated utilizing an on-line enrichment column prior to chromatographic separation on a reverse phase nanospray column (Thermo Scientific). Spectra of eluted peptides were collected from a mass spectrometer (Thermo Scientific Orbitrap Velos) over a m/z range of 400-2000 Da with a dynamic exclusion limit of 2 MS/MS spectra of a peptide mass for 30 seconds (exclusion duration of 90 seconds). Resulting spectra was generated using Xcalibur 2.2 software (Thermo Scientific) with a signal-to-noise ratio threshold of 1.5 and 1 scan/group.

Tandem mass spectra were extracted, charge state was deconvoluted and deisotoped by ProteoWizard (MSConvert) version 3.0. MS/MS samples were analyzed by Mascot (Matrix Science, London, UK; version 2.3.02) set up to search the uniprot\_feline\_rev\_100214 database

(unknown version, 42512 entries). Searches were performed assuming trypsin digestion, with a fragment ion mass tolerance of 0.80 Da, and a parent ion tolerance of 20 PPM. Oxidation of methionine and carbamidomethyl of cysteine were specified in Mascot as variable modifications. Scaffold (version Scaffold\_4.4.1.1, Proteome Software Inc., Portland, OR) was used to validate MS/MS based peptide and protein identifications. Peptide identifications were accepted if they could be established at greater than 95.0% probability by the Scaffold Local FDR algorithm. Protein identifications were accepted if they could be established at greater than 99.9% probability and contained at least 2 identified peptides. Protein probabilities were assigned by the Protein Prophet algorithm.<sup>16</sup> Proteins that contained similar peptides and could not be differentiated based on MS/MS analysis alone were grouped to satisfy the principles of parsimony.

### *5.3.7 Statistics*

To investigate an association between the presence of anti- $\alpha$ -enolase antibodies in the serum of cats with or without CKD and between CKD groups (i.e. vaccine status and IRIS stage) was determined by Fisher's exact test and chi-square analysis, respectively. A non-parametric t test (Mann Whitney) was used to compare mean absorbance and %ELISA results between controls and CKD cats while a non-parametric one-way analysis of variance (Kruskal Wallis) was used to compare mean absorbance and %ELISA results between CKD groups (i.e. vaccine status and IRIS stage) with a post hoc Dunn's multiple comparison. Correlation analysis of ELISA assays and serum creatinine concentrations were achieved by a non-parametric Spearman rank correlation. All statistical analyses were performed on GraphPad Prism version 5.00 for Windows (GraphPad Software, San Diego California USA, [www.graphpad.com](http://www.graphpad.com)). Statistical significance was set at  $p < 0.05$ .

## 5.4 Results

### 5.4.1 Samples

A total of 29 CKD cats classified into Stages II-IV as well as 8 healthy, non-azotemic control cats were included in this study. Control cats were  $\leq 1 \frac{1}{2}$  years old, domestic shorthair, and consisted of 2 males and 6 females. Mean serum creatinine concentration for control cats was 1.1 md/dl (range 0.9-1.6 md/dl). A total of 9 Stage II cats, 8 Stage III and 12 Stage IV CKD cats were included in this study. The mean age of cats with CKD was 14.7 years (range 8-20  $\frac{1}{2}$  years) and included 14 castrated male and 15 spayed female cats. Domestic shorthair cats were most prevalent (n=17) with lesser domestic longhair (n=6), 3 Siamese, 1 Tonkinese, and 1 Ragdoll breeds. The mean serum creatinine concentration for Stage II cats was 2.3 mg/dl (range 1.8-2.7 mg/dl), Stage III 3.5 mg/dl (2.9-4 mg/dl), and Stage IV 8.2 mg/dl (4.2-12.6 mg/dl). Vaccine histories were collected from medical records and primary veterinarians were contacted to confirm dates, routes of administration, and type of FVRCP vaccine given. This information was only available for 9/29 CKD cats. Because of the limited number of cats with available vaccine histories statistical comparisons of antibody levels were not analyzed.

### 5.4.2 Western Blot Immunoassay

Of the 29 CKD cats, 19 were positive for  $\alpha$ -enolase antibodies while 10 were negative by Western blot (Figure 5.1). The mean molecular weight (MW) of CKD bands was 72.7 kDa. Five Stage II cats, 6 Stage III, and 8 Stage IV cats had anti- $\alpha$ -enolase antibodies in serum by western blot. All eight control cats were positive for anti- $\alpha$ -enolase antibodies with a mean band MW of 71.8 kDa. The theoretical molecular weight for recombinant  $\alpha$ -enolase protein was 73.5 kDa. No association was found between the presence of anti- $\alpha$ -enolase antibodies in serum and cats



with or without CKD by western blot ( $p=0.08$ ). A majority of CKD cats in each stage had  $\alpha$ -enolase antibodies in serum albeit a statistically significant association was not found ( $p=0.70$ ).

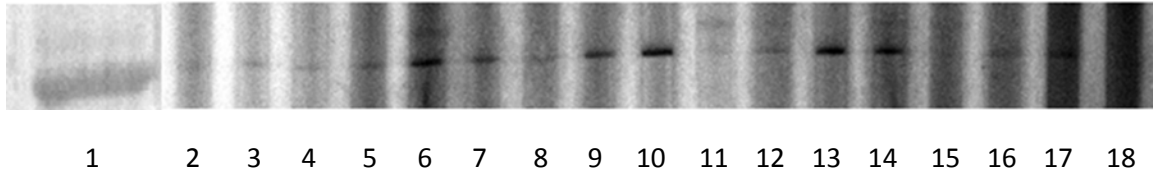


Figure 5.1 Alpha-enolase western blot with cat serum. Lane 1 is the molecular weight standard at 64 kDa. Mean band molecular weight is approximately 72kDa. (Lane 2 and 3) control cats, (Lanes 4-16) CKD cats, (Lane 17) positive control, and (Lane 18) negative control.

### 5.4.3 ELISA

Results from  $\alpha$ -enolase ELISAs are summarized in Table 5.1. The mean absorbance for  $\alpha$ -enolase ELISAs in healthy, non-azotemic control cats was 0.44 (standard error of the mean 0.06) which was significantly less than CKD cats ( $1.21 \pm 0.10$ ,  $p < 0.0001$ ; Figure 5.2). The median %ELISA for  $\alpha$ -enolase antibodies in 8 control cats was 0 (range 0-23.6) while CKD cats were significantly greater at 77.47 (range 0-371.9;  $p < 0.0001$ ; Figure 5.3).

Table 5.1 Mean absorbance and calculated %ELISA results of  $\alpha$ -enolase ELISA. %ELISA measurements were determined by the following equation: (mean absorbance test sample - mean absorbance of negative control) / (mean absorbance of the positive control - mean absorbance of the negative control) x 100.

	Mean Absorbance			%ELISA	
	Mean	Standard error (SEM)	Median	Median	Range
Control	0.44	0.06	0.42	0.00	0-23.6
CKD, IRIS Stage					
Stage II (n=9)	1.05	0.15	1.11	69.67	0-158.8
Stage III (n=8)	1.17	0.09	1.19	80.13	20.8-122.4
Stage IV (n=12)	1.35	0.20	1.22	83.47	42.6-371.9

Mean absorbance values for  $\alpha$ -enolase in non-azotemic, healthy control cats were significantly less than CKD cats at all IRIS stages ( $p < 0.05$ , Figure 5.4). Median  $\alpha$ -enolase %ELISA measurements for control cats were less than all CKD stages, however, statistical significant difference was only found between controls and CKD Stages III and IV ( $p < 0.05$ , Figure 5.5).

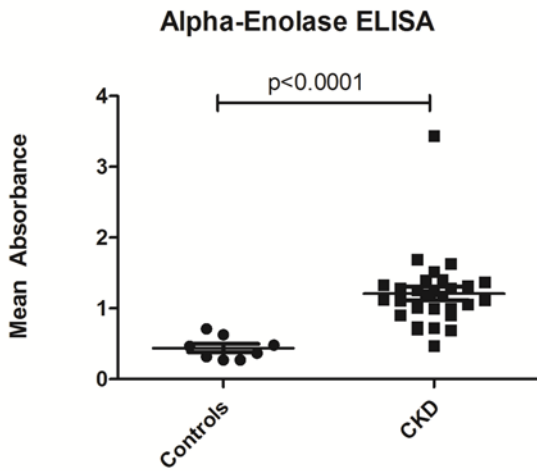


Figure 5.2 Mean absorbance for  $\alpha$ -enolase ELISA. CKD cats had significantly higher  $\alpha$ -enolase antibodies than healthy controls,  $p < 0.001$ .

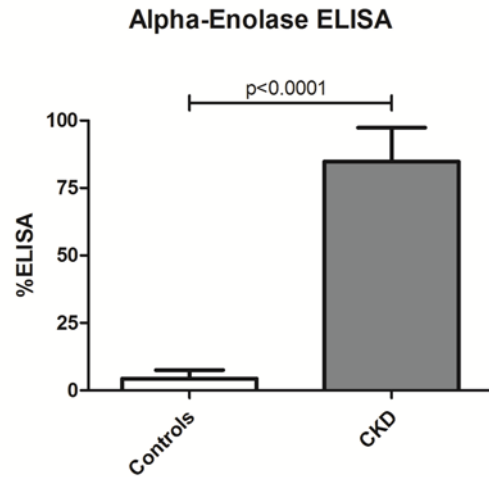


Figure 5.3 %ELISA for the  $\alpha$ -enolase ELISA. CKD cats had significantly higher  $\alpha$ -enolase antibodies than healthy controls,  $p < 0.001$ .

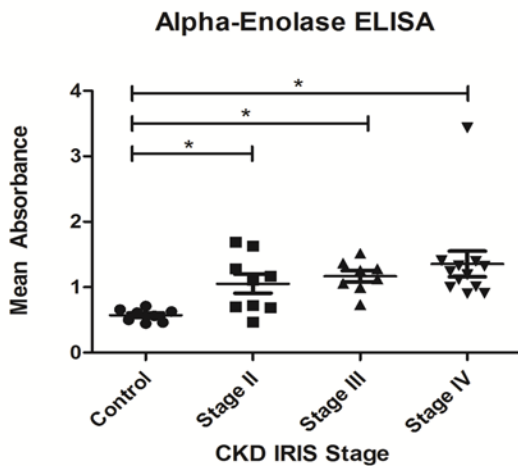


Figure 5.4 Mean absorbance for  $\alpha$ -enolase ELISA by IRIS stage. Healthy controls had significantly less  $\alpha$ -enolase antibodies than CKD cats at Stages II-IV,  $p < 0.05$ .

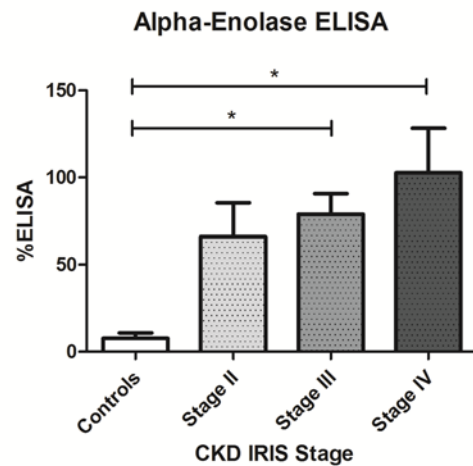


Figure 5.5 %ELISA for  $\alpha$ -enolase ELISA by IRIS stage. Healthy controls had significantly less  $\alpha$ -enolase antibodies than CKD cats at Stages III and IV,  $p < 0.05$ .

The mean absorbance of  $\alpha$ -enolase by ELISA increased with increasing IRIS stage; however, the results were not statistically significant (Figure 5.4). Stage II cats had a mean absorbance of 1.05 ( $\pm$  0.15) and a median %ELISA value of 69.67 (range 0-158.8). Stage III cats had a mean absorbance of 1.17 ( $\pm$ 0.09) and median %ELISA of 80.13 (range 20.8-122.4); while Stage IV cats had a mean absorbance of 1.35 ( $\pm$ 0.20) and median %ELISA value of 83.47 (range 42.6-371.9). No difference in %ELISA measurements was found among IRIS stages (Figure 5.5).

No significant correlation between either mean absorbance ( $r=0.20$ ,  $p=0.29$ ) or %ELISA ( $r=0.21$ ,  $p=0.28$ ) and serum creatinine concentration of CKD cats was found (Figures 5.6 and 5.7). Removal of single outlier did not make data statistically significant. Additionally, the mean absorbance and %ELISA from CKD cats that were negative by  $\alpha$ -enolase western blot and those that were positive were not statistically different ( $p=0.19$ ; Figures 5.8 and 5.9 ). If western blot negative cats were removed from the analysis, detectable  $\alpha$ -enolase antibody by ELISA remained significantly greater than controls (mean absorbance,  $p=0.0002$ ; %ELISA,  $p=0.0003$ ; Figures 5.10 and 5.11).

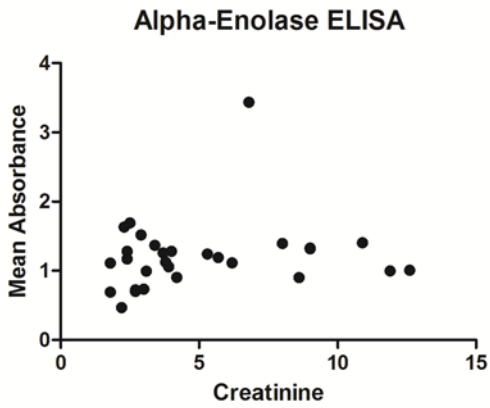


Figure 5.6 Spearman correlation of Mean absorbance and serum creatinine for CKD cats. No significant correlation was found ( $r=0.20$ ,  $p=0.29$ ).

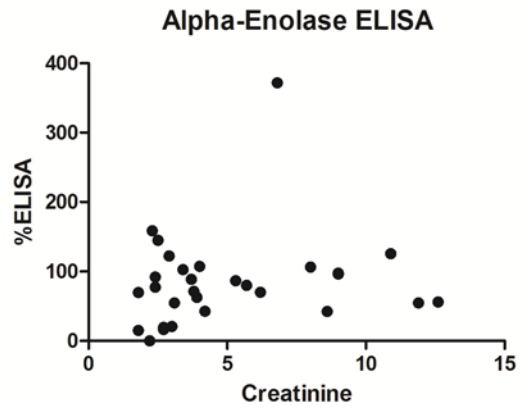


Figure 5.7 Spearman correlation of %ELISA and serum creatinine for CKD cats. No significant correlation was found ( $r=0.21$ ,  $p=0.28$ ).

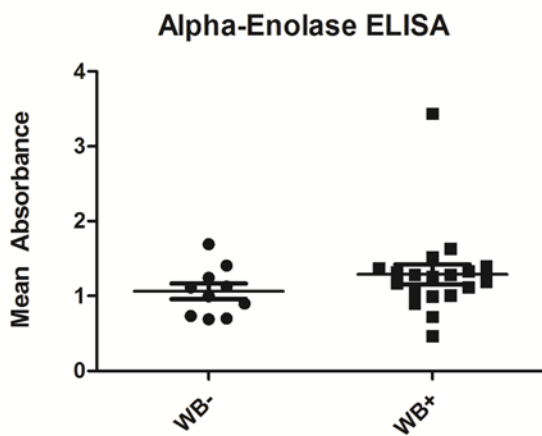


Figure 5.8 Mean absorbance for  $\alpha$ -enolase ELISA. CKD cats that were negative by western blot immunoassay did not have significantly different levels of  $\alpha$ -enolase antibodies by ELISA,  $p=0.19$ .

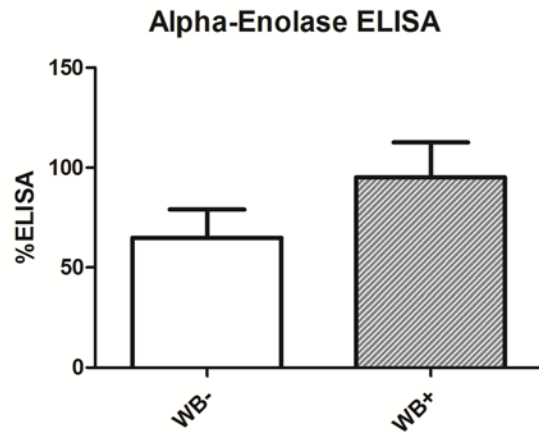


Figure 5.9 %ELISA for  $\alpha$ -enolase ELISA. CKD cats that were negative by western blot immunoassay did not have significantly different levels of  $\alpha$ -enolase antibodies by ELISA,  $p=0.19$ .

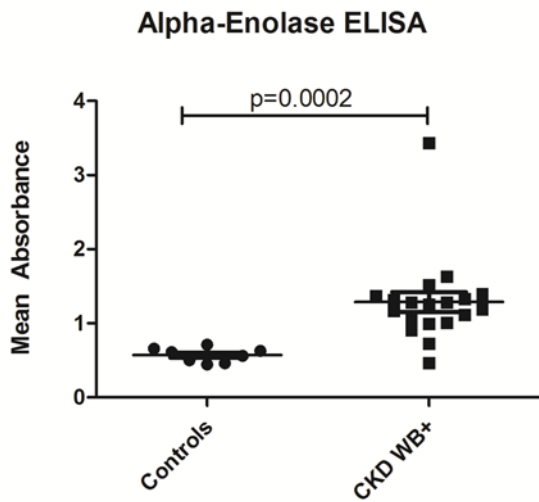


Figure 5.10 Mean absorbance for  $\alpha$ -enolase by ELISA. Control cats had significantly less  $\alpha$ -enolase antibodies than western blot positive CKD cats,  $p=0.0002$ .

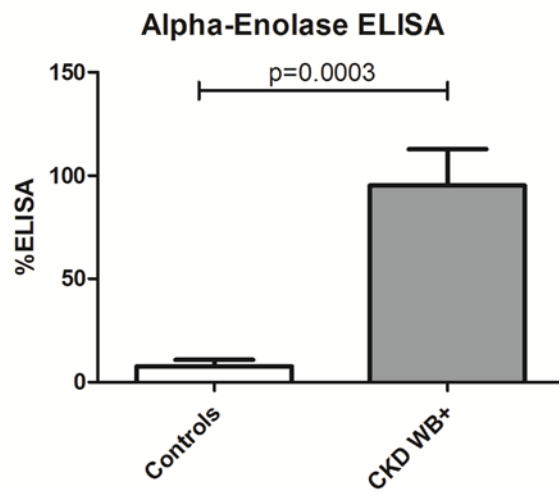


Figure 5.11 %ELISA for  $\alpha$ -enolase by ELISA. Control cats had significantly less  $\alpha$ -enolase antibodies than western blot positive CKD cats,  $p=0.0003$ .

#### 5.4.4 Immunoprecipitation (IP) and Mass Spectrometry

Immunoglobulin G eluted from serum by affinity chromatography was incubated with feline renal cortical homogenate. Elutes were run on PAGE and bands excised for mass spectrometry. Protein bands were present in all immunoglobulin dilutions. Eluted heavy chain immunoglobulin protein bands (50 kDa) were not distinct from eluted antigen in the CKD samples and the entire band was submitted for proteomics. A total of 30 proteins with 100% protein identification probability were found in the protein band excised from CKD immunoprecipitation (IP) gel. Nineteen proteins with 100% protein identification probability were identified from monoclonal  $\alpha$ -enolase antibody IP gel. Enolase was identified in the feline renal homogenate precipitated with recombinant  $\alpha$ -enolase antibody along with numerous keratin contaminants. Enolase was not found from excised gel bands in the CKD sample. A majority of proteins identified were keratin contaminants. However, when elutes were analyzed by mass

spectrometry prior to gel electrophoresis  $\alpha$ -enolase was identified from feline renal homogenate precipitated with CKD immunoglobulin at 2 and 5 ug titrations.

## 5.5 Discussion

Spontaneous development of anti- $\alpha$ -enolase antibodies in serum have been shown to be associated with nephritis in humans with autoimmune diseases.<sup>12, 17</sup> In cats, autoantibodies to  $\alpha$ -enolase can be induced with parenteral administration of FVRCP vaccine.<sup>9, 10</sup> Additionally, inoculation with the vaccine contaminate, CRFK lysates, has been linked to the development of interstitial nephritis in hyperinoculated cats--a common lesion seen in cats with naturally occurring kidney disease.<sup>6</sup> Our findings show that cats with CKD do develop significant levels of anti- $\alpha$ -enolase antibodies detectable by serum ELISA when compared to healthy, non-azotemic controls. While there was subtle increases in the mean absorbance measurements between CKD stages no statistically significant association between serum creatinine concentrations or IRIS stage and antibody levels were found. Due to unavailable vaccine histories for all study cats an association between parenteral FVRCP and  $\alpha$ -enolase antibodies in CKD cat sera could not be determined. Future directions in determining this relationship would include similar assays with sample sets from age-matched cats with and without CKD and detailed vaccine histories which would include the route of administration, type of vaccine (e.g. modified live), frequency and timeframe of vaccination from sample date.

Ten CKD cats were negative on western blot immunoassay but had detectable levels of  $\alpha$ -enolase antibodies by ELISA. Those cats that were negative for  $\alpha$ -enolase antibodies by western blot did have less mean absorbance and %ELISA measurements compared to CKD western blot positive CKD cats; however, this difference was not statistically significant (Figures 5.8 and 5.9). Alpha-enolase western blot immunoassay could be a less sensitive method of  $\alpha$ -

enolase antibody detection compared to ELISA. However, all control cats were positive by immunoblot but had significantly less antibody by ELISA than immunoblot negative CKD cats negative cats ( $p=0.002$ ). A potential reason for this discrepancy could be from failure of protein transfer from the gel to the PVDF membrane in those particular locations, however, negative samples were spread out over the membrane and not necessarily concentrated to one location. Lastly,  $\alpha$ -enolase antibody in sera of cats with CKD could have low affinity binding for recombinant  $\alpha$ -enolase resulting in reduction in the level of detection by immunoblot.<sup>18, 19</sup>

Alpha-enolase was sequenced by mass spectrometry from immunoprecipitated cat sera and recombinant, monoclonal antibody with feline kidney homogenate. The absence of identifiable  $\alpha$ -enolase by mass spectrometry in gel bands from immunoprecipitated cat sera could be the consequence of interference of immunoglobulin heavy chain.<sup>14</sup> It is likely that due to confluent bands between the location of Ig heavy chain (50 kDa) and the protein of interest (47 kDa) on the gel that immunoglobulin was included with excision of the sample band. Exclusion of immunoglobulin could be achieved by a different immunoprecipitation technique that covalently binds antibody to the IP agarose matrix allowing for elution of only the antigen (Thermo Scientific). Despite potential interference of Ig heavy chain whole elution's of feline immunoglobulin and precipitated kidney homogenates yielded identification of  $\alpha$ -enolase with 100% protein identification probability. A potential cause for this discrepancy between the crude elution and the gel band could be in the method of band excision. Perhaps gel bands were excised or handled incorrectly yielding mostly keratin contaminants by mass spectrometry. It is our opinion, based on the results of this assay, that immunoglobulin present within CKD cat sera binds endogenous renal  $\alpha$ -enolase.



In conclusion, the findings of this study show that cats with naturally occurring CKD have high levels of serum anti- $\alpha$ -enolase antibodies. While cats with CKD have significantly greater amounts of  $\alpha$ -enolase autoantibodies when compared to healthy controls, no significant difference was found when comparing groups based on severity of disease (i.e. IRIS stage). Lastly, immunoglobulin present within the serum of cats with CKD is capable of binding endogenous feline renal  $\alpha$ -enolase.

## REFERENCES

1. Marino CL, Lascelles BD, Vaden SL, et al. Prevalence and classification of chronic kidney disease in cats randomly selected from four age groups and in cats recruited for degenerative joint disease studies. *J Feline Med Surg* 2013.
2. Lulich J, Osborne C, O'Brien T, et al. Feline renal failure: questions, answers, questions. *Compendium on Continuing Education for the Practicing Veterinarian* 1992;14(2):26.
3. Elliott J, Barber PJ. Feline chronic renal failure: clinical findings in 80 cases diagnosed between 1992 and 1995. *J Small Anim Pract* 1998;39(2):78-85.
4. Chakrabarti S, Syme HM, Brown CA, et al. Histomorphometry of feline chronic kidney disease and correlation with markers of renal dysfunction. *Vet Pathol* 2013;50(1):147-155.
5. Nadasdy T, Sedmak D. Acute and Chronic Tubulointerstitial Nephritis. In: Jennette JC, Olson JL, Schwartz MM, et al., eds. *Heptinstall's Pathology of the Kidney*. Vol II. 6th ed. Philadelphia, PA: Lippincott Williams & Wilkins; 2007:1083-1137.
6. Lappin MR, Basaraba RJ, Jensen WA. Interstitial nephritis in cats inoculated with Crandell Rees feline kidney cell lysates. *J Feline Med Surg* 2006;8(5):353-356.
7. Scherk MA, Ford RB, Gaskell RM, et al. 2013 AAFP Feline Vaccination Advisory Panel Report. *J Feline Med Surg* 2013;15(9):785-808.
8. Crandell RA, Fabricant CG, Nelson-Rees WA. Development, characterization, and viral susceptibility of a feline (*Felis catus*) renal cell line (CRFK). *In Vitro* 1973;9(3):176-185.
9. Lappin MR, Jensen WA, Jensen TD, et al. Investigation of the induction of antibodies against Crandell-Rees feline kidney cell lysates and feline renal cell lysates after parenteral administration of vaccines against feline viral rhinotracheitis, calicivirus, and panleukopenia in cats. *Am J Vet Res* 2005;66(3):506-511.
10. Whittemore JC, Hawley JR, Jensen WA, et al. Antibodies against Crandell Rees feline kidney (CRFK) cell line antigens, alpha-enolase, and annexin A2 in vaccinated and CRFK hyperinoculated cats. *J Vet Intern Med* 2010;24(2):306-313.
11. Pratesi F, Moscato S, Sabbatini A, et al. Autoantibodies specific for alpha-enolase in systemic autoimmune disorders. *J Rheumatol* 2000;27(1):109-115.
12. Migliorini P, Pratesi F, Bongiorno F, et al. The targets of nephritogenic antibodies in systemic autoimmune disorders. *Autoimmun Rev* 2002;1(3):168-173.
13. Gitlits VM, Toh BH, Sentry JW. Disease association, origin, and clinical relevance of autoantibodies to the glycolytic enzyme enolase. *J Investig Med* 2001;49(2):138-145.

14. Bruschi M, Sinico RA, Moroni G, et al. Glomerular autoimmune multicomponents of human lupus nephritis in vivo:  $\alpha$ -enolase and annexin AI. *J Am Soc Nephrol* 2014;25(11):2483-2498.
15. Novartis Animal Health Inc. IRIS staging CKD. <http://www.iris-kidney.com/guidelines/staging.shtml> (2013, accessed 1 April 2015).
16. Nesvizhskii AI, Keller A, Kolker E, et al. A statistical model for identifying proteins by tandem mass spectrometry. *Anal Chem* 2003;75(17):4646-4658.
17. Terrier B, Degand N, Guilpain P, et al. Alpha-enolase: a target of antibodies in infectious and autoimmune diseases. *Autoimmun Rev* 2007;6(3):176-182.
18. Janeway C, P T, M W, et al. *Autoimmune responses are directed against self antigens*. 5 ed. New York: Garland Science; 2001.
19. Nagele EP, Han M, Acharya NK, et al. Natural IgG autoantibodies are abundant and ubiquitous in human sera, and their number is influenced by age, gender, and disease. *PLoS One* 2013;8(4):e60726.

## CHAPTER 6: QUANTIFICATION OF RENAL $\alpha$ -ENOLASE IN FELINE CHRONIC KIDNEY DISEASE

### 6.1 Chapter Summary

Alpha-enolase, a ubiquitous, glycolytic enzyme known for catalyzing the conversion of 3-phosphoglycerate to phosphoenolpyruvate has been implicated as a self-antigen in various autoimmune diseases. Autoantibodies in serum are capable of eliciting renal injury and ultimately can contribute to patient morbidity and mortality. Furthermore, endogenous renal  $\alpha$ -enolase has been shown to be overexpressed in human patients with systemic lupus nephritis and mixed cryoglobulinemia. Kidney disease is common in companion animals and affects a significant proportion of geriatric cats. Alpha-enolase protein expression in the kidney has not been determined in healthy or diseased cats. The purpose of this study was to identify and characterize  $\alpha$ -enolase expression in feline tissues as well as to compare the pattern of expression between healthy kidneys and kidneys from cats with chronic kidney disease (CKD). A total of 29 cats with CKD and 8 non-azotemic, healthy controls were evaluated for this study. An immunohistochemistry technique for semi-quantitative measurement of  $\alpha$ -enolase protein expression in feline tissue was optimized utilizing a commercially available monoclonal  $\alpha$ -enolase antibody. In healthy kidneys,  $\alpha$ -enolase was moderately expressed in tubular epithelium but absent in glomeruli. In contrast,  $\alpha$ -enolase expression was significantly decreased in tubules that were degenerative or atrophic in kidneys of CKD cats with significantly more expression in glomeruli relative to healthy controls. There was no significant difference in  $\alpha$ -enolase expression in hepatocytes between groups. This study shows that renal  $\alpha$ -enolase expression is altered in cats with CKD.

## 6.2 Introduction

Lohman and Mayerhof in 1934 discovered the glycolytic enzyme, enolase, while studying the conversion of 3-phosphoglycerate to pyruvate in muscle extracts.<sup>1</sup> To date, enolase has been described in both prokaryotic and eukaryotic organisms. The mammalian enolase enzyme family consists of 3 isoenzyme subunits: alpha, beta, and gamma; forming homo- or heterodimers.<sup>2-6</sup> Alpha-enolase isoenzyme is ubiquitous, found in a variety of tissues, with the highest concentration within the thymus and kidney.<sup>4,7</sup> This isoform predominates during morphogenesis which eventually transitions into beta and gamma dimers with development of mature skeletal muscle and nervous tissues, respectively.<sup>2,3,5,6</sup> Although originally characterized as a cytoplasmic, glycolytic enzyme, enolase has been shown to have multiple functions as well as variable cellular expression.<sup>4,8-11</sup> Products of *enol* gene can participate in transcriptional repression; cellular defense against hypoxia; and function as a plasminogen receptor.<sup>12-17</sup>

Circulating  $\alpha$ -enolase antibodies have been repeatedly detected in serum of patients with autoimmune diseases such as but not limited to rheumatoid arthritis, systemic lupus erythematosus (SLE), and mixed cryoglobulinemia.<sup>7,18-22</sup> Of particular interest, 70% of SLE patients with detectable anti-alpha-enolase antibodies have active nephritis.<sup>22,23</sup> Renal expression of  $\alpha$ -enolase is primarily within the cytoplasm of healthy renal tubular epithelium but lacking within glomeruli.<sup>19,24</sup> In human patients with lupus nephritis,  $\alpha$ -enolase is overexpressed in tubules and glomeruli in comparison to healthy patients.<sup>19</sup> Similar descriptive or quantitative studies of enolase expression in healthy or diseased feline kidneys have not been reported.

The aim of the current study was firstly to utilize immunohistochemistry to determine protein expression of alpha-enolase in feline tissues and compare expression in the kidney

between healthy control cats and cats with chronic kidney disease (CKD). In addition, immunoreactivity of  $\alpha$ -enolase in liver tissues was used in order to determine if systemic  $\alpha$ -enolase protein expression was affected by CKD.

## **6.3 Methods and Materials**

### *6.3.1 Samples*

Cats with CKD presenting to Colorado State University Diagnostic Medical Center for necropsy from 2012 to 2014 were used for this study. Kidney (n=29) and liver tissues (n=5) from cats with CKD was sampled at the time of necropsy. Tissues were fixed in 10% neutral buffered formalin solution, paraffin embedded and sectioned at 5 microns. Liver (n=5) and kidney (n=8) tissue from non-azotemic, young ( $\leq 1.5$  years), healthy cats acquired from the humane society or laboratory reared were used as controls, respectively. Acquisition of tissues was approved by Colorado State University's Institutional Animal Care and Use Committee (IACUC). Liver tissue was sampled and scored in order to determine if systemic  $\alpha$ -enolase protein expression was variable with chronic kidney disease. Thymic tissue from a young cat that was euthanized unrelated to the current study and necropsied for diagnostic purposes was collected and used for antibody optimization and assay validation. Thymic tissue was used for assay validation and optimization due to its reported high level of  $\alpha$ -enolase protein expression.<sup>7</sup>

### *6.3.2 Clinicopathologic Data*

Using the IRIS staging scheme for CKD, study cats were assigned into a stage between II and IV based on elevated serum creatinine concentration, a urine specific gravity  $< 1.035$ , and clinical history consistent with CKD.<sup>25</sup> Cats with a normal serum creatinine concentration ( $< 1.6$  mg/dl), which include IRIS Stage I, were not included. Stages II, III, and IV were defined by serum

creatinine concentrations measuring 1.6-2.8 mg/dl, 2.9-5.0 mg/dl and >5.0 mg/dl, respectively. Non-azotemic control cats had no clinical evidence or history of renal disease, USG >1.035, and serum creatinine concentration  $\leq$  1.6 mg/dl.

### *6.3.3 Immunohistochemistry*

Tissues were fixed in 10% neutral buffered formalin solution, paraffin embedded and sectioned at 5 microns. Immunohistochemistry (IHC) on all tissues was performed on a Leica Bond-Max autostainer (Leica Microsystems) according to established manufacturer's protocol. Tissue sections were deparaffinized and rehydrated. Antigen retrieval consisted of heating slides for 20 minutes with Bond Epitope Retrieval Solution 1 at pH 6 (Leica Microsystems). Endogenous peroxidase activity was blocked with 3% hydrogen peroxide solution. Slides were incubated with mouse monoclonal ENO1 antibody (Abnova Taiwan Corp.) for 15 minutes at room temperature. Primary antibody was replaced with Bond Ready-to-Use Mouse Negative Control antibody for negative controls (Leica Microsystems). Antibody detection was accomplished by applying 3,3'-diaminobenzidine chromagen and hematoxylin counterstain.

Determining optimal antibody concentration for appropriate signal intensity was determined by applying serial dilutions of primary antibody (ENO1, Abnova) to thymic tissue. The optimal concentration of antibody that provided the highest intensity with the least background staining was 1:2000, compared with more concentrated dilutions (1:500 and 1:1000). Primary antibody at a concentration of 1:2000 was used in all IHC procedures as described above with thymus as a positive control. Assay validation was achieved by scoring thymic tissue at the optimal antibody concentration on 3 separate occasions and scored separately. Interassay variation was determined from the quotient of the standard deviations and mean (i.e. coefficient of variation).

Each section of kidney and liver was evaluated for positive immunoreactivity and assigned a score based on signal intensity—immunoreactivity—ranging from 0 to 3. Scoring was defined as follows: 0=no staining, 1=light brown/tan, 2=moderate brown staining, 3=dark brown which may obscure the nucleus. Ten high powered fields (40X) were selected from a subgross grid for each section of liver and kidney. A total of 20 hepatocytes, 2 per single grid block were scored. Similarly renal cortical tubules, either 20 tubules from controls or 10 injured and 10 normal tubules from CKD cats, and 20 non-sclerotic glomeruli for each cat were scored. Injured tubules were defined as those that were degenerative or atrophic. Sections from bilateral kidneys were evaluated separately and compared to determine if there was variability between kidneys in individual CKD (n=5) and control (n=2) cats.

#### *6.3.4 Statistics*

Immunoreactivity scores for renal cortical tubules and glomeruli from non-azotemic controls and CKD cats were compared by non-parametric one-way analysis of variance (Kruskal-Wallis) with post-hoc Dunn's comparison tests. Additionally, tubules and glomeruli from bilateral kidneys of CKD and control cats were compared by non-parametric, paired t test (Wilcoxon signed rank test). Hepatocytes of controls and CKD cats were compared by a non-parametric t test. Statistical significance for all analyses were set at  $p < 0.05$  and performed in GraphPad Prism version 5.00 for Windows (GraphPad Software, San Diego California USA, [www.graphpad.com](http://www.graphpad.com)).



## 6.4 Results

### 6.4.1 Signalment and Clinicopathologic Data

A total of 29 cats with CKD and 8 non-azotemic, young, healthy controls were included in this study. Control cats were  $\leq 1 \frac{1}{2}$  years old, domestic shorthair, and consisted of 2 males and 6 females. A total of 9 Stage II cats, 8 Stage III and 12 Stage IV CKD cats were included in this study. The mean age of cats with CKD was 14.7 years (range 8-20  $\frac{1}{2}$  years) and included 14 castrated male and 15 spayed female cats. Domestic shorthair cats were most prevalent (n=17) with lesser domestic longhair (n=6), 3 Siamese, 1 Tonkinese, and 1 Ragdoll breeds.

### 6.4.2 Immunohistochemistry

#### 6.4.2.1 Thymus

Immunohistochemistry of feline tissues utilizing a mouse monoclonal  $\alpha$ -enolase antibody (Abnova, Taiwan) was validated and optimized with thymic tissue from a young cat without renal disease. At the ideal dilution, 1:2000, the coefficient of variation for interassay variation was determined to be 8.2%. Pale to light staining was present in the cytoplasm of most thymic epithelial cells with a mean staining intensity of 0.99 on a visual scale of 0-3. Infrequently, a thin rim of moderate cytoplasmic staining could be identified around small lymphocytic nuclei. Determining cytoplasmic versus membrane staining was equivocal in lymphocytes.

Additionally, periparenchymal adipocytes were positive for cytoplasmic enolase.

#### 6.4.2.2 Liver

Hepatocellular  $\alpha$ -enolase expression was not significantly different between cats with or without CKD ( $p > 0.05$ , Figure 6.1). The median immunoreactivity score for young control cats and CKD was 1 (range 0-2). No score of 3 was given to any hepatocyte for either group while a majority were given a score of 1 (controls 62/100, CKD 73/100). Remaining cats were given a score of

either 2 (controls 20/100, CKD 12/100) or no staining was detected (controls 18/100, CKD 15/100). Alpha-enolase staining was restricted to the cytoplasm of hepatocytes (Figure 6.2).

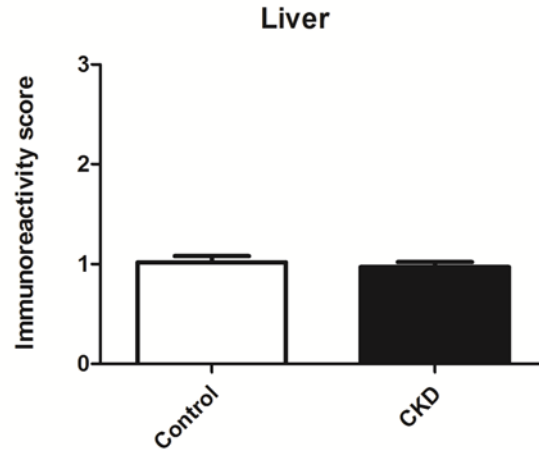


Figure 6.1 Mean immunoreactivity scores for hepatocytes of healthy controls (n=5) and CKD cats (n=5). Whiskers represent the standard error of mean.

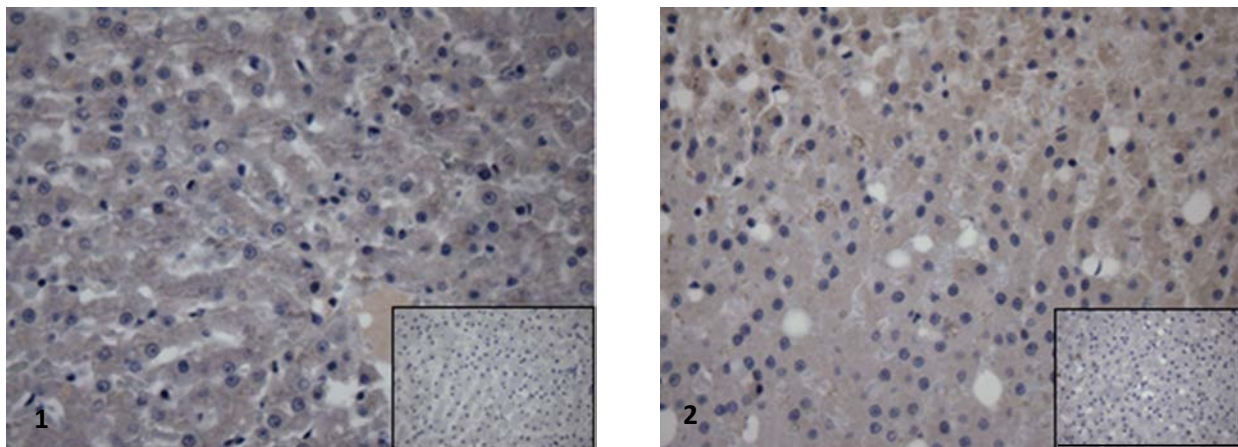


Figure 6.2 Immunohistochemistry of the liver from a (1) non-azotemic, healthy control and (2) chronic kidney disease cat, mouse monoclonal  $\alpha$ -enolase antibody, 20X (Inset: negative control).

### 6.4.2.3 Kidney

Alpha-enolase immunoreactivity scores for CKD and control cats are summarized in Figure 6.3 with descriptive statistics outlined in Table 6.1. When comparing bilateral kidney scores from either CKD (n=5) or control (n=2) cats statistical difference was not found in staining intensities of CKD tubules (injured tubules, p=0.57; normal tubules, p=0.11) and glomeruli (CKD, p=0.77; controls, p=0.09). All tubules from bilateral kidneys of control cats were scored a 2 and so statistical analysis could not be performed because all values were equal. Because no difference between kidneys within individual cats was found, either those with CKD or healthy controls, a single kidney was evaluated for each cat for the remainder of the study.

Table 6.1 Summary of immunoreactivity scores in non-azotemic, healthy control cats (n=8) and chronic kidney disease cats (n=29). Immunoreactivity scores are given as the total number and (percentage) of glomeruli or tubule with each score

	Median	Range	Immunoreactivity score				
			0	1	2	3	
<b>Glomeruli</b>							
Control	1	0-2	49 (31)	90 (56)	21 (13)	0 (0)	
CKD	2	0-3	95 (16)	96 (17)	243 (42)	146 (25)	
<b>Tubules</b>							
Control	2	2-3	0 (0)	0 (0)	158 (99)	2 (1)	
CKD, Normal	2	1-3	0 (0)	19 (7)	203 (70)	68 (23)	
CKD, Injured	1	0-3	34 (12)	151 (52)	74 (26)	31 (11)	

### Immunoreactivity of feline renal alpha-enolase

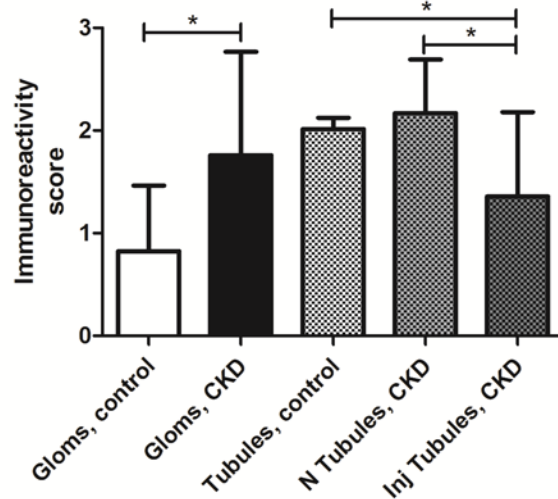


Figure 6.3 Mean immunoreactivity scores for glomeruli and tubules from healthy controls and CKD cats. Normal and injured tubules in CKD cats were scored separately. Whiskers represent the standard error of mean. Glomerular  $\alpha$ -enolase expression was significantly greater in CKD cats than controls ( $p < 0.05$ ). Tubular  $\alpha$ -enolase was significantly greater in control tubules and normal CKD tubules when compared to injured CKD tubules ( $p < 0.05$ ).

A total of 8 young, non-azotemic, healthy cats were used as controls. Twenty glomeruli and 20 tubules were evaluated per cat. The median glomerular immunoreactivity score for control cats was 1 (range 0-2). The majority of glomeruli (139/160) had either absent staining for  $\alpha$ -enolase or occasional pale staining of a few epithelial cells (Figure 6.4). The median tubular immunoreactivity score for control cats was 2 (range 2-3). Nearly all control cats had moderate, monochromatic, cytoplasmic staining of tubular epithelial cells (158/160) with only a few tubules that stained intensely (2/160, Figure 6.4).

Twenty-nine cats at various stages of CKD were evaluated for this study. Glomerular staining in CKD cats was variable with a median score of 2 (range 0-3). Immunopositivity for  $\alpha$ -enolase was variable even within the same kidney of some cats with some glomeruli having absent staining while in other regions staining intensity was marked (Figure 6.5). However, moderate staining was most common (243/580) and present within the cytoplasm of glomerular epithelial cells (visceral and parietal) and less frequently mesangial cells. Degenerative and atrophic tubules (i.e. injured) were scored separately from tubules that morphologically were normal in cats with CKD. Injured tubules had a median score of 1 (range 0-3) while morphologically normal tubules had a median score of 2 (range 1-3). There was a greater variability in staining intensity in injured tubules while a majority of morphologically normal tubules had moderate staining (203/290).

Glomerular  $\alpha$ -enolase expression by immunohistochemistry was significantly greater in cats with CKD than controls ( $p < 0.05$ ). Immunoreactivity was not significantly different between morphologically normal tubules and control tubules, however, injured tubules from CKD cats had significantly less  $\alpha$ -enolase staining than both tubules from control cats and morphologically normal tubules from CKD cats (Figure 6.5).

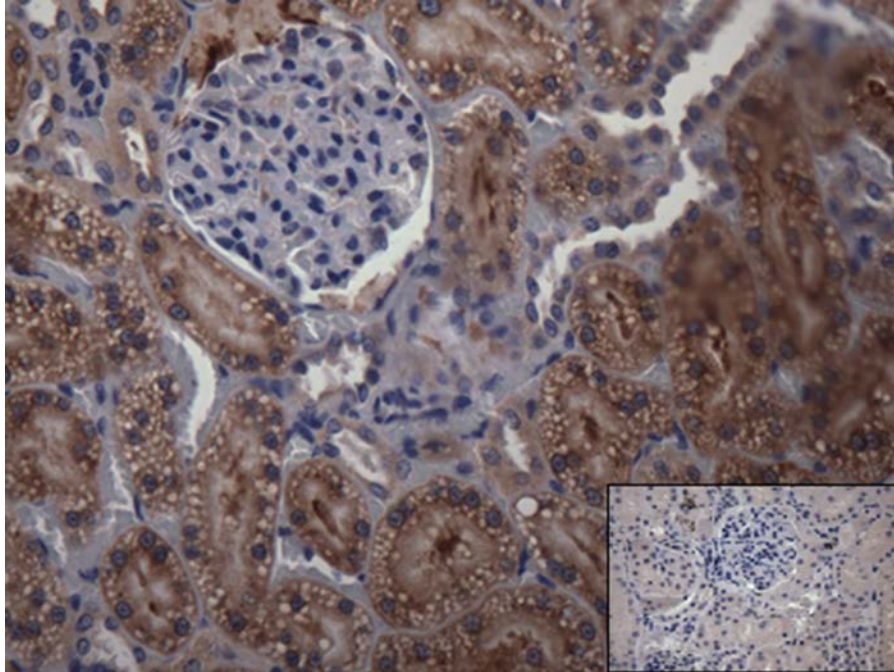


Figure 6.4 Immunohistochemistry of the kidney in a healthy control cat, mouse monoclonal  $\alpha$ -enolase antibody. Minimal staining in glomeruli with moderate, monochromatic staining of tubules, 20X (Inset: negative control).

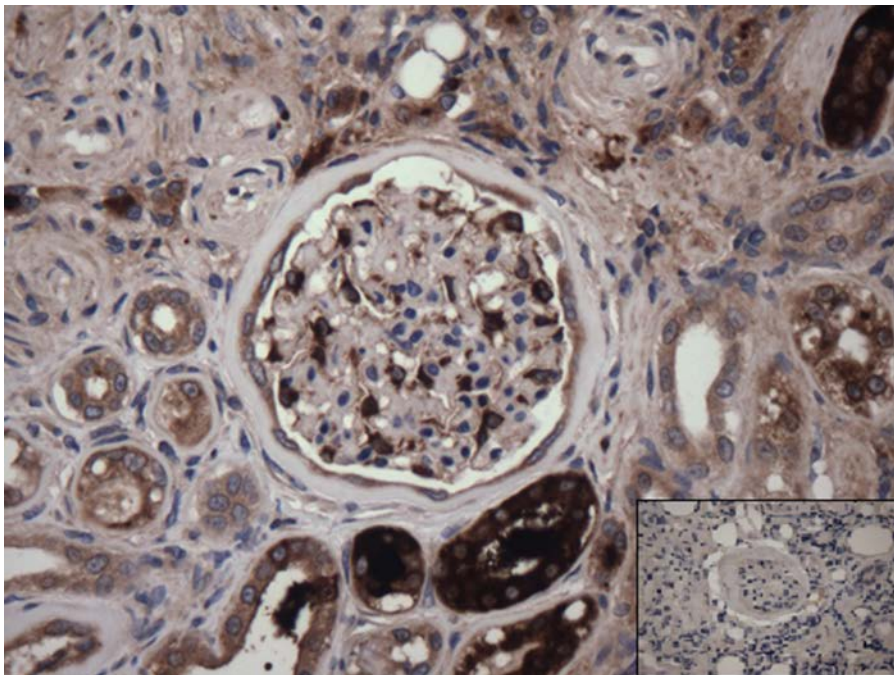


Figure 6.5 Immunohistochemistry of the kidney in a CKD cat, mouse monoclonal  $\alpha$ -enolase antibody. There is moderate to marked glomerular staining in epithelial and few mesangial cells. Tubules have variable staining intensities, 20X (Inset: negative control).

Immunoreactivity of  $\alpha$ -enolase was compared between CKD stages. Results are summarized in Figure 6.6 with descriptive statistics outlined in Table 6.2. Of the 29 CKD cats included in this study 9 were in Stage II, 8 Stage III, and 12 were in Stage IV. The median expression of  $\alpha$ -enolase in glomeruli was 2 (range 0-3) for all stages with no statistical significance found between stages. Median immunoreactivity for normal tubules was 2 (range 1-3) for all stages with no significant difference between stages. Injured tubules of cats at any stage of CKD had significantly less  $\alpha$ -enolase expression when compared to normal tubules at any stage ( $p < 0.05$ ). The median immunoreactivity score for all stages of injured tubules was 1 (range 0-3). No statistically significant difference was found between stages when  $\alpha$ -enolase expression in injured tubules was compared. Alpha-enolase expression in glomeruli of CKD cats was significantly less than normal tubules at all stages ( $p < 0.05$ ). Injured tubules from all stages had significantly less  $\alpha$ -enolase expression than glomeruli from Stage IV cats ( $p < 0.05$ ). However, expression was similar between injured tubules of Stage II cats and glomeruli of both Stage II and III cats ( $p > 0.05$ ).

Immunoreactivity of alpha-enolase by IRIS Stage

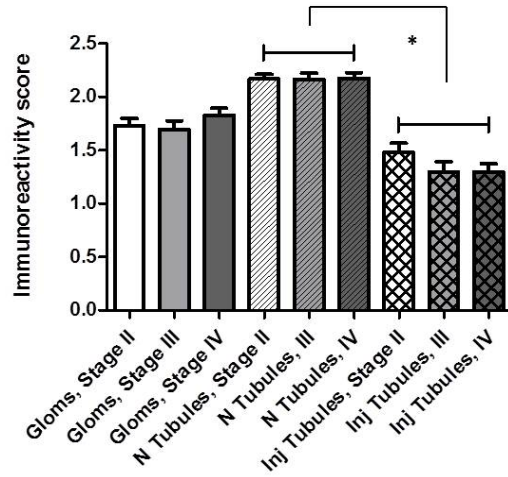


Figure 6.6 Mean immunoreactivity scores for glomeruli and tubules from healthy controls and CKD cats. Normal and injured tubules in CKD cats were scored separately. Whiskers represent the standard error of mean. Glomerular  $\alpha$ -enolase expression was significantly greater in CKD cats than controls ( $p < 0.05$ ). Tubular  $\alpha$ -enolase was significantly greater in control tubules and normal CKD tubules when compared to injured CKD tubules ( $p < 0.05$ ).

Table 6.2 Summary of immunoreactivity scores in CKD cats grouped by IRIS. Immunoreactivity scores are given as the total number and (percentage) of glomeruli or tubule with each score.

	Median	Range	Immunoreactivity score			
			0	1	2	3
<b>Glomeruli</b>						
Stage II	2	0-3	27 (15)	26 (14)	96 (53)	31 (17)
Stage III	2	0-3	30 (19)	28 (18)	63 (39)	39 (24)
Stage IV	2	0-3	38 (16)	42 (18)	84 (35)	76 (32)
<b>Tubules</b>						
<b>Normal</b>						
Stage II	2	1-3	0 (0)	2 (2)	71 (79)	17 (19)
Stage III	2	1-3	0 (0)	6 (8)	55 (69)	19 (24)
Stage IV	2	1-3	0 (0)	11 (9)	77 (64)	32 (27)
<b>Injured</b>						
Stage II	1	0-3	8 (9)	43 (48)	27 (30)	12 (13)
Stage III	1	0-3	11 (14)	42 (53)	19 (24)	8 (10)
Stage IV	1	0-3	15 (13)	65 (54)	29 (24)	11 (9)



## 6.5 Discussion

In this study we have described  $\alpha$ -enolase protein expression in feline thymic, hepatic, and renal tissues. We demonstrated that there is a difference between renal  $\alpha$ -enolase expression in cats with CKD compared to healthy controls. Renal  $\alpha$ -enolase is primarily expressed in renal cortical tubules in healthy cats with absent to minimal expression in glomeruli. In contrast, tubular expression was decreased in injured tubules while glomerular expression was increased in CKD cats compared to healthy controls. Alpha-enolase expression in the glomeruli of CKD cats was present in the cytoplasm of mesangial cells, visceral and parietal epithelium similar to the pattern described in patients with SLE nephritis with the exception of crescents in SLE which was not a feature found in CKD cats.<sup>19</sup>

The mechanism for  $\alpha$ -enolase protein overexpression in the kidney has not been definitively determined.<sup>19</sup> Possible mechanisms include glycolytic and non-glycolytic pathways in response to hypoxic conditions and increased anaerobic metabolism.<sup>4, 12, 13</sup> In response to hypoxic conditions, endothelial cells but not renal tubular epithelial cells were shown to up regulate  $\alpha$ -enolase.<sup>12, 13, 26</sup> Therefore, at least in cases of SLE nephritis with overexpression of  $\alpha$ -enolase in renal tubules another function for the protein other than glycolysis may be the cause for increased levels. Glomerular expression described in this current study is similar to that seen in SLE nephritis biopsies. Therefore, it seems plausible that up regulation of  $\alpha$ -enolase in cats with CKD has a similar pathogenesis and function, although at present has not been described. Similar mechanisms are likely playing a role in increased protein expression in glomeruli and normal tubules of cats with CKD. The decreased protein expression in injured tubules of CKD cats could be the result of tubular degeneration and atrophy a common histologic feature of feline CKD.<sup>27, 28</sup> Another potential cause for decreased protein expression in injured tubules

could be the presence of nephritogenic autoantibodies that are bound to tubular  $\alpha$ -enolase and thus blocking available epitopes for detection by monoclonal antibody in the immunohistochemistry assay. However, this was not a reported interference for protein detection in similar assays with known nephritogenic autoantibodies in human patients.<sup>19</sup>

Alpha-enolase expression in the liver of cats was not affected by CKD.

Immunoreactivity was mild in both CKD and healthy control groups. Thymic  $\alpha$ -enolase immunoreactivity in both CKD and control cats were unexpected in the current study. Alpha-enolase is considered a ubiquitous protein with the thymus and kidney containing greater amounts of protein than other organs.<sup>4,7</sup> This conclusion was based on intense reactivity of rabbit  $\alpha$ -enolase antiserum to rabbit thymic tissue extracts via an immunoblot assay.<sup>7</sup> In this aforementioned study rabbit polyclonal anti- $\alpha$ -enolase serum was applied to several tissue extracts. The thymus in particular was extracted from rabbit while the others were rat and human derived. Perhaps the markedly intense immunoreactivity was due to high primary antibody concentrations, nonspecific staining or cross reactivity rather than an optimized protein quantification in this tissue. Based on the findings in the current study, the kidney has greater protein expression than that of the thymus or liver by immunohistochemistry utilizing a monoclonal, mouse antibody.

In conclusion, renal  $\alpha$ -enolase is increased in glomeruli and decreased in injured tubules of CKD cats when compared to healthy controls. The mechanism for alteration of protein expression could be the result of hypoxia, increased anaerobic metabolism; or tubulointerstitial injury. Additional studies to further elucidate the role of  $\alpha$ -enolase enzyme in the pathogenesis of feline CKD are needed such as quantifying  $\alpha$ -enolase mRNA, localizing cellular expression as well as identifying nephritogenic autoantibodies in feline tissues.

## REFERENCES

1. Lohman K, Meyerhof O. Enzymatic transformation of phosphoglyceric acid into pyruvic and phosphoric acid. *Biochem Z* 1934;273:13.
2. Fletcher L, Rider CC, Taylor CB. Developmental changes in brain-specific enolase isoenzymes. *Biochem Soc Trans* 1976;4(6):1135-1136.
3. Fletcher L, Rider CC, Taylor CB. Enolase isoenzymes. III. Chromatographic and immunological characteristics of rat brain enolase. *Biochim Biophys Acta* 1976;452(1):245-252.
4. Pancholi V. Multifunctional alpha-enolase: its role in diseases. *Cell Mol Life Sci* 2001;58(7):902-920.
5. Rider CC, Taylor CB. Enolase isoenzymes in rat tissues. Electrophoretic, chromatographic, immunological and kinetic properties. *Biochim Biophys Acta* 1974;365(1):285-300.
6. Rider CC, Taylor CB. Enolase isoenzymes. II. Hybridization studies, developmental and phylogenetic aspects. *Biochim Biophys Acta* 1975;405(1):175-187.
7. Sabbatini A, Dolcher MP, Marchini B, et al. Alpha-enolase is a renal-specific antigen associated with kidney involvement in mixed cryoglobulinemia. *Clin Exp Rheumatol* 1997;15(6):655-658.
8. Moscato S, Pratesi F, Sabbatini A, et al. Surface expression of a glycolytic enzyme, alpha-enolase, recognized by autoantibodies in connective tissue disorders. *Eur J Immunol* 2000;30(12):3575-3584.
9. Moscato S, Pratesi F, Bongiorno F, et al. Endothelial cell binding by systemic lupus antibodies: functional properties and relationship with anti-DNA activity. *J Autoimmun* 2002;18(3):231-238.
10. Wygrecka M, Marsh LM, Morty RE, et al. Enolase-1 promotes plasminogen-mediated recruitment of monocytes to the acutely inflamed lung. *Blood* 2009;113(22):5588-5598.
11. Díaz-Ramos A, Roig-Borrellas A, García-Melero A, et al.  $\alpha$ -Enolase, a multifunctional protein: its role on pathophysiological situations. *J Biomed Biotechnol* 2012;2012:156795.
12. Aaronson RM, Graven KK, Tucci M, et al. Non-neuronal enolase is an endothelial hypoxic stress protein. *J Biol Chem* 1995;270(46):27752-27757.
13. Graven KK, Zimmerman LH, Dickson EW, et al. Endothelial cell hypoxia associated proteins are cell and stress specific. *J Cell Physiol* 1993;157(3):544-554.

14. Miles LA, Dahlberg CM, Plescia J, et al. Role of cell-surface lysines in plasminogen binding to cells: identification of alpha-enolase as a candidate plasminogen receptor. *Biochemistry* 1991;30(6):1682-1691.
15. Redlitz A, Fowler BJ, Plow EF, et al. The role of an enolase-related molecule in plasminogen binding to cells. *Eur J Biochem* 1995;227(1-2):407-415.
16. López-Alemaný R, Suelves M, Muñoz-Cánoves P. Plasmin generation dependent on alpha-enolase-type plasminogen receptor is required for myogenesis. *Thromb Haemost* 2003;90(4):724-733.
17. López-Alemaný R, Longstaff C, Hawley S, et al. Inhibition of cell surface mediated plasminogen activation by a monoclonal antibody against alpha-Enolase. *Am J Hematol* 2003;72(4):234-242.
18. Terrier B, Degand N, Guilpain P, et al. Alpha-enolase: a target of antibodies in infectious and autoimmune diseases. *Autoimmun Rev* 2007;6(3):176-182.
19. Migliorini P, Pratesi F, Bongiorno F, et al. The targets of nephritogenic antibodies in systemic autoimmune disorders. *Autoimmun Rev* 2002;1(3):168-173.
20. Lee KH, Chung HS, Kim HS, et al. Human alpha-enolase from endothelial cells as a target antigen of anti-endothelial cell antibody in Behçet's disease. *Arthritis Rheum* 2003;48(7):2025-2035.
21. Lee JH, Cho SB, Bang D, et al. Human anti-alpha-enolase antibody in sera from patients with Behçet's disease and rheumatologic disorders. *Clin Exp Rheumatol* 2009;27(2 Suppl 53):S63-66.
22. Pratesi F, Moscato S, Sabbatini A, et al. Autoantibodies specific for alpha-enolase in systemic autoimmune disorders. *J Rheumatol* 2000;27(1):109-115.
23. Hanrotel-Saliou C, Segalen I, Le Meur Y, et al. Glomerular antibodies in lupus nephritis. *Clin Rev Allergy Immunol* 2011;40(3):151-158.
24. Haimoto H, Takashi M, Koshikawa T, et al. Enolase isozymes in renal tubules and renal cell carcinoma. *Am J Pathol* 1986;124(3):488-495.
25. Novartis Animal Health Inc. IRIS staging CKD. <http://www.iris-kidney.com/guidelines/staging.shtml> (2013, accessed 1 April 2015).
26. Zimmerman LH, Levine RA, Farber HW. Hypoxia induces a specific set of stress proteins in cultured endothelial cells. *J Clin Invest* 1991;87(3):908-914.
27. Lucke VM. Renal disease in the domestic cat. *J Pathol Bacteriol* 1968;95(1):67-91.

28. McLeland SM, Cianciolo RE, Duncan CG, et al. A Comparison of Biochemical and Histopathologic Staging in Cats With Chronic Kidney Disease. *Vet Pathol* 2014.

## CHAPTER 7: CELLULAR LOCALIZATION OF RENAL ALPHA-ENOLASE

### 7.1 Chapter Summary

Alpha-enolase is a ubiquitous glycolytic enzyme that is alternatively expressed on the plasma membrane where it can be targeted by autoantibodies in sera of patients with autoimmune diseases involving the kidney. Anti- $\alpha$ -enolase antibodies can be induced experimentally in cats with prophylactic viral vaccines and occur naturally in cats with chronic kidney disease (CKD). The purpose of this study was to evaluate the cellular location of  $\alpha$ -enolase in feline renal tissue homogenates. A total of 29 CKD cats at various IRIS stages and 2 healthy controls were included in this study. Renal tissue homogenates were fractionated and  $\alpha$ -enolase protein was identified by western blot immunoassay. Twenty-eight cats with CKD and both control cats had cytosolic  $\alpha$ -enolase protein while only 16 CKD cats and a single control cat had membranous protein expression. The number of cats with membranous  $\alpha$ -enolase was significantly greater in later stages of kidney disease ( $p=0.006$ ). Eluted immunoglobulin from both azotemic and non-azotemic cats bound endogenous cytosolic and membrane proteins at the approximate molecular weight as  $\alpha$ -enolase.

### 7.2 Introduction

Autoimmune diseases occur due to the production of an adaptive immune response to self-antigen.<sup>1</sup> Specific T lymphocytes that recognize self-antigen are capable of causing tissue damage directly or indirectly by antigen presentation and subsequent antibody production by B lymphocytes.<sup>1</sup> Frequently highly conserved intracellular enzymes are the target of autoantibodies in autoimmune diseases.<sup>2</sup> The loss of self-tolerance is often spontaneous or idiopathic; however there is evidence that autoimmunity can be triggered by infectious agents via

molecular mimicry.<sup>1, 3</sup> Regardless of the inciting cause, there is dysregulation of the immune response resulting in systemic or tissue specific injury by cellular or humoral defenses.

Alpha-enolase is frequently reported as the target for autoantibodies in a myriad of diseases.<sup>3-5</sup> Specifically, glomerular podocyte  $\alpha$ -enolase has been identified as a target for autoantibodies by *in vivo* co-localization in human membranous glomerulonephritis and lupus nephritis biopsies.<sup>6, 7</sup> Renal injury results from immune complex deposition, activation of complement and recruitment of inflammatory cells.<sup>8</sup> In cats, interstitial nephritis has been documented to occur in association with the presence of experimentally induced anti- $\alpha$ -enolase antibodies.<sup>9, 10</sup> Antibodies were induced by repeated administration of vaccines containing cellular contaminants as well as cell line lysates.<sup>9</sup> Furthermore, azotemic client owned cats with known FVRCP vaccine histories were more likely to have  $\alpha$ -enolase antibodies than non-azotemic cats.<sup>11</sup>

Alpha-enolase is a ubiquitous glycolytic enzyme with highest concentrations in the thymus and kidney.<sup>12, 13</sup> However, its function and location do not appear to be restricted to the cytoplasm to participate in glycolytic metabolism. In addition to catalyzing the conversion of 2-phosphoglycerate to phosphoenolpyruvate,  $\alpha$ -enolase can be expressed on the plasma membrane as a plasminogen receptor or act as a marker of hypoxia and heat stress.<sup>13-17</sup> As a membrane bound protein it can also act as a target for autoantibodies.<sup>2</sup> Shifting of enzyme expression to the plasma membrane may provide clues to possible pathogenesis of disease, such as its role in hypoxic stress or inflammation, and is in part the aim of this particular study. In addition to localizing  $\alpha$ -enolase cellular expression in the kidney we analyzed the affinity of cat sera to renal fractionated proteins.

## 7.3 Material and Methods

### 7.3.1 Samples

Cats with CKD presenting to Colorado State University Diagnostic Medical Center for necropsy and available serum from 2012 to 2014 were used for this study. Samples were collected from any residual serum that remained after ante mortem routine biochemistry, at the owner's permission. Samples were stored at -20°C until assays could be run in batches. Renal cortical tissue was taken at the time of necropsy, stored in RNAlater preservative, and frozen at -80°C. Similarly, tissues and serum from two healthy, non-azotemic, laboratory reared cats were used as controls. Acquisition of tissues and serum was approved by Colorado State University's Institutional Animal Care and Use Committee (IACUC). Additional serum from non-azotemic, aged cats (>10 years old) from a previous study that were screened for  $\alpha$ -enolase antibodies by western blot immunoassay were included for affinity chromatography assays.<sup>11</sup>

### 7.3.2 Subcellular fractionation

Renal cortical tissue was weighed (20mg), minced, rinsed in cold PBS, and disrupted by a hand held tissue homogenizer (Omni International, Inc). Subcellular fractionation of membrane and cytosolic compartments was achieved using Qproteome Cell Compartment Kit (Qiagen) according to the manufacturer's protocol. Briefly, extraction buffer was added to homogenized tissue to disrupt the plasma membrane. After centrifugation at 4000 rcf for 10 minutes at 4°C, the supernatant which contained cytosolic proteins was separated from the pellet. The pellet which contained the plasma membrane and organelles was resuspended in a separate extraction buffer, incubated and centrifuged at 6000 rcf for 10 minutes at 4°C. This supernatant contained plasma membranes proteins. Cellular fractions were then desalted with acetone precipitation and resuspended with 0.5% Tween 20 in PBS (0.5% PBST). Protein concentrations were determined



by the Pierce BCA Protein Assay Kit (Thermo Scientific). Five micrograms of protein from each fraction was mixed with lithium dodecyl sodium (LDS) sample buffer, reducing agent, denatured and loaded on a precast 10% Bis-Tris mini gel along with a molecular weight standard (Thermo Scientific). Gels were electrophoresed in 3-(N-Morpholino)-propanesulfonic acid running buffer at 200V for 50 minutes. Proteins were then transferred to a polyvinylidene difluorure (PVDF) membrane in transfer buffer with 20% methanol in a XCell II Blot Module (NuPage, Intitrogen, Carlsbad) at 25V for 90 minutes.

Membranes were blocked with 5% nonfat dry milk in PBS with 0.2% Tween 20 (0.2% PBST; Fisher Scientific) and then incubated with a primary mouse monoclonal anti-alpha-enolase antibody (2.5 $\mu$ g/mL) overnight at 4°C (Abnova Taiwan Corp.). Monoclonal mouse anti-Na-K-ATPase (0.05 $\mu$ g/mL) and anti-GAPDH (Glyceraldehyde-3-phosphate-dehydrogenase, 1:1000) blocked with 3% milk in PBS were optimized and used for confirmation of plasma membrane and cytosolic compartments, respectively (Millipore). All membranes were washed with 5% nonfat dry milk in PBS with 0.2% PBST and subsequently incubated in goat-anti-mouse IgG (heavy and light chain) secondary antibody conjugated to horseradish peroxidase at room temperature for 1 hour (Abnova Taiwan Corp.). Protein bands were visualized by colorimetric horseradish peroxidase (HRP) detection with 3, 3'-diaminobenzidine in 10% hydrogen peroxide buffer and analyzed by Quantity One (Bio-Rad) software. Prevalence of  $\alpha$ -enolase protein bands in subcellular fractions were compared between IRIS stages by chi-square analysis on GraphPad Prism version 5.00 for Windows (GraphPad Software, San Diego California USA, [www.graphpad.com](http://www.graphpad.com)).

### *7.3.3 Affinity chromatography*

Serum samples from each of the following groups were pooled for a total final volume of 250-300  $\mu$ L and utilized for affinity chromatography assay: CKD and aged, non-azotemic cats that were positive and negative for  $\alpha$ -enolase antibody by western blot immunoblot. Immunoglobulin G was purified with a commercially available antibody purification kit (Thermo Scientific) according to the manufacturer's protocol as previously described.<sup>18-20</sup> Briefly, serum was incubated with a Protein A agarose column in order to elute immunoglobulin G. Gel electrophoresis and western blot membranes were prepared as previously described with recombinant  $\alpha$ -enolase, cytosolic, and membrane fractions and stored at  $-20^{\circ}\text{C}$ . Membranes were thawed, rinsed with methanol and then with distilled water before blocked with TNTP + 10% milk at room temperature on a rocker for one hour. Immunoglobulin concentration was optimized at 15 $\mu$ g in 10mL of TNTP + 10% milk (1.5 $\mu$ g/mL). Membranes were incubated at  $4^{\circ}\text{C}$  overnight with gentle rocking then washed with PBS-Tween 80 three times for 5 minutes. Secondary goat-anti-cat antibody was diluted 1:25 with 20mL of TNTP+milk. Membranes were incubated with secondary antibody in the dark for 1 hour with gentle rocking at room temperature and rinsed with PBS-Tween 80. Protein bands were visualized by colorimetric horseradish peroxidase (HRP) detection with 3, 3'-diaminobenzidine in 10% hydrogen peroxide buffer and analyzed by Quantity One (Bio-Rad) software.

## **7.4 Results**

### *7.4.1 Subcellular fractionation*

Optimal concentrations of primary and secondary antibody were determined. Serial dilutions of primary Na-K-ATPase antibody at 0.1  $\mu$ g/mL, 0.05 $\mu$ g/mL, and 0.075  $\mu$ g/mL were evaluated by western blot immunoassay with protein from membrane fractions. Similarly, dilutions of 1:250,

1:500, and 1:1000 for GAPDH were evaluated by western blot immunoassay with protein from cytosolic fractions. For each antibody, serial dilutions of secondary goat anti-mouse antibody at 1:2000, 1:3000, and 1:5000 were employed. Optimal concentration for Na-K-ATPase was 0.05 µg/mL while GAPDH antibody was optimal at 1:1000 both at 1:5000 dilution of secondary antibody. Homogenized fractions required addition of detergent (0.5% PBS-Tween 20) to solubilize the protein pellet after acetone precipitation which reduced the appearance of multiple bands in the final immunoblot.

Subcellular fractionation of renal cortical tissue from all CKD cats and 2 non-azotemic, healthy cats was achieved by the aid of a commercially available kit (Qiagen). Cytosolic and membrane fractions were confirmed by the presence of positive bands at the appropriate molecular weight (MW) for GAPDH and Na-K-ATPase in respective fractions (Figure 7.1). A prominent protein band was present in the cytosolic fraction at an approximate molecular weight of 62.3 kDa (range 60.2-63.5 kDa) that bound  $\alpha$ -enolase monoclonal antibody in all but a single CKD cat (CKD 28/29, controls 2/2 Figure 7.2). Sixteen CKD cats and a single control cat had a faint band at a similar molecular weight in the membrane fractions (mean 64.1 kDa, range 62.8-65.2 kDa, Figure 7.3). The single CKD cat that did not have detectable cytosolic  $\alpha$ -enolase protein was negative in the membrane fraction as well. Of the CKD cats, 8/9 Stage II cats had cytosolic protein and only 1/9 had  $\alpha$ -enolase in the membrane fraction. All Stage III cats (8/8) had cytosolic  $\alpha$ -enolase while 6/8 had protein in the membrane fraction. Similarly all Stage IV cats (12/12) had cytosolic and 9/12 had membrane protein. Cats in higher stages (i.e. Stages III and IV) of CKD were more likely to have  $\alpha$ -enolase in the membrane fraction ( $p=0.006$ , Figure 7.4). Additional bands were present at approximately 182.7, 79.2, 76.1, 70.9, and 53.4 kDa in

the cytosolic fractions. In the membrane fractions additional bands were present at approximately 149.8, 33.0, and 15.0 kDa.

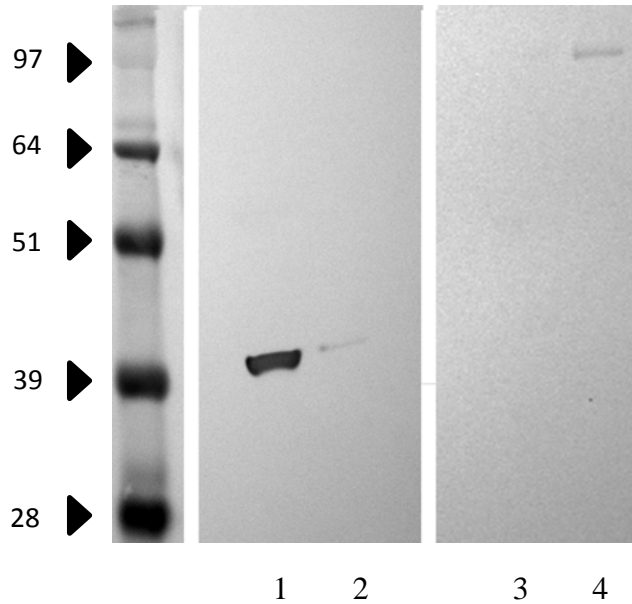


Figure 7.1 Western blots of renal cortical cytosolic (Lane 1 and 3) and membrane (Lane 2 and 4) fractions. Lanes 1 and 2 GAPDH, Lanes 3 and 4 Na-K-ATPase.

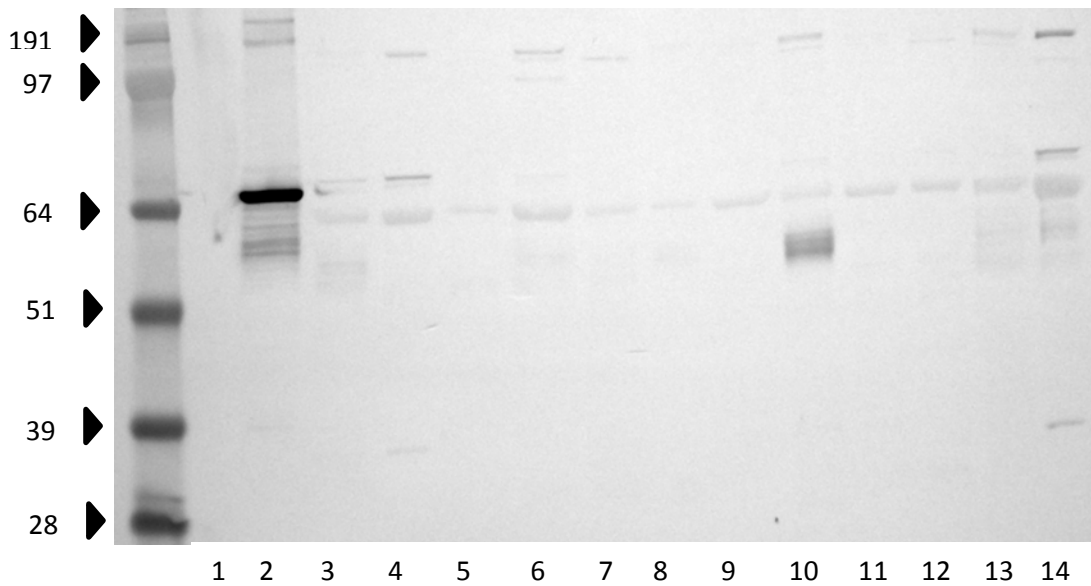


Figure 7.2 Cytosolic fractions from CKD cats with a common, dominant band at a mean molecular weight of 62.3 kDa. Lane 1, blocking buffer (negative); Lane 2, recombinant  $\alpha$ -enolase protein; Lanes 3-14, cytosolic fractions from CKD cats.

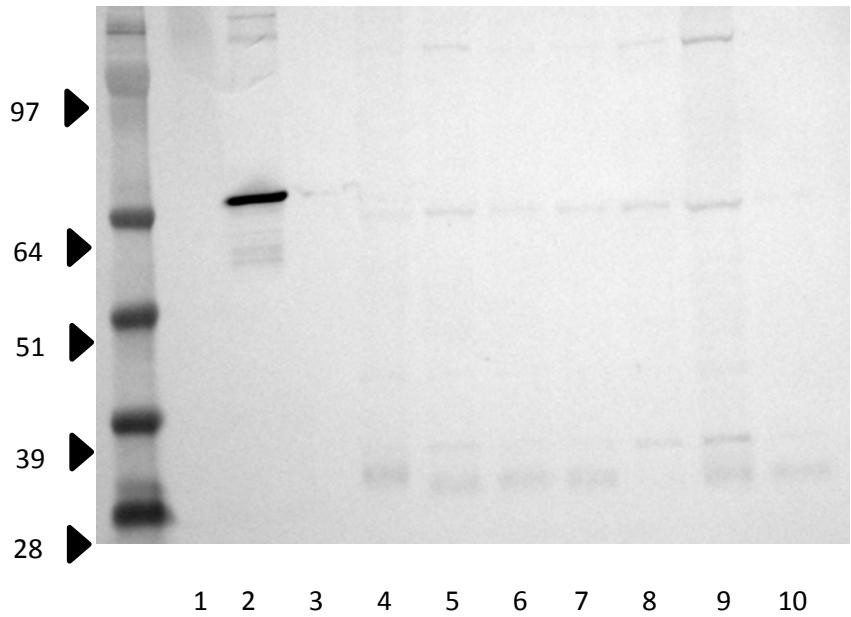


Figure 7.3 Membrane fractions from CKD cats with a common, dominant band at a mean molecular weight of 64.1 kDa. Lane 1, blocking buffer (negative); Lane 2, recombinant  $\alpha$ -enolase protein; Lanes 3-10, membrane fractions from CKD cats.

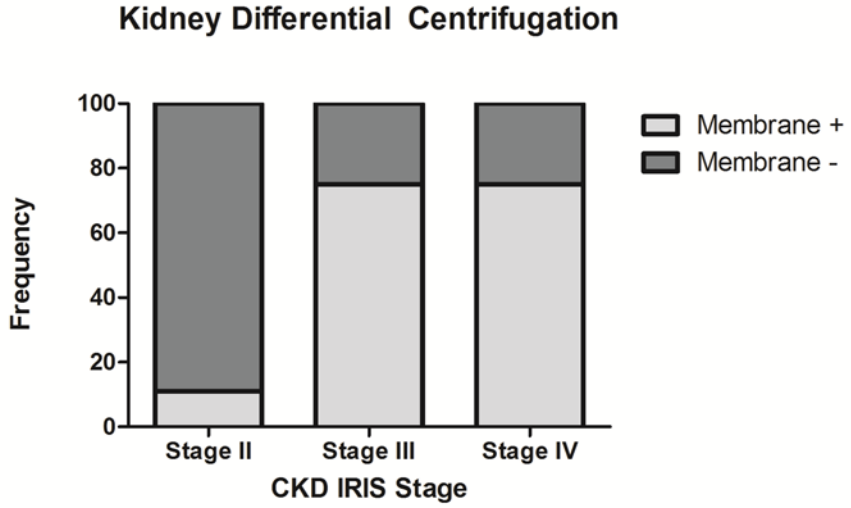


Figure 7.4 Prevalence of CKD cats with membranous expression of  $\alpha$ -enolase by IRIS stage expressed as a percentage of the group. Expression was significantly more common in later stages ( $p=0.006$ ).

#### 7.4.2 Affinity chromatography

Serum with and without  $\alpha$ -enolase antibodies, confirmed by western blot immunoassay, from both CKD and aged, non-azotemic cats were used for this assay. Immunoglobulin G was extracted from serum by affinity chromatography as described. Immunoglobulin was quantitated and applied to western blots of renal cortical fractions at various dilutions (1.5  $\mu\text{g}/\text{mL}$ , 7.5  $\mu\text{g}/\text{mL}$  and 15.0  $\mu\text{g}/\text{mL}$ ). Optimal concentration of IgG was determined to be 1.5  $\mu\text{g}/\text{ml}$ . Immunoblots containing recombinant  $\alpha$ -enolase, feline renal cytosolic and membrane proteins were incubated separately with IgG from aforementioned groups. Immunodominant bands were similar between groups (Figure 7.5). Recombinant enolase bands appeared at 54.3 kDa which was less than the theoretical MW of 73.5 kDa. Dominant cytosolic protein bands were present at 51.7 kDa, 80.2 kDa, and 43.7 kDa. Membrane protein bands were present at 52.2 kDa and a single band at 30.6 kDa in the membrane incubated with aged, non-azotemic feline serum that was negative by immunoassay for  $\alpha$ -enolase antibody.

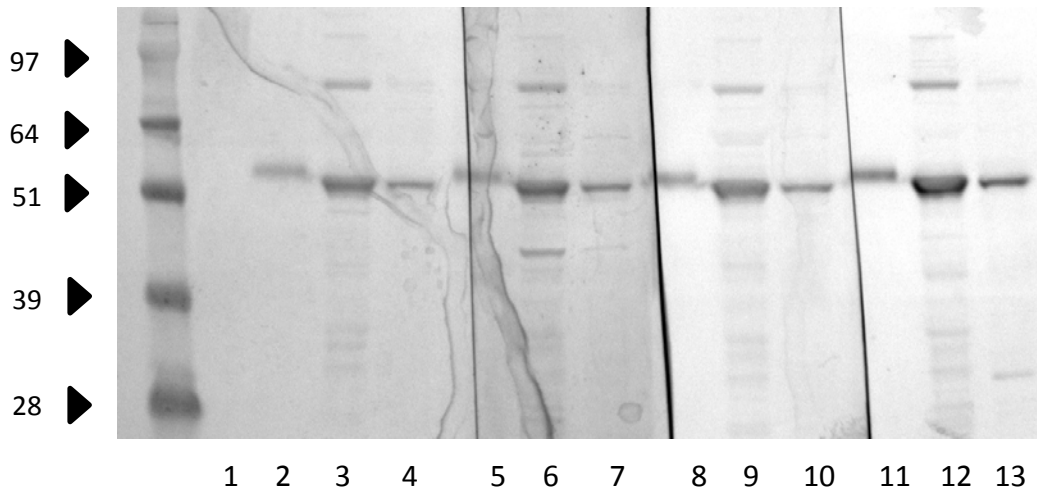


Figure 7.5 Western blot of feline renal subcellular fractions incubated with 1.5  $\mu\text{g/mL}$  of IgG from CKD cats (Lanes 2-7) and aged, non-azotemic cats (Lanes 8-13) that were either positive (Lanes 5-7 and 11-13) or negative (Lanes 2-4 and 8-10) for  $\alpha$ -enolase antibody by western blot immunoblot. Lane 1 blocking buffer (negative); Lanes 2,5, 8, and 11 recombinant  $\alpha$ -enolase; Lanes 3,6, 9, and 12 cytosolic fractions; Lanes 4, 7,10, and 13 membrane fractions.

## 7.5 Discussion

Alpha-enolase has been characterized as an abundant, highly conserved cytosolic protein which is capable of acting as a plasminogen receptor on the cell membrane or up regulated in response to metabolic stress such as hypoxia.<sup>17</sup> However, knowledge of protein expression and its role in disease states is mostly restricted to human and rodent models. The purpose of this study was to characterize cellular expression of  $\alpha$ -enolase in the cat kidney both in health and in CKD. In addition, to complement previous serologic studies we were able to demonstrate that immunoglobulin present in cat sera was capable of binding to endogenous feline renal protein *in vitro*.

Subcellular fractionation of renal cortical tissue from CKD cats revealed the presence of dominant protein band that bound  $\alpha$ -enolase monoclonal antibody in a majority of study cats. This protein was present in cytosolic and lesser membrane fractions in 28 and 16 CKD cats, respectively. However, the identified protein was not at the expected molecular weight (MW) for  $\alpha$ -enolase which should be approximately 47 kDa. In general, discrepancies in the expected molecular weight of proteins separated by gel electrophoresis can be the result of post-translational modifications such as nitration, carbonylation, and phosphorylation, alternative splicing, or intrinsic factors such as protein charge or dimerization.<sup>21</sup> Post-translational modifications of  $\alpha$ -enolase have been documented in association with neoplasia, diabetic cardiomyopathy, aging, and Alzheimer's disease.<sup>17</sup> Oxidative stress can result in carbonylation and nitration of  $\alpha$ -enolase which will modify the isoelectric point of the protein without change to the protein's molecular weight.<sup>22, 23</sup> It has been demonstrated that cats with CKD have increased markers of oxidative stress.<sup>24</sup> This stress could potentially lead to protein modifications, altering  $\alpha$ -enolase isoelectric point or molecular weight. In the present study, additional proteomics analyses to assess the presence of post-translational modifications in the kidney of CKD cats would be required to identify if such changes were present in feline renal  $\alpha$ -enolase. Alternatively, protein bands at higher molecular weight could be the result of sample viscosity. While optimizing the subcellular fractionation for gel electrophoresis and western blot immunoassay samples were eventually solubilized in 0.5% PBS-Tween 20 which resulted in a moderately to markedly viscous sample. It is possible that the sample viscosity inhibited the electrophoretic mobility to some extent resulting in a slightly increased molecular weight by gel electrophoresis.<sup>25, 26</sup> Additionally, the positive control--recombinant  $\alpha$ -enolase--was not at the exact expected MW of 73.5 kDa but less at approximately 54.3 kDa in the affinity



chromatography western blots. In this assay, the reduction in weight could be the consequence of loss of the GST tag (26 kDa) from the recombinant protein.

Extraction of immunoglobulin by affinity chromatography revealed positive bands in samples that had previously tested negative for anti- $\alpha$ -enolase antibodies by western blot immunoassay. A potential explanation for this could be that there was a soluble substance interfering with the immunoglobulin in the serum of cats with negative western blot immunoassays. Or perhaps  $\alpha$ -enolase antibody was less concentrated in these cats sera which brought about a false negative result by western blot immunoassay.

In conclusion, this study has shown that  $\alpha$ -enolase is predominantly expressed within the cytosol of cats with and without chronic kidney disease. As the stage of CKD progresses (i.e. from Stage II to IV) membranous expression of  $\alpha$ -enolase occurs more frequently. Although a mechanism for the shift to membranous  $\alpha$ -enolase expression has not been defined the data gathered in this study suggests that a relationship, either cause or effect, between the severity of CKD and a shift in cellular localization exists.<sup>2</sup> Alpha-enolase can function as a plasminogen receptor, the site for conversion of plasminogen to plasmin in the fibrinolysis pathway, when expressed on cell membranes.<sup>27</sup> Impaired fibrin clearance due to blocking of plasminogen receptors by anti- $\alpha$ -enolase antibodies leading to increased inflammation has been proposed.<sup>2, 27</sup> Further work to define the functional role of membranous  $\alpha$ -enolase in cats with CKD, such as a plasminogen receptor, is needed. Furthermore, determining if there is an association between the presence and severity of renal inflammation and membranous  $\alpha$ -enolase expression in cats with CKD may provide insight into the role of  $\alpha$ -enolase as a plasminogen receptor in feline CKD.

## REFERENCES

1. Janeway C, P T, M W, et al. *Autoimmune responses are directed against self antigens*. 5 ed. New York: Garland Science; 2001.
2. Moscato S, Pratesi F, Sabbatini A, et al. Surface expression of a glycolytic enzyme, alpha-enolase, recognized by autoantibodies in connective tissue disorders. *Eur J Immunol* 2000;30(12):3575-3584.
3. Gitlits VM, Toh BH, Sentry JW. Disease association, origin, and clinical relevance of autoantibodies to the glycolytic enzyme enolase. *J Investig Med* 2001;49(2):138-145.
4. Pratesi F, Moscato S, Sabbatini A, et al. Autoantibodies specific for alpha-enolase in systemic autoimmune disorders. *J Rheumatol* 2000;27(1):109-115.
5. Terrier B, Degand N, Guilpain P, et al. Alpha-enolase: a target of antibodies in infectious and autoimmune diseases. *Autoimmun Rev* 2007;6(3):176-182.
6. Bruschi M, Carnevali ML, Murtas C, et al. Direct characterization of target podocyte antigens and auto-antibodies in human membranous glomerulonephritis: Alfa-enolase and borderline antigens. *J Proteomics* 2011;74(10):2008-2017.
7. Bruschi M, Sinico RA, Moroni G, et al. Glomerular autoimmune multicomponents of human lupus nephritis in vivo:  $\alpha$ -enolase and annexin AI. *J Am Soc Nephrol* 2014;25(11):2483-2498.
8. Migliorini P, Anzilotti C, Caponi L, et al. Autoantibodies and nephritis: Different roads may lead to Rome. *Molecular Autoimmunity* 2005:16.
9. Lappin MR, Jensen WA, Jensen TD, et al. Investigation of the induction of antibodies against Crandell-Rees feline kidney cell lysates and feline renal cell lysates after parenteral administration of vaccines against feline viral rhinotracheitis, calicivirus, and panleukopenia in cats. *Am J Vet Res* 2005;66(3):506-511.
10. Lappin MR, Basaraba RJ, Jensen WA. Interstitial nephritis in cats inoculated with Crandell Rees feline kidney cell lysates. *J Feline Med Surg* 2006;8(5):353-356.
11. Sonius C, Whittemore J, Hawley J, et al. Association Between Feline Antibody Responses to Alpha-Enolase and Azotemia in Privately-Owned Cats (poster). American College of Veterinary Internal Medicine Annual Forum, Denver CO; 2011.
12. Sabbatini A, Dolcher MP, Marchini B, et al. Alpha-enolase is a renal-specific antigen associated with kidney involvement in mixed cryoglobulinemia. *Clin Exp Rheumatol* 1997;15(6):655-658.
13. Pancholi V. Multifunctional alpha-enolase: its role in diseases. *Cell Mol Life Sci* 2001;58(7):902-920.

14. Plow EF, Herren T, Redlitz A, et al. The cell biology of the plasminogen system. *FASEB J* 1995;9(10):939-945.
15. Wistow GJ, Lietman T, Williams LA, et al. Tau-crystallin/alpha-enolase: one gene encodes both an enzyme and a lens structural protein. *J Cell Biol* 1988;107(6 Pt 2):2729-2736.
16. Aaronson RM, Graven KK, Tucci M, et al. Non-neuronal enolase is an endothelial hypoxic stress protein. *J Biol Chem* 1995;270(46):27752-27757.
17. Díaz-Ramos A, Roig-Borrellas A, García-Melero A, et al.  $\alpha$ -Enolase, a multifunctional protein: its role on pathophysiological situations. *J Biomed Biotechnol* 2012;2012:156795.
18. Whittemore JC, Hawley JR, Jensen WA, et al. Antibodies against Crandell Rees feline kidney (CRFK) cell line antigens, alpha-enolase, and annexin A2 in vaccinated and CRFK hyperinoculated cats. *J Vet Intern Med* 2010;24(2):306-313.
19. Baldwin CI, Denham DA. Isolation and characterization of three subpopulations of IgG in the common cat (*Felis catus*). *Immunology* 1994;81(1):155-160.
20. Yamamoto S, Omura M, Hirata H. Isolation of porcine, canine and feline IgG by affinity chromatography using protein A. *Vet Immunol Immunopathol* 1985;9(2):195-200.
21. Ahmad QR, Nguyen DH, Wingerd MA, et al. Molecular weight assessment of proteins in total proteome profiles using 1D-PAGE and LC/MS/MS. *Proteome Sci* 2005;3(1):6.
22. Lu N, Zhang Y, Li H, et al. Oxidative and nitrate modifications of alpha-enolase in cardiac proteins from diabetic rats. *Free Radic Biol Med* 2010;48(7):873-881.
23. Baraibar MA, Hyzewicz J, Rogowska-Wrzesinska A, et al. Oxidative stress-induced proteome alterations target different cellular pathways in human myoblasts. *Free Radic Biol Med* 2011;51(8):1522-1532.
24. Keegan RF, Webb CB. Oxidative stress and neutrophil function in cats with chronic renal failure. *J Vet Intern Med* 2010;24(3):514-519.
25. Westermeier R. Electrophoresis in gels. *Methods Biochem Anal* 2011;54:365-377.
26. Hellman LM, Fried MG. Electrophoretic mobility shift assay (EMSA) for detecting protein-nucleic acid interactions. *Nat Protoc* 2007;2(8):1849-1861.
27. Migliorini P, Pratesi F, Bongiorno F, et al. The targets of nephritogenic antibodies in systemic autoimmune disorders. *Autoimmun Rev* 2002;1(3):168-173.

## CHAPTER 8: CONCLUDING REMARKS

### 8.1 Significance of Work

It has been well established that feline chronic kidney disease (CKD) affects many cats and can have significant consequences. There are many gaps in our current knowledge as to the leading cause(s) and pathogenesis of this syndrome. The ultimate goal for this dissertation was to elevate our knowledge in an attempt to bridge some of these gaps. In Chapter 3, we described various patterns and characteristics of renal lesions at the different stages of CKD. Unique lesions and specific patterns will hopefully guide future studies in potential etiologies and therapies. In Chapter 4 we characterized gastric lesions in cats with CKD. Our findings will undoubtedly impact current therapeutic regimens. For the second part of this dissertation we explored the role of  $\alpha$ -enolase and autoantibodies in feline CKD. Chapter 5 demonstrated the presence of anti- $\alpha$ -enolase antibodies in the serum of cats with CKD that were capable of binding to endogenous renal proteins. Chapter 6 characterized the expression of  $\alpha$ -enolase protein in healthy and CKD cats while Chapter 7 went a step further and described the subcellular protein expression. The data generated from the second portion of this project are in large descriptive but have some interesting potential etiopathogenic implications for feline CKD.

### 8.2 Specific Aim 1 (Chapter 3: Histopathology of CKD IRIS stages)

This chapter documented differences in histologic lesions and patterns among the four stages of CKD. The severity of tubular degeneration, interstitial inflammation, fibrosis, and glomerulosclerosis was significantly greater in later stages of CKD compared to early stages of disease, although glomerulosclerosis was the only variable that increased significantly with each disease stage. This latter finding is unique to this study as glomerulosclerosis was mild and not different among stages in a previous study of cats with CKD.<sup>1</sup> Sclerosis, or hardening of the

glomerulus can occur for a variety of reasons. Maladaptive hyperfiltration and ischemia can result in glomerulosclerosis with the latter considered in the aforementioned study to be the more probable pathogenesis based on pattern of glomeruli histopathologically.<sup>1,2</sup> This is of particular interest in conjunction with the vascular findings in this study. Fibrointimal hyperplasia, a thickening of the vascular intima, was found in 56.5% of CKD cats and could have potential hemodynamic consequences that warrant further investigation. Proteinuria was associated with increased severity of tubular degeneration, inflammation, fibrosis, tubular epithelial single cell necrosis and decreased normal parenchyma. These findings will help pinpoint therapeutic targets and the stage of disease at which they should be initiated, in addition to potential implications as to the pathogenesis of CKD in the cat.

### **8.3 Specific Aim 2 (Chapter 4: Uremic gastropathy)**

Uremic gastritis, consisting of necrosis, hemorrhage, and ulceration has been documented in humans with renal failure.<sup>3</sup> While dogs appear to be less affected by necrosis and mucosal ulceration, no histologic assessment of gastric pathology in cats with CKD has been performed.<sup>4</sup><sup>5</sup> The aim of this chapter was to evaluate the type and prevalence of histopathologic lesions in the stomach of cats with CKD, and to determine whether the degree of azotemia, calcium-phosphorus products and serum gastrin concentrations correlated with gastric pathology.

The most significant gastric lesions in CKD cats were fibrosis and mineralization. Gastric ulceration, hemorrhage, edema, and vascular injury, were not observed in cats with CKD. Only cats with moderate and severe azotemia had gastric mineralization. Calcium-phosphorus product (CPP) was correlated to disease severity. Severely azotemic CKD cats had significantly greater CPP when compared to non-azotemic controls, and to mildly and moderately azotemic cats.

Gastrin concentrations were significantly greater in CKD cats when compared to non-azotemic controls but elevated concentrations were not associated with gastric ulceration.

These data suggest that the therapeutic administration of gastric protectants such as sucralfate may not be justified in cats with CKD. Medical management of gastrointestinal symptoms with anti-emetic and anti-nausea drugs may be more appropriate in ameliorating clinical symptoms attributable to uremia. Gastric mineralization, likely the consequence of metastatic mineralization, suggests that interventions to reduce hyperphosphatemia and renal secondary hyperparathyroidism are indicated. Lastly, the exact role of hypergastrinemia in contributing to gastric hyperacidity and/or gastric lesions in cats with CKD is still unclear. Further studies to determine gastric acidity and normal gastric pathology in cats are needed in order to close this gap in our understanding of the etiopathogenesis of hypergastrinemia in feline uremia.

#### **8.4 Specific Aim 3 (Chapter 5: Alpha-enolase antibodies in serum and endogenous renal targets)**

Systemic lupus erythematosus (SLE) is an autoimmune disease in which patients have autoantibodies that target a variety of cellular components. Of interest, anti- $\alpha$ -enolase antibodies have been associated with active nephritis and recovery in SLE patients.<sup>6-8</sup> Anti- $\alpha$ -enolase antibodies can be induced experimentally in cats and inducible autoantibodies have been associated with interstitial nephritis.<sup>9, 10</sup> In this chapter, the goal was to determine if cats with naturally occurring CKD at various stages and with variable vaccine exposure had significant serum anti- $\alpha$ -enolase antibodies. In addition, it was determined that endogenous renal  $\alpha$ -enolase was a target for circulating autoantibodies.

Cats with CKD had significantly higher levels of serum anti- $\alpha$ -enolase antibodies than healthy, non-azotemic control cats. Alpha-enolase antibodies increased with each stage (Stage II-IV); however the difference between each stage was not statistically significant. Lack of statistical significance may be a consequence of a small sample size for each stage. If autoantibodies to  $\alpha$ -enolase do indeed increase with stage then there are potential diagnostic or pathogenic implications of these antibodies. Autoantibodies can be produced in response to cellular injury for tissue repair.<sup>11, 12</sup> Renal tubular injury in feline CKD, which includes degeneration and epithelial cell death, were described in Chapter 3. These histologic variables of tubular injury increase with stage and thus could potentially be the cause for an increase in autoantibodies. Alternatively, autoantibodies induced by vaccination could be the cause for renal injury. Vaccination status could only be confirmed in 9/29 CKD cats in this study and thus an association between vaccination exposure and antibody levels could not be determined. Future studies should be concentrated on evaluating anti- $\alpha$ -enolase antibodies in cats with and without naturally occurring CKD with known vaccine histories. Furthermore, correlation of antibody levels and histologic variables of renal injury in cats with CKD are warranted to evaluate the potential pathogenicity of  $\alpha$ -enolase antibodies.

#### **8.5 Specific Aim 4 (Chapter 6: Renal $\alpha$ -enolase protein expression)**

Alpha-enolase is best known as a cytoplasmic, glycolytic enzyme in most cell types.<sup>13, 14</sup> However, It is not restricted to its glycolytic role in the cytosol. It can be up regulated in the cell in response to physiologic stress, expressed on the cell membrane as a plasminogen receptor, C-peptide receptor, or marker of apoptosis to name a few.<sup>15-20</sup> In addition protein expression in kidneys of patients with active nephritis is differentially expressed and is targeted by

autoantibodies.<sup>6-8</sup> Differences in protein expression could give clues to the metabolic state of tissues or pathogenesis of a particular disease.

In this chapter, an immunohistochemical assay utilizing a monoclonal mouse antibody was optimized and validated in feline tissues to assess protein expression in health and CKD. Renal  $\alpha$ -enolase was primarily expressed in renal cortical tubules in healthy cats with absent to minimal expression in glomeruli. In contrast, tubular expression was less in injured tubules while glomerular expression was increased in CKD cats compared to healthy controls. Alpha-enolase expression in the glomeruli of CKD cats was present in the cytoplasm of mesangial cells, visceral and parietal epithelium. Hepatic protein expression was similar between healthy and CKD cats which indicates that there is not likely a systemic down regulation of  $\alpha$ -enolase enzyme in cats with CKD. Implications of the differential expression may be an indicator of the metabolic state of the kidney. Perhaps there is increased expression in glomeruli and a few remaining morphologic normal tubules as a response to local tissue hypoxia or increased metabolic demand on remaining, functioning nephrons. Studies have shown that whilst renal tubular epithelial cells did not up regulate enolase in response to hypoxic conditions the *in vitro* conditions were extreme.<sup>20, 21</sup> It is more likely that local tissue oxygen tension could be reduced, due to loss of peritubular capillaries, increased interstitial fibrosis and inflammation, but not absent and it would be of interest to explore what the metabolic response of tubular cells and glomerular epithelial cells are under these conditions. This may include investigating expression of hypoxic markers like hypoxia inducible factor (HIF-1 $\alpha$ ) or vascular endothelial growth factor (VEGF-A) in correlation with  $\alpha$ -enolase expression in cats with CKD. Lastly, including a group of age matched cats that do not have CKD in future experiments should be performed.



## 8.6 Specific Aim 5 (Chapter 7: Cellular localization of $\alpha$ -enolase)

To complement the previous chapter which addressed  $\alpha$ -enolase protein expression in cats with CKD, this aim expanded our understanding of protein expression to the subcellular level. Alpha-enolase has multiple functions as a membranous protein. A few include plasminogen receptor, apoptotic marker, and target for autoantibodies.<sup>6, 7, 16-18, 22-24</sup> Localization of protein in cats with CKD has possible etiopathogenic implications.

In this chapter, kidney homogenate was fractionated into cytosolic and membranous fractions and  $\alpha$ -enolase protein was identified by immunoblot. Protein expression was predominately in the cytosolic fractions as would be expected; however in over half of CKD cats had membranous  $\alpha$ -enolase, albeit subjectively weaker. Membranous expression in cats with CKD could indicate that in this disease there is a functional shift for this protein. Perhaps in these cells,  $\alpha$ -enolase is acting as a plasminogen receptor or externalized as a result of apoptosis. In the case of the latter it would be plausible that in cats with CKD that due to ongoing tissue injury that there is some degree of apoptosis. In addition, we were able to show that immunoglobulin in cat sera is capable of binding renal endogenous proteins in both cytosolic and membranous fractions. It is debatable if this binding translates *in vivo* or if autoantibodies are indeed pathogenic as there is little evidence that feline CKD is an immune-complex mediated disease.<sup>1, 9, 11</sup> Additional studies such as that done by Bruschi et al co-localizing protein and antibodies in tissues would be of interest.<sup>6, 7</sup> Lastly, evaluating a subset of aged matched cats without CKD would be beneficial in further understanding these findings.

## REFERENCES

1. Chakrabarti S, Syme HM, Brown CA, et al. Histomorphometry of feline chronic kidney disease and correlation with markers of renal dysfunction. *Vet Pathol* 2013;50(1):147-155.
2. Hughson MD, Johnson K, Young RJ, et al. Glomerular size and glomerulosclerosis: relationships to disease categories, glomerular solidification, and ischemic obsolescence. *Am J Kidney Dis* 2002;39(4):679-688.
3. Jaffe R, Laing, DR. Changes of the Digestive Tract in Uremia. A Pathologic Anatomic Study. *JAMA Internal Medicine* 1934;53(6):851-864.
4. Cheville N. Uremic Gastropathy in the Dog. *Veterinary Pathology* 1979;16:292-309.
5. Peters RM, Goldstein RE, Erb HN, et al. Histopathologic Features of Canine Uremic Gastropathy: A Retrospective Study. *JVIM* 2005;19:315-320.
6. Bruschi M, Carnevali ML, Murtas C, et al. Direct characterization of target podocyte antigens and auto-antibodies in human membranous glomerulonephritis: Alfa-enolase and borderline antigens. *J Proteomics* 2011;74(10):2008-2017.
7. Bruschi M, Sinico RA, Moroni G, et al. Glomerular autoimmune multicomponents of human lupus nephritis in vivo:  $\alpha$ -enolase and annexin AI. *J Am Soc Nephrol* 2014;25(11):2483-2498.
8. Migliorini P, Pratesi F, Bongiorno F, et al. The targets of nephritogenic antibodies in systemic autoimmune disorders. *Autoimmun Rev* 2002;1(3):168-173.
9. Lappin MR, Basaraba RJ, Jensen WA. Interstitial nephritis in cats inoculated with Crandell Rees feline kidney cell lysates. *J Feline Med Surg* 2006;8(5):353-356.
10. Whittemore JC, Hawley JR, Jensen WA, et al. Antibodies against Crandell Rees feline kidney (CRFK) cell line antigens, alpha-enolase, and annexin A2 in vaccinated and CRFK hyperinoculated cats. *J Vet Intern Med* 2010;24(2):306-313.
11. Nagele EP, Han M, Acharya NK, et al. Natural IgG autoantibodies are abundant and ubiquitous in human sera, and their number is influenced by age, gender, and disease. *PLoS One* 2013;8(4):e60726.
12. Janeway C, P T, M W, et al. *Autoimmune responses are directed against self antigens*. 5 ed. New York: Garland Science; 2001.
13. Lohman K, Meyerhof O. Enzymatic transformation of phosphoglyceric acid into pyruvic and phosphoric acid. *Biochem Z* 1934;273:13.

14. Pancholi V. Multifunctional alpha-enolase: its role in diseases. *Cell Mol Life Sci* 2001;58(7):902-920.
15. Ishii T, Fukano K, Shimada K, et al. Proinsulin C-peptide activates  $\alpha$ -enolase: implications for C-peptide--cell membrane interaction. *J Biochem* 2012;152(1):53-62.
16. Miles LA, Dahlberg CM, Plescia J, et al. Role of cell-surface lysines in plasminogen binding to cells: identification of alpha-enolase as a candidate plasminogen receptor. *Biochemistry* 1991;30(6):1682-1691.
17. Redlitz A, Fowler BJ, Plow EF, et al. The role of an enolase-related molecule in plasminogen binding to cells. *Eur J Biochem* 1995;227(1-2):407-415.
18. Ucker DS, Jain MR, Pattabiraman G, et al. Externalized glycolytic enzymes are novel, conserved, and early biomarkers of apoptosis. *J Biol Chem* 2012;287(13):10325-10343.
19. Nakajima K, Hamanoue M, Takemoto N, et al. Plasminogen binds specifically to alpha-enolase on rat neuronal plasma membrane. *J Neurochem* 1994;63(6):2048-2057.
20. Aaronson RM, Graven KK, Tucci M, et al. Non-neuronal enolase is an endothelial hypoxic stress protein. *J Biol Chem* 1995;270(46):27752-27757.
21. Graven KK, Farber HW. Endothelial cell hypoxic stress proteins. *J Lab Clin Med* 1998;132(6):456-463.
22. Moscato S, Pratesi F, Sabbatini A, et al. Surface expression of a glycolytic enzyme, alpha-enolase, recognized by autoantibodies in connective tissue disorders. *Eur J Immunol* 2000;30(12):3575-3584.
23. Terrier B, Degand N, Guilpain P, et al. Alpha-enolase: a target of antibodies in infectious and autoimmune diseases. *Autoimmun Rev* 2007;6(3):176-182.
24. Wygrecka M, Marsh LM, Morty RE, et al. Enolase-1 promotes plasminogen-mediated recruitment of monocytes to the acutely inflamed lung. *Blood* 2009;113(22):5588-5598.